Outline of today's lecture

- ☑ **CMB secondary anisotropies**
- ☑ **Polarization signal of the CMB**
- ☑ **Observation of the CMB: receivers, telescopes**
- ☑ **CMB data analysis**

Questions?

Recap: Temperature anisotropies

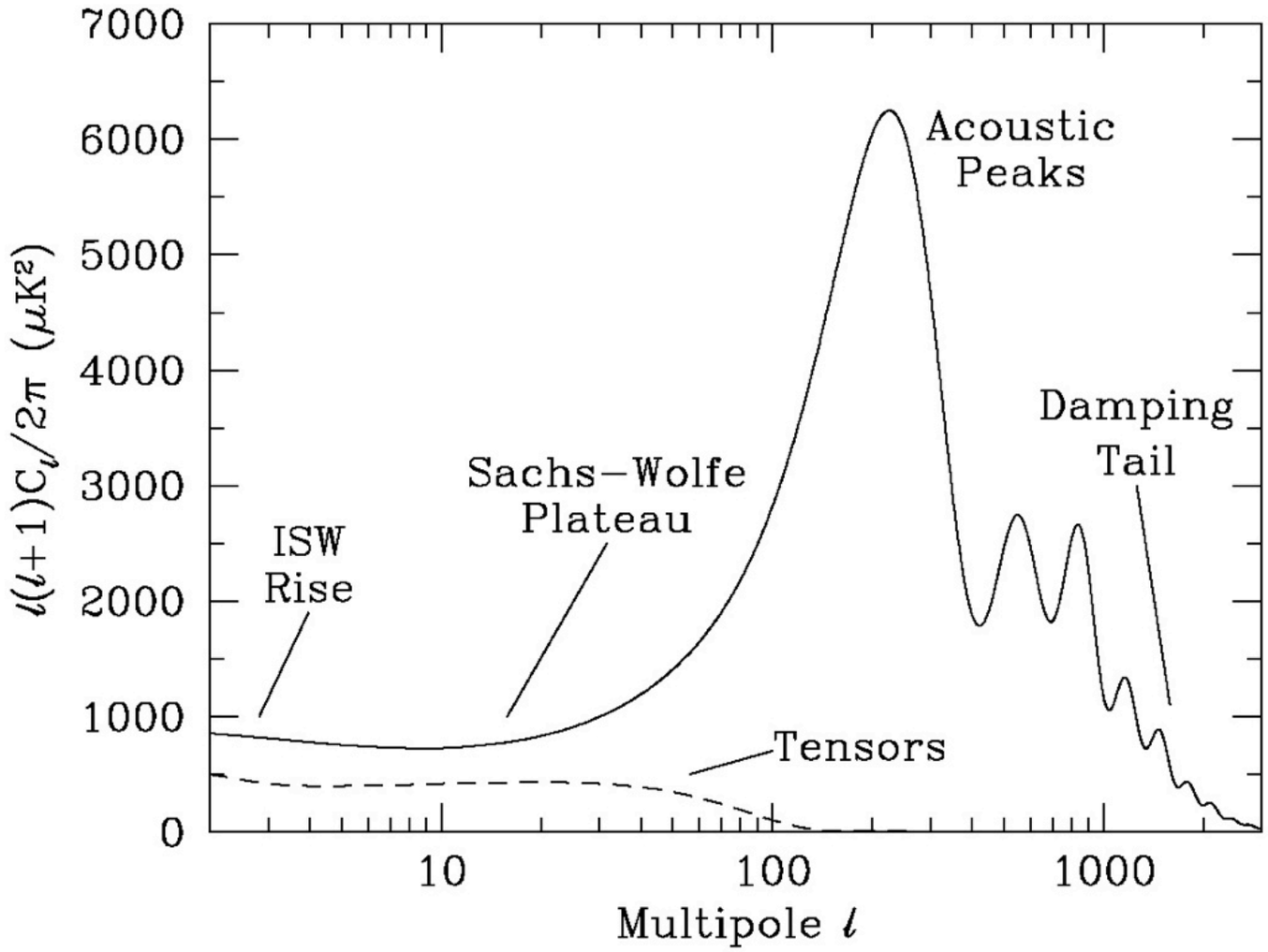

Three acoustic peak observables:

- angular scale
- photon-to-baryon ratio
- radiation-to-matter ratio

(plus information about the shape of initial matter power spectrum)

Recap: Dependance on parameters

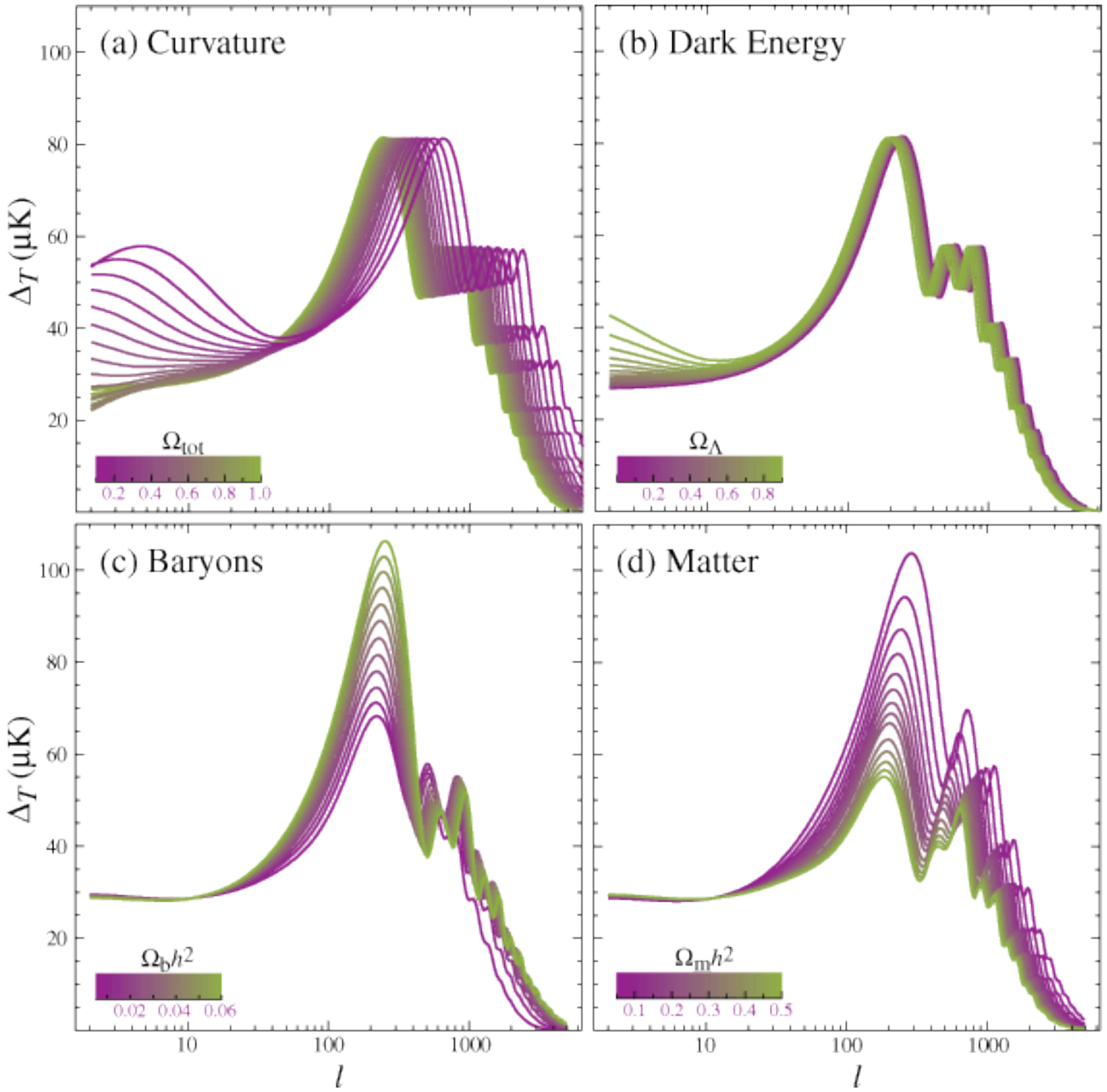

Summary of temperature anisotropies

Table 1. Sources of temperature fluctuations.

PRIMARY	Gravity	
	Doppler	
	Density fluctuations	
	Damping	
	Defects	Strings
		Textures
SECONDARY	Gravity	Early ISW
		Late ISW
		Rees-Sciama
		Lensing
	Local reionization	Thermal SZ
		Kinematic SZ
	Global reionization	Suppression
		New Doppler
		Vishniac
"TERTIARY" (foregrounds & headaches)	Extragalactic	Radio point sources
		IR point sources
	Galactic	Dust
		Free-free
		Synchrotron
	Local	Solar system
		Atmosphere
		Noise, *etc.*

Integrated Sachs-Wolfe effect

Temperature anisotropies due to density change and associated gravitational potential (scaler perturbations) at a given point **x** along the direction **n**

$$\frac{\delta T}{T} = \frac{1}{4}\frac{\delta \rho_\gamma}{\rho_\gamma}(\mathbf{x}) + \Phi(\mathbf{x}) + \mathbf{n}\cdot\mathbf{v}_\gamma(\mathbf{x}) + \int_{t_r}^{t_0} dt\ (\dot{\Phi} - \dot{\Psi}),$$

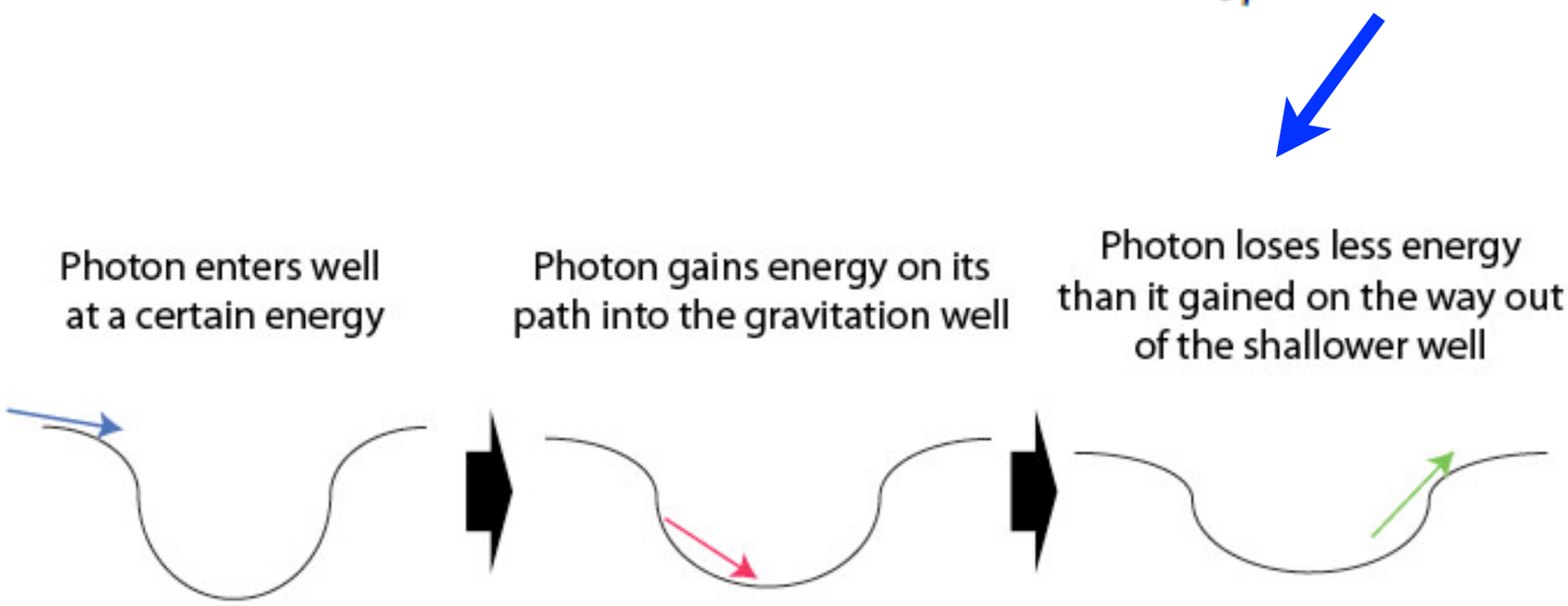

Gravitational well of galaxy supercluster - the depth shrinks as the universe (and cluster) expands

Integrated Sachs-Wolfe effect

- The early ISW effect is caused by the small but non-negligible contribution of photons to the density of the universe

- The late ISW effect

- Gravitational blueshift on infall does not cancel redshift on climb-out

- Contraction of spatial metric doubles the effect: $\Delta T/T \sim 2\Delta\Phi$

- Effect of potential hills and wells cancel out on small scales

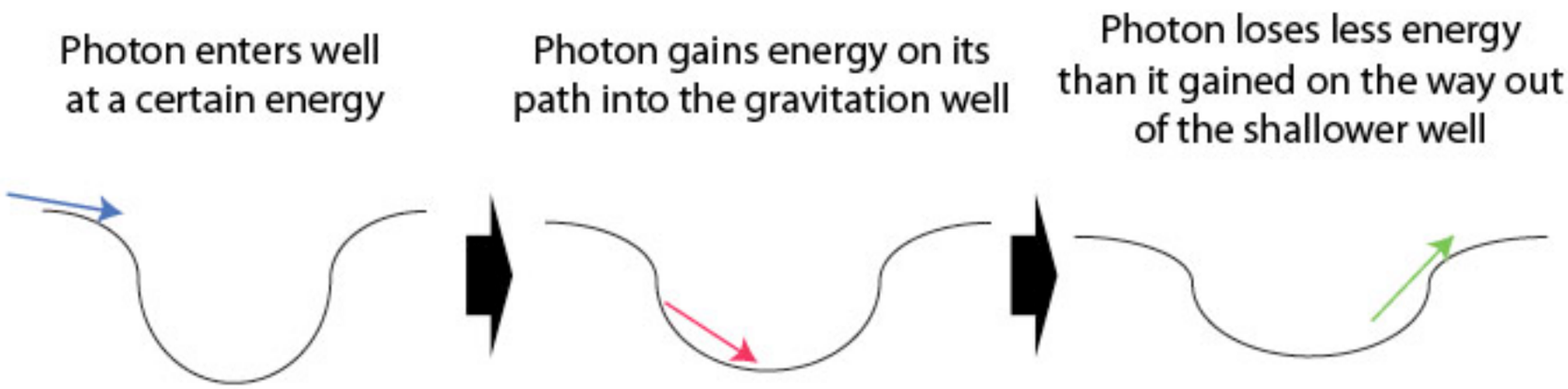

ISW effect as Dark Energy probe

The ISW effect constraints the dynamics of acceleration

Cosmic evolution of dark energy is parametrized by $w(a) \equiv p_{DE}/\rho_{DE}$
for cosmological constant, w=−1. In general, $\rho_{DE} \sim a^{-3(1+w)}$

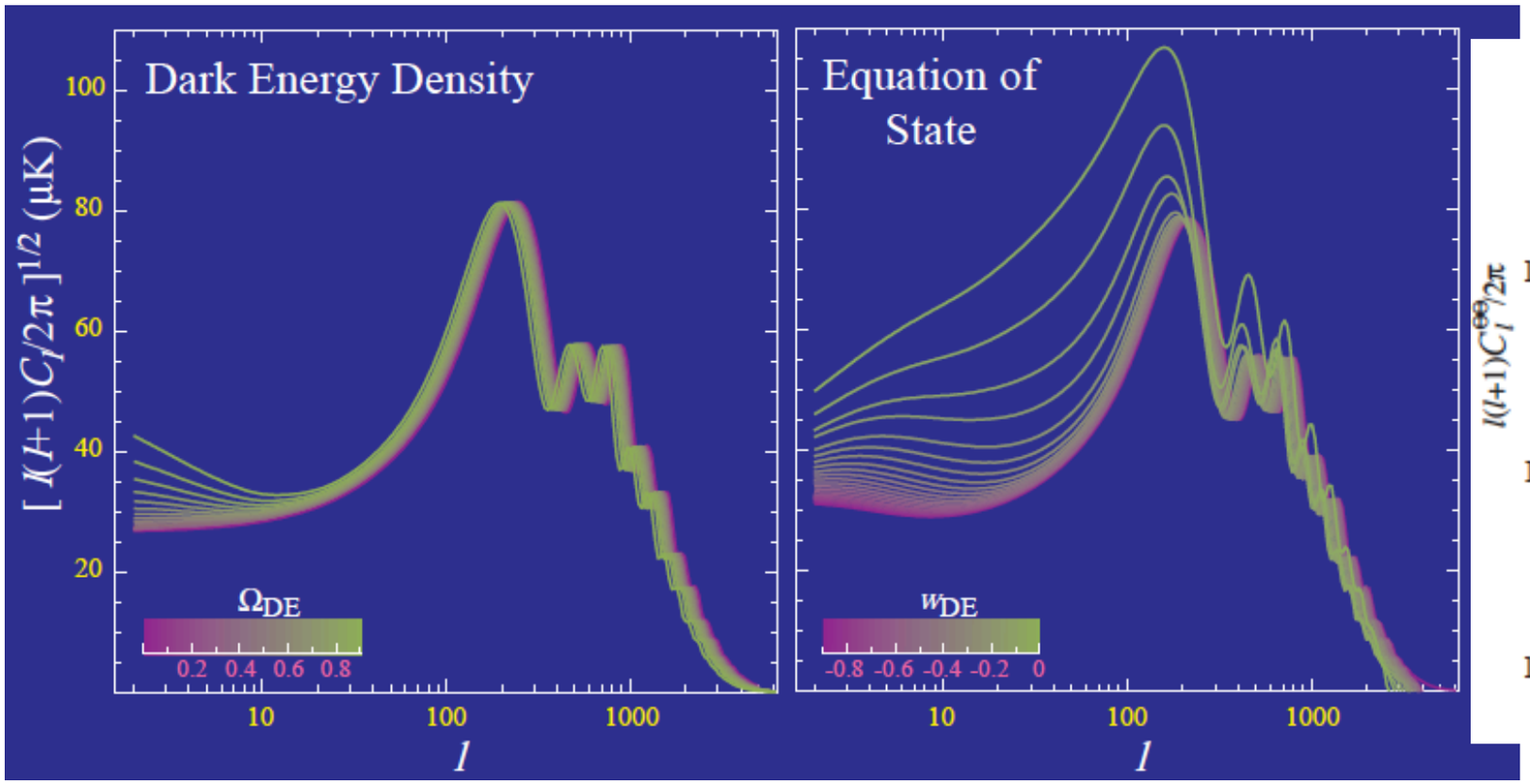

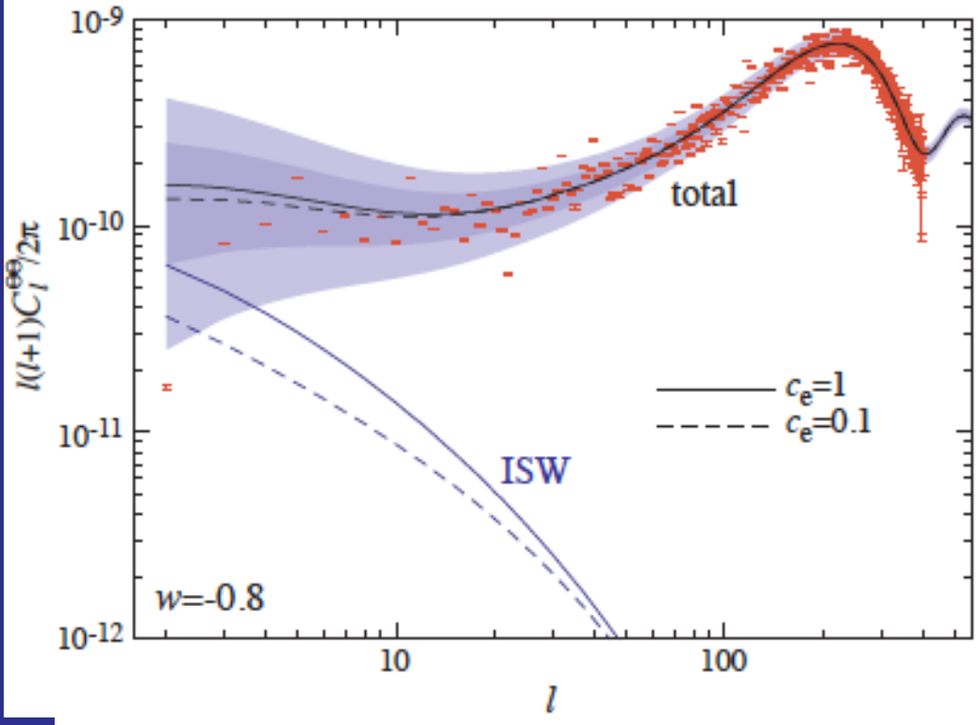

Cosmic variance problem

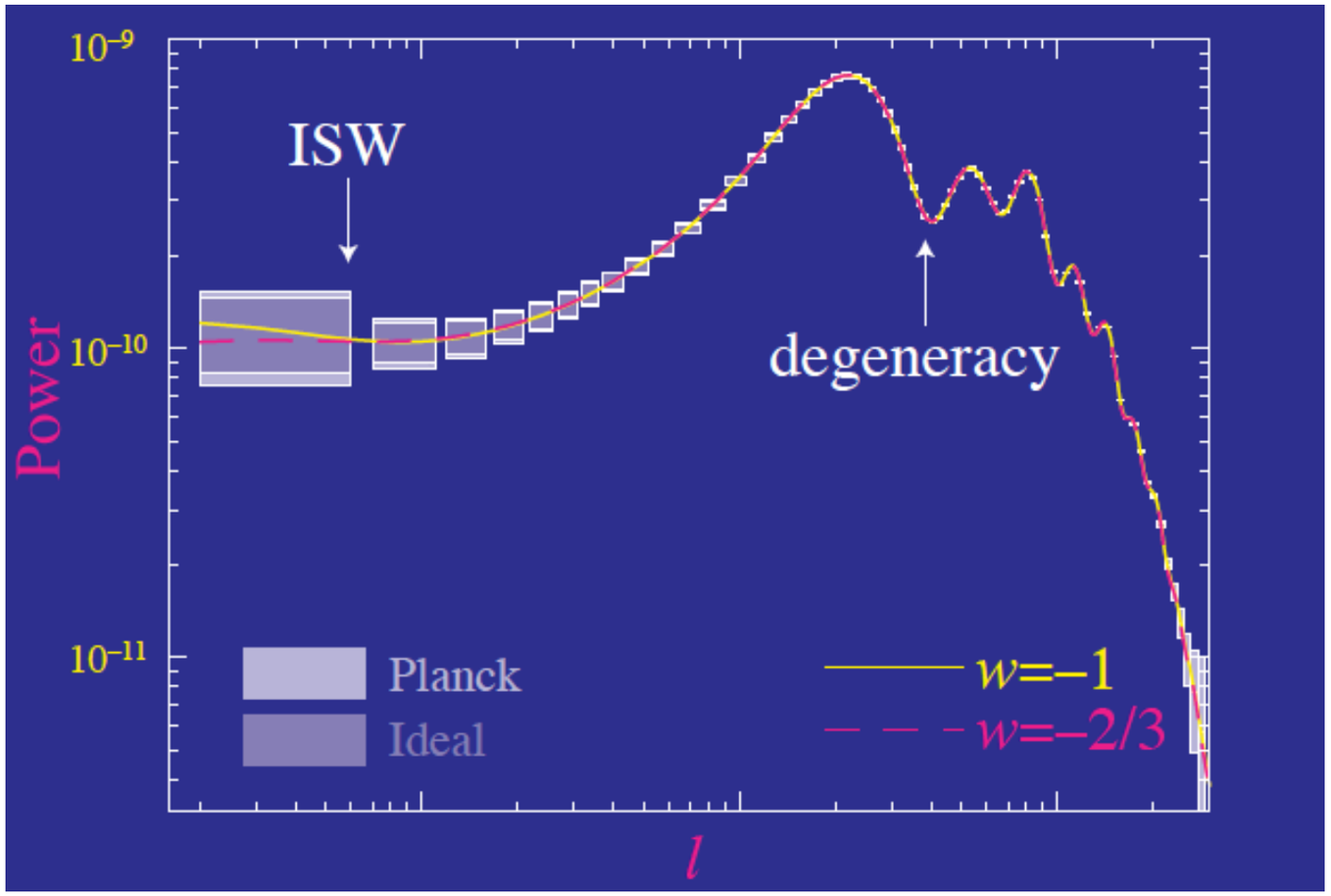

Low multipole signals are severely cosmic variance limited

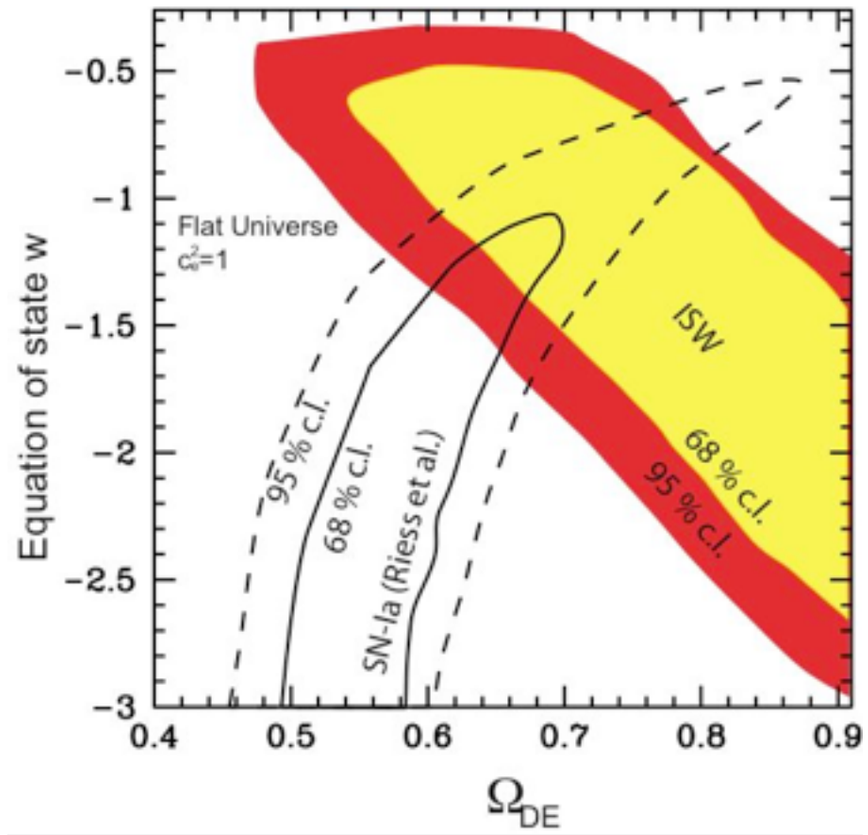

Corasaniti, Giannantonio, Melchiorri 2005

Solution: Cross-correlate with other probes of dark energy, with large sky coverage (optical, X-ray or radio surveys)

How to go further with CMB?

Cosmic Variance

› We only have one realization (our sky), i.e., one event.

› TT at small l (incl. first peak) is now cosmic variance limited.

To go further:

› TT at large l

› Polarization

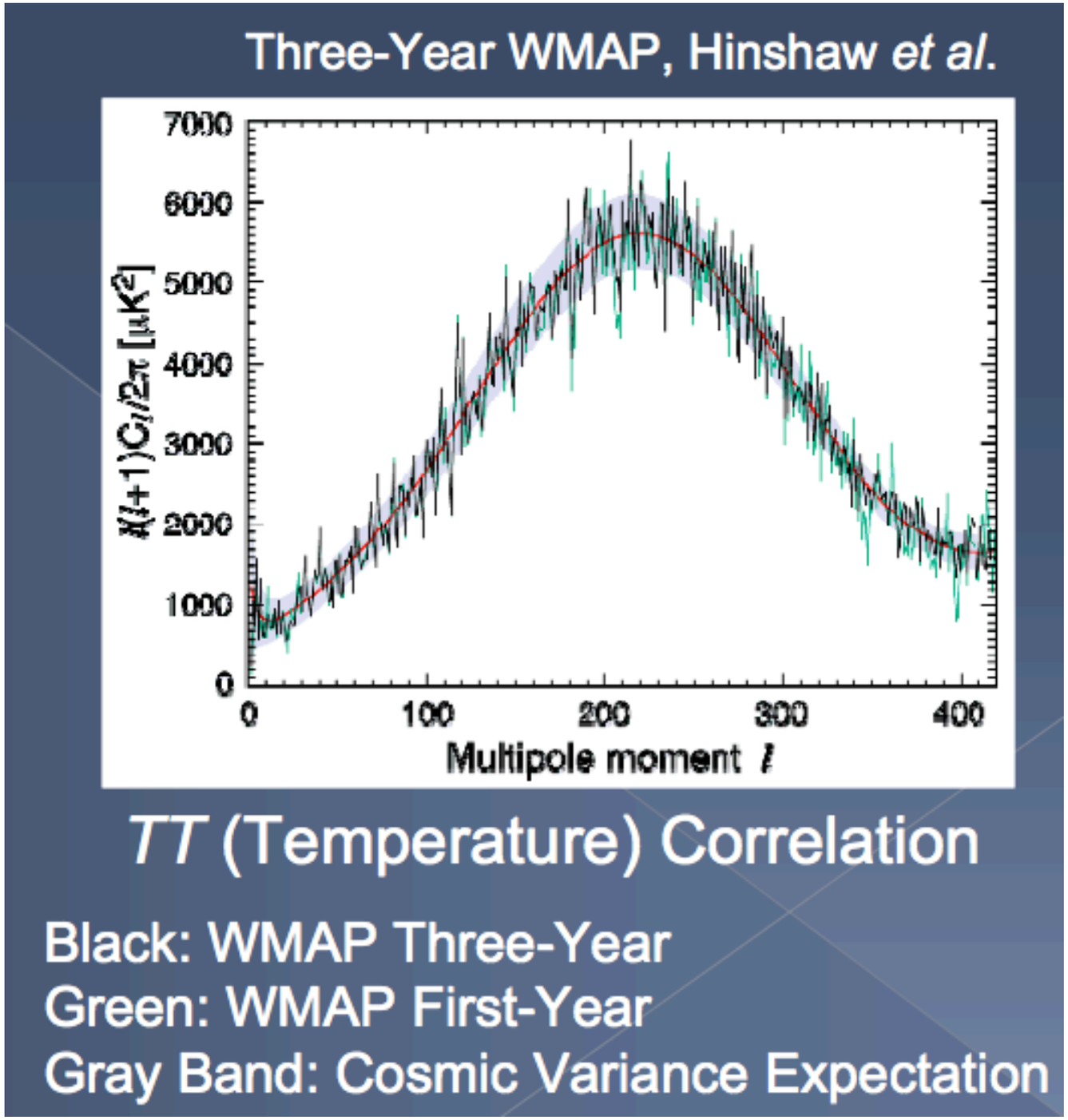

ΔT from reionization

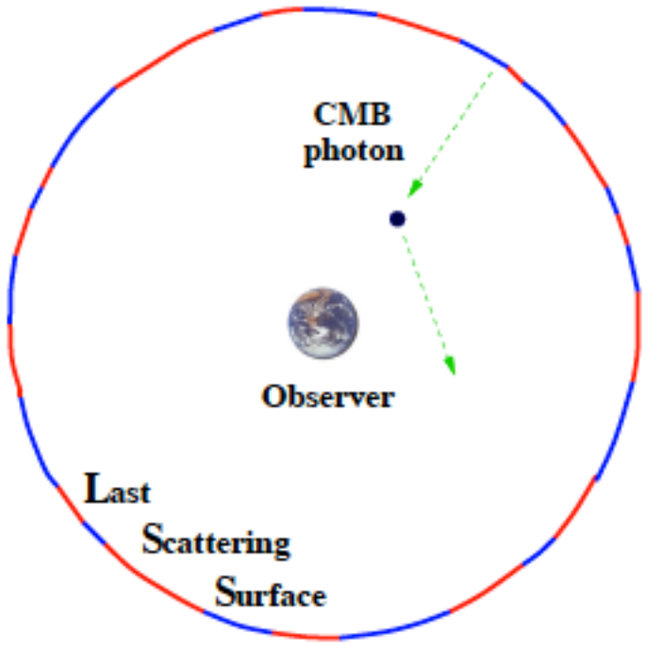

$$\frac{\Delta T}{T_0}(\theta) = e^{-\tau} \left.\frac{\Delta T}{T_0}(\theta)\right|_{orig.} + \left.\frac{\Delta T}{T_0}(\theta)\right|_{new}$$

"suppression (blurring)" & "generation"

Re-scattering of CMB photons damps anisotropy power as $e^{-2\tau}$, with τ the optical depth to Thomson scattering

New perturbations are generated on small scales due to the bulk motion of electrons in over-dense regions (Ostriker-Vishniac effect)

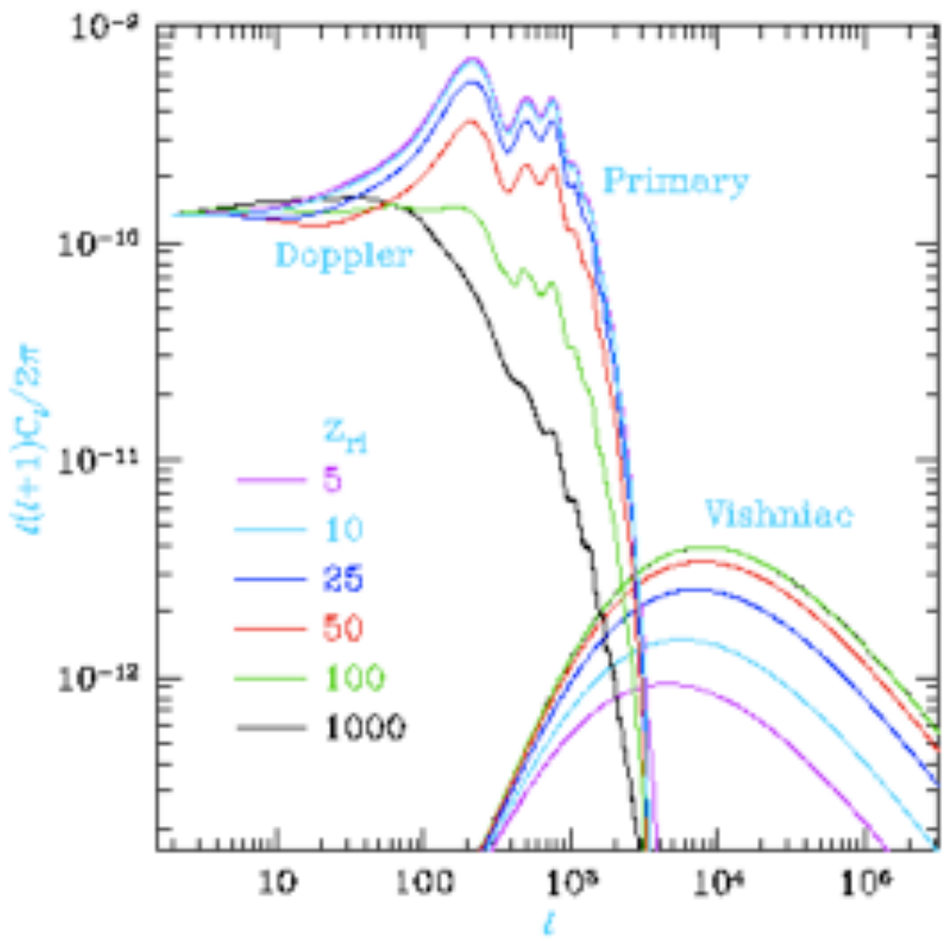

Local reionization: SZ effect

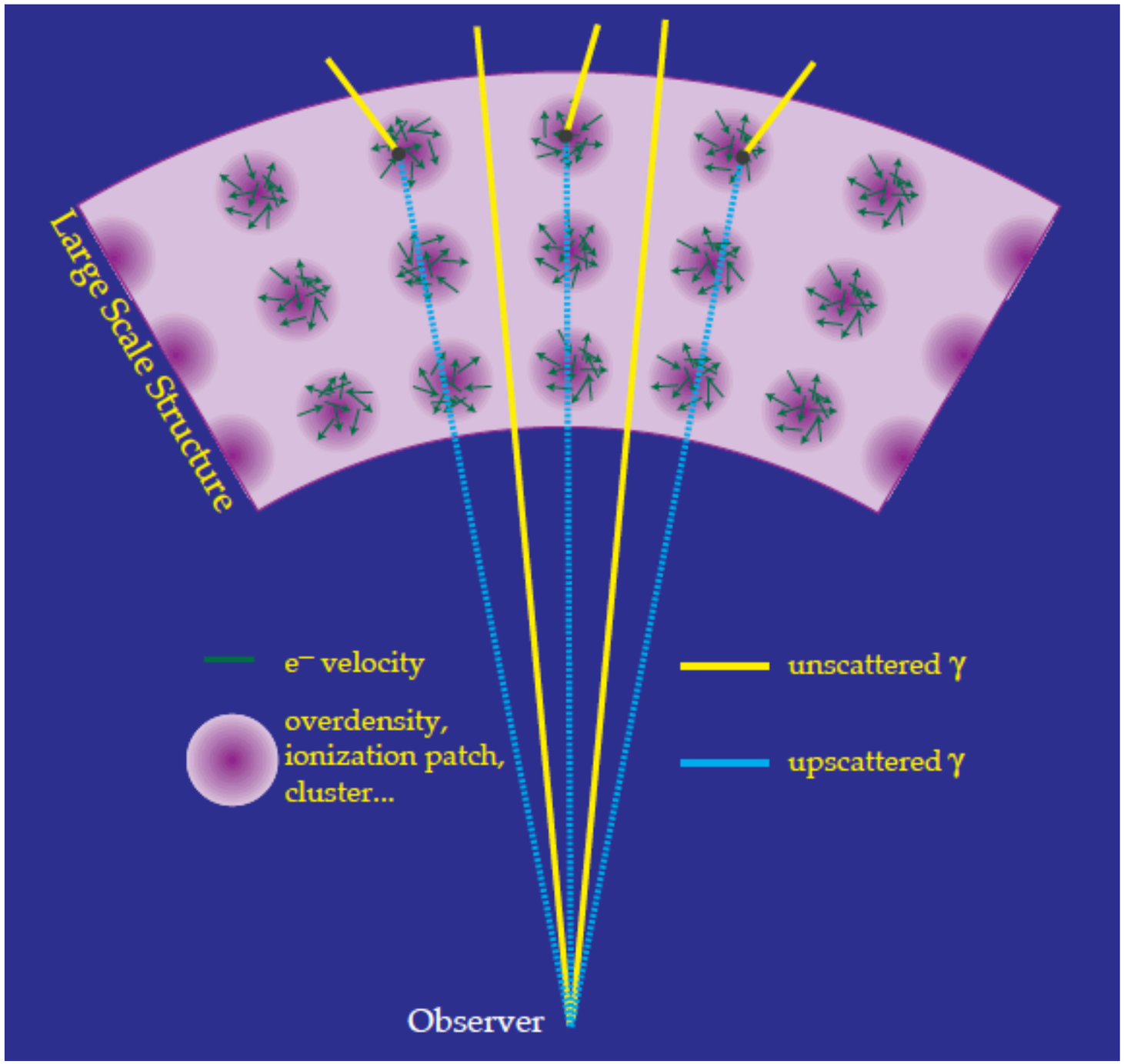

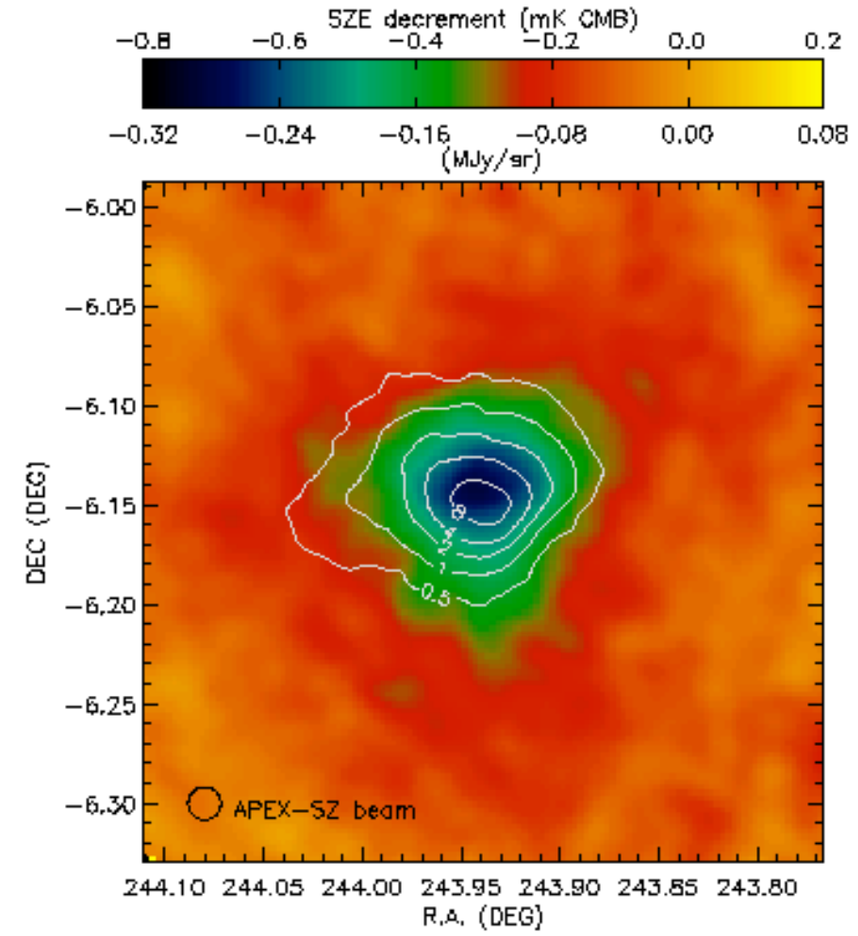

$$\frac{\Delta T}{T_{\rm CMB}} = -2y$$

$$y = \int n_{\rm e}(r)\sigma_{\rm T}\frac{k_{\rm B}T_{\rm e}(r)}{m_{\rm e}c^2}dl$$

SZ power spectrum

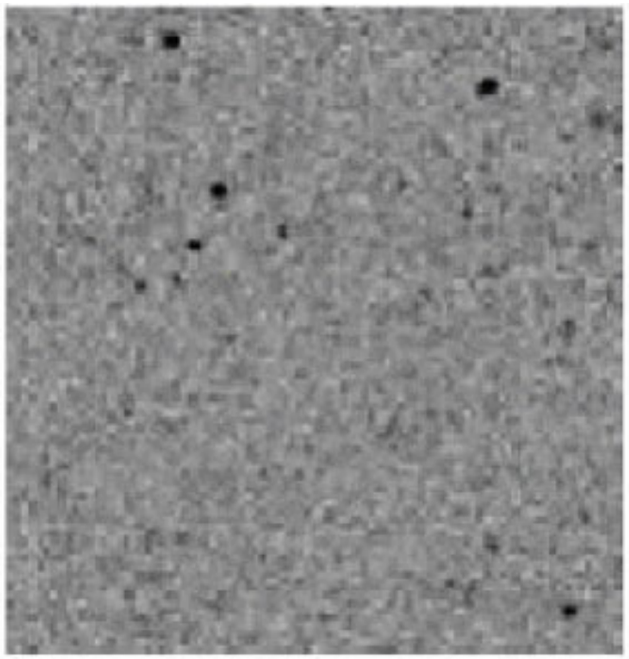

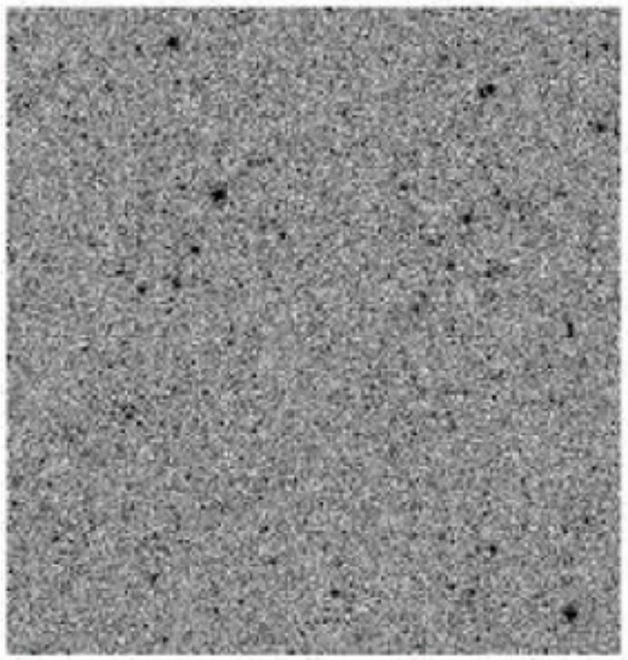

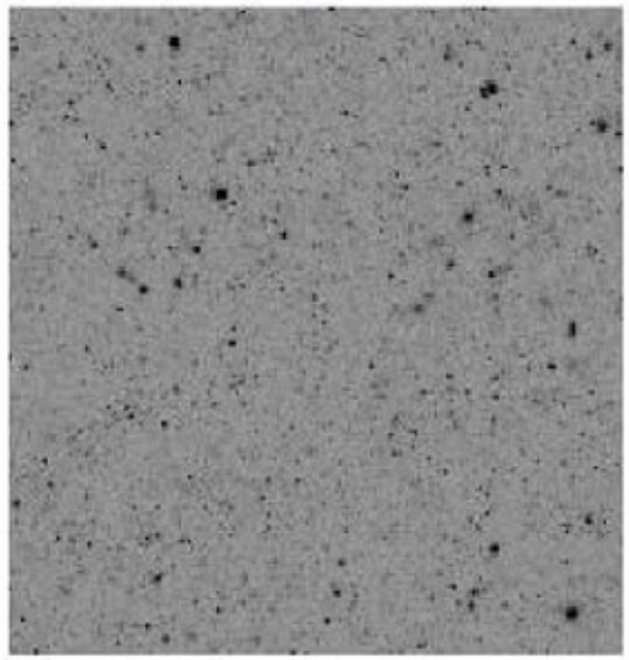

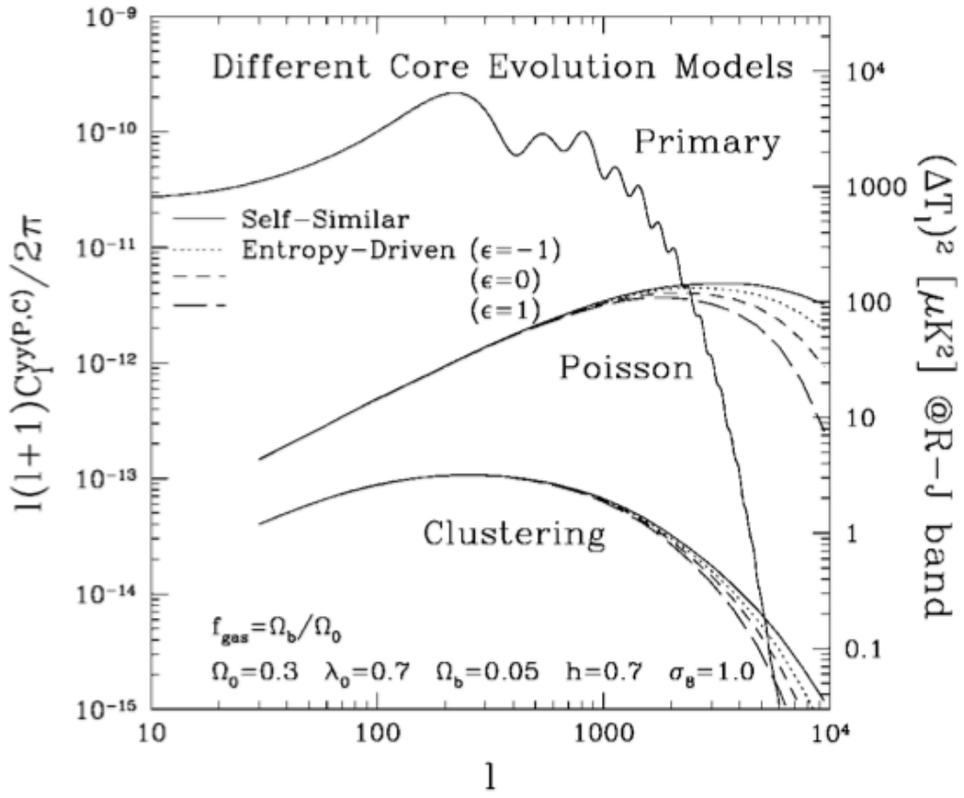

Komatsu & Kiayama (1999)

SZ power spectrum

SZ power spectrum is a powerful probe of cosmology, primarily through its strong dependance on σ_8

$$\frac{l(l+1)C_l}{2\pi} \simeq 330\ \mu\mathrm{K}^2\sigma_8^7\left(\frac{\Omega_\mathrm{b}h}{0.035}\right)^2$$

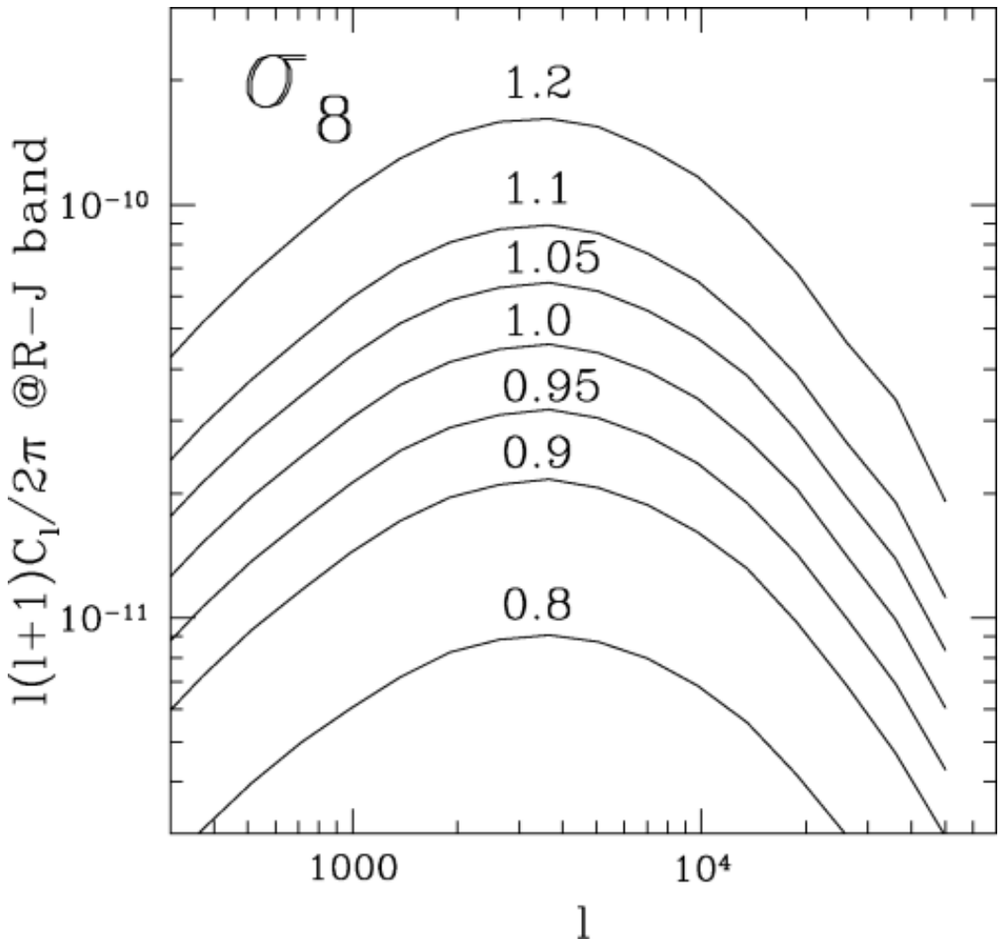

Text

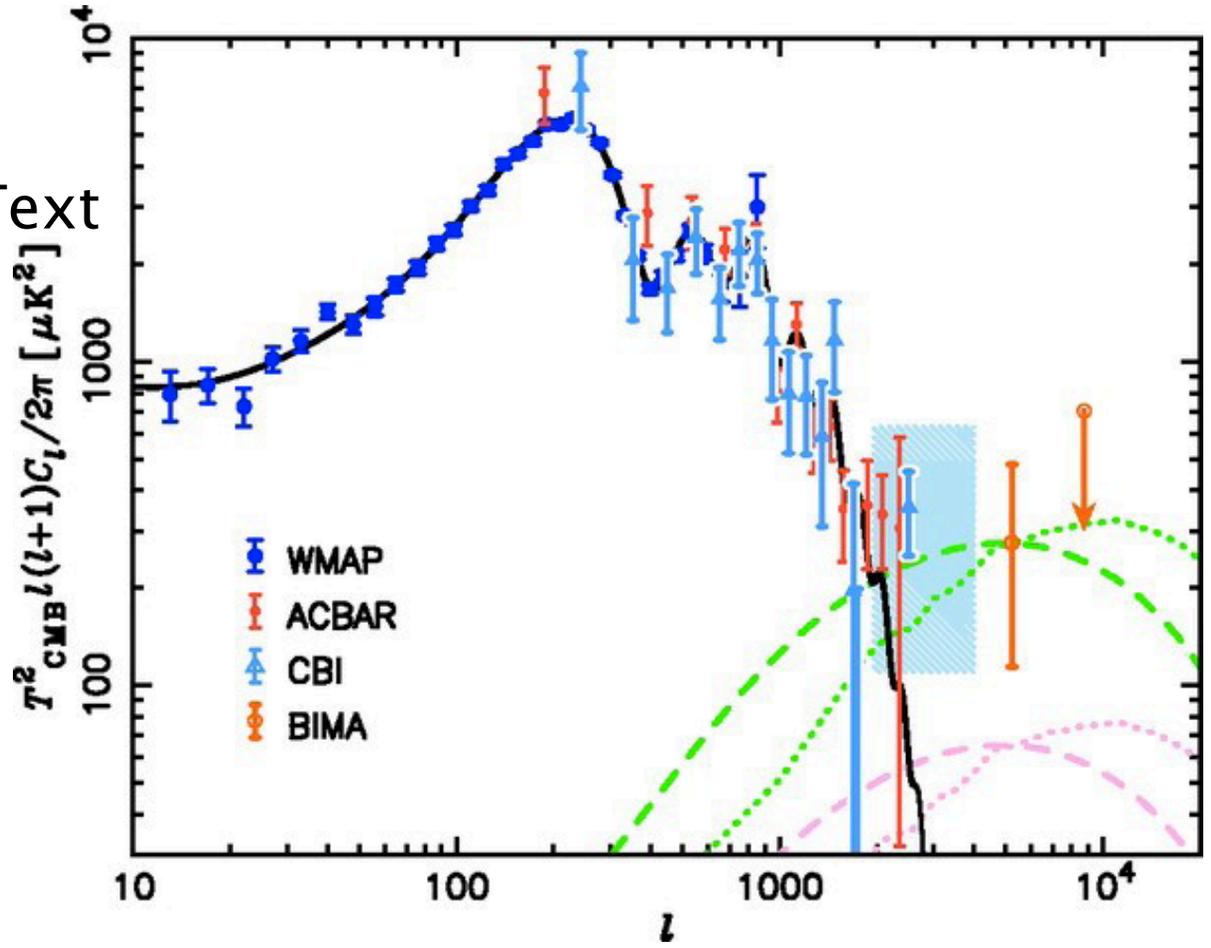

Lensing of the power spectrum

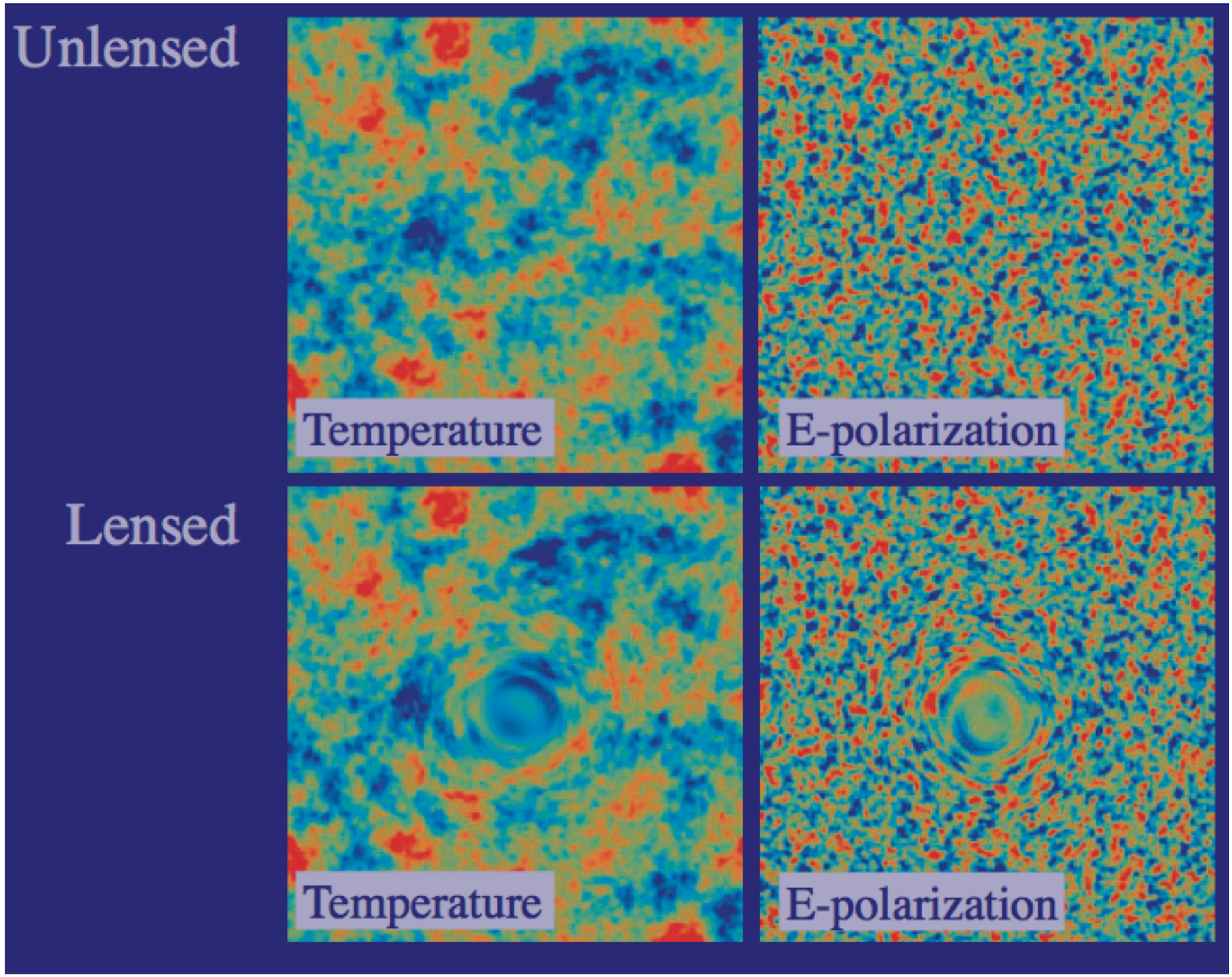

Lensing of the power spectrum

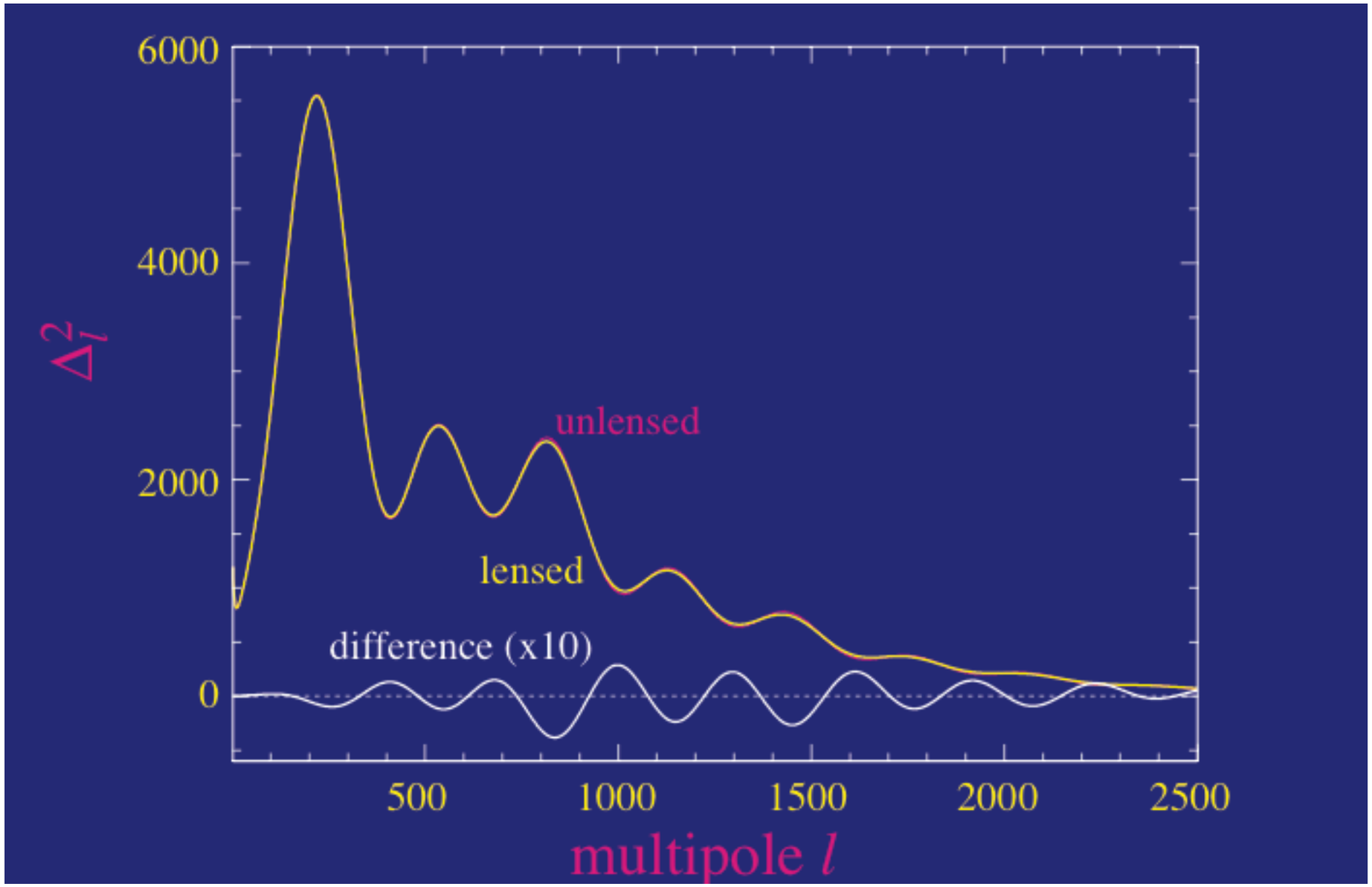

Lensing smooths the power spectrum (and E mode polarization) with a width Δl~60

This is a small effect, reaching ~10% deep in the damping tail.

Lensing measurement from SPT

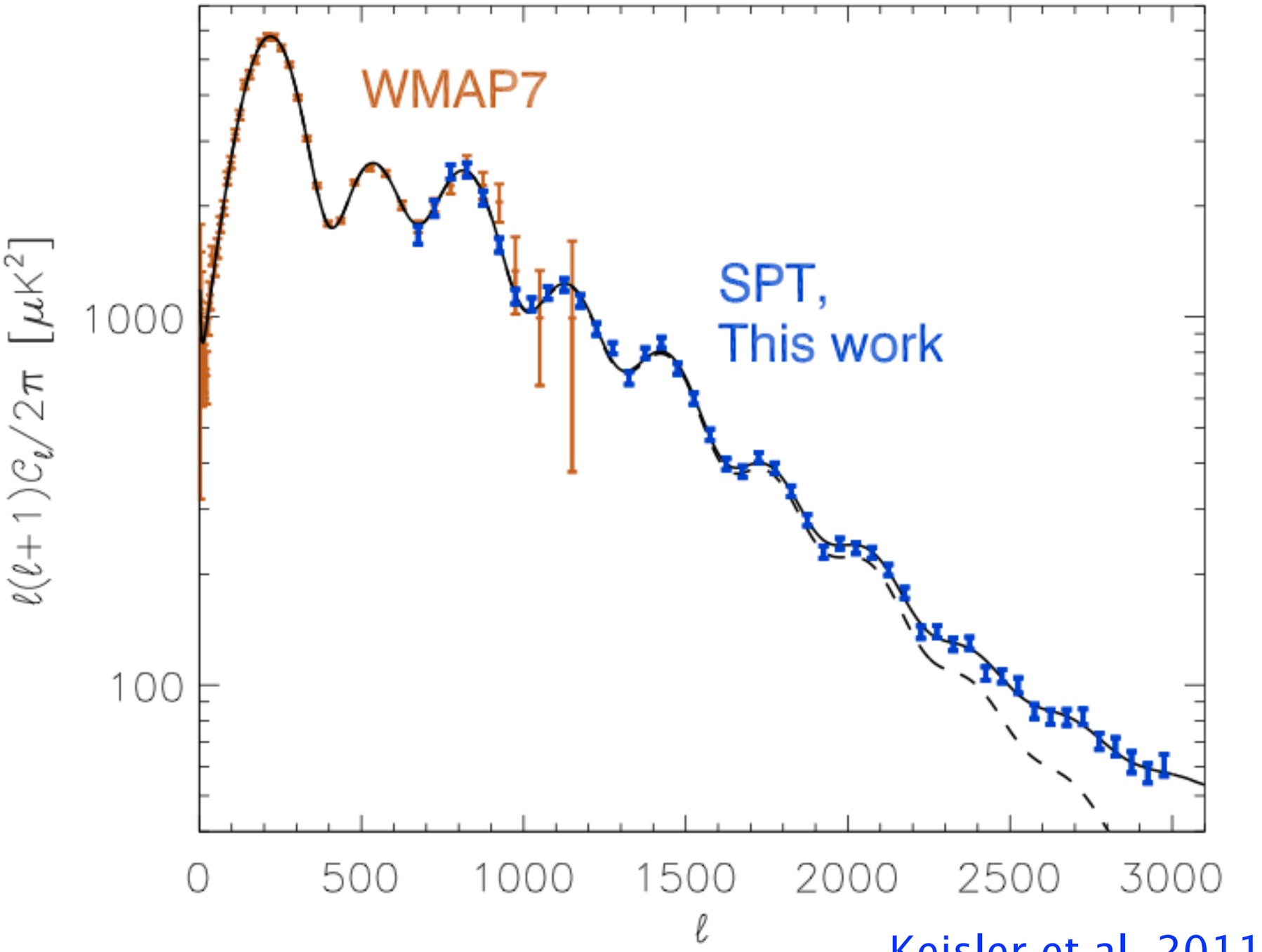

Keisler et al. 2011

Other small effects..

Resonant scattering by atoms and molecules (CMB spectroscopy!)

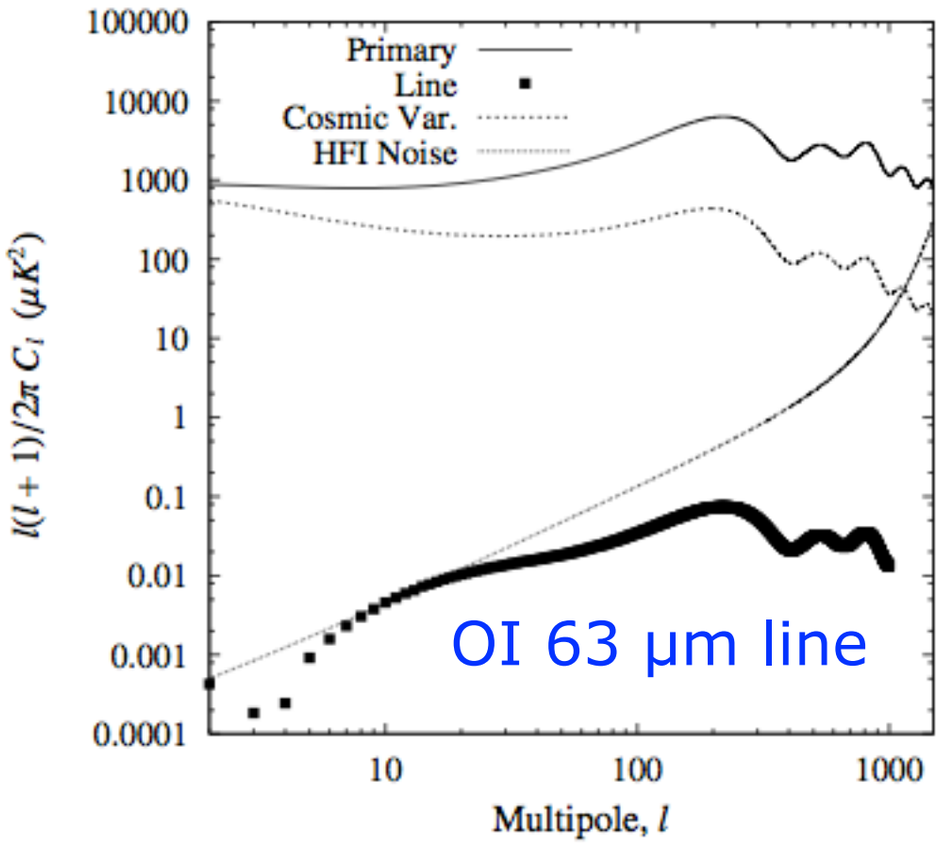

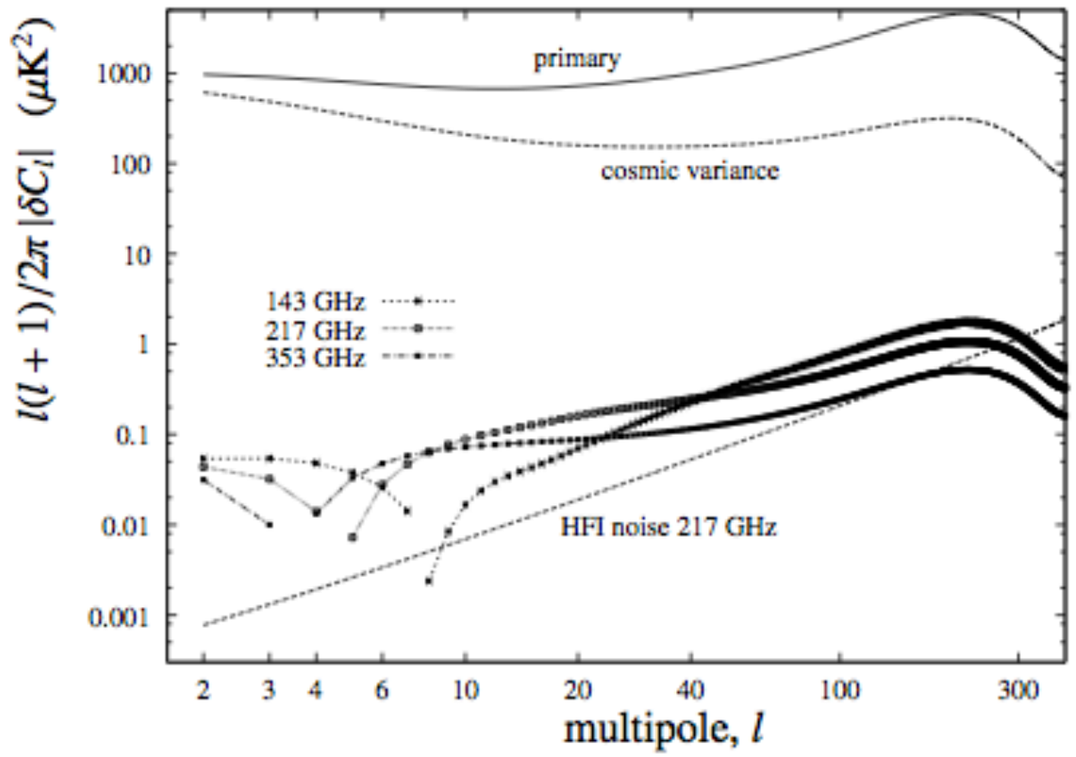

Basu, Hernandez-Monteagudo & Sunyaev 2004

$$\frac{\delta T}{T_0}(\boldsymbol{n}, z=0) = (1-\tau_{X_i})\ \frac{\delta T}{T_0}(\boldsymbol{n}, z_{X_i}) + \tau_{X_i}\ \frac{\delta T}{T_0}\Big|_{\rm new}^{\rm lin}(\boldsymbol{n}, z_{X_i}) + O\left[\tau_{X_i}^2\right].$$

$$\Rightarrow \quad \delta C_l \equiv C_l^{X_i} - C_l = \tau_{X_i}\cdot C_1 + \tau_{X_i}^2\cdot C_2 + O\left(\tau_{X_i}^3\right).$$

Power at small angular scales

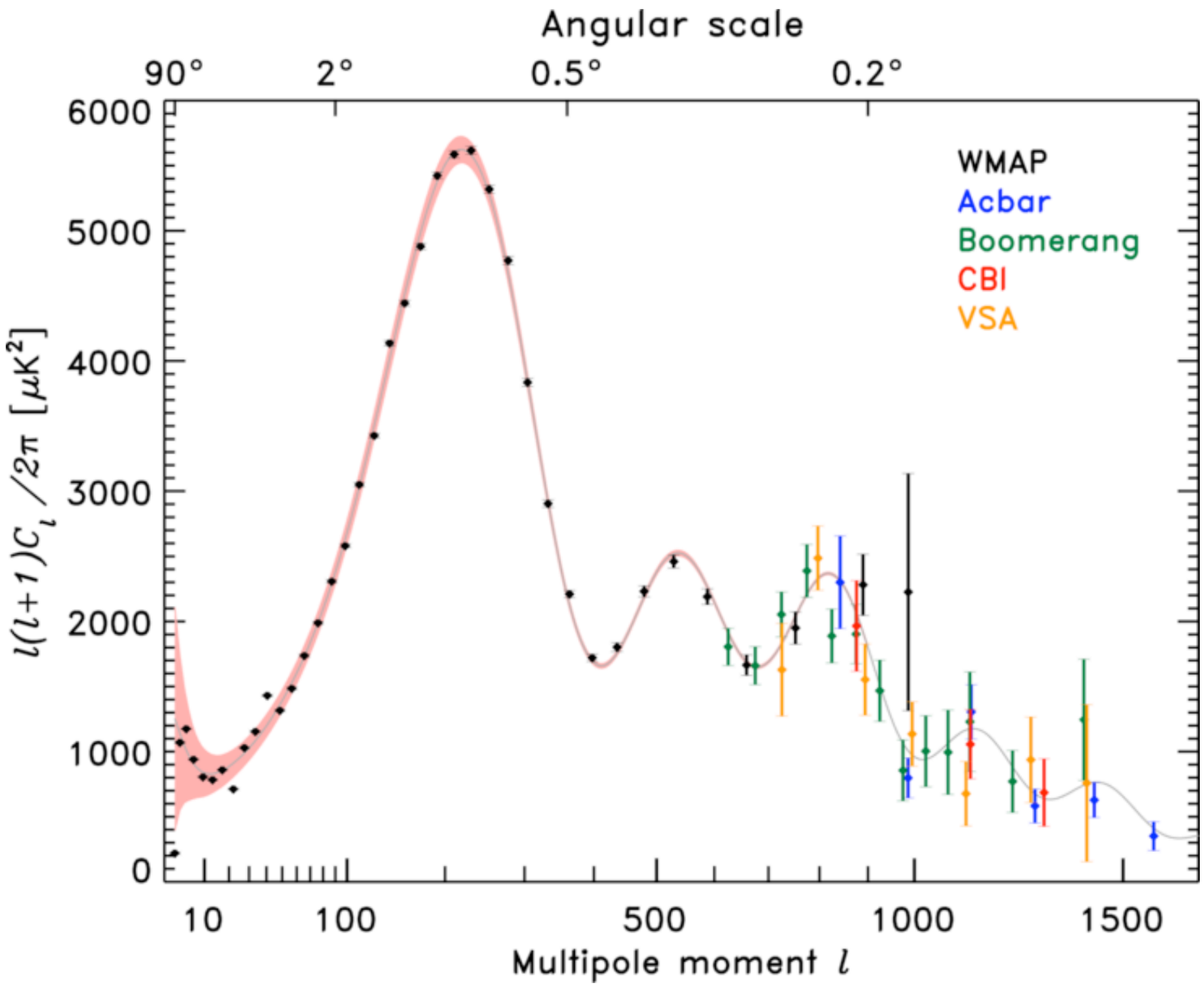

The signal is actually C_l! Our power spectrum plots boosts the apparent variance at large l by a factor l^2! Observations at high-l therefore requires far greater sensitivity.

Polarization of the CMB

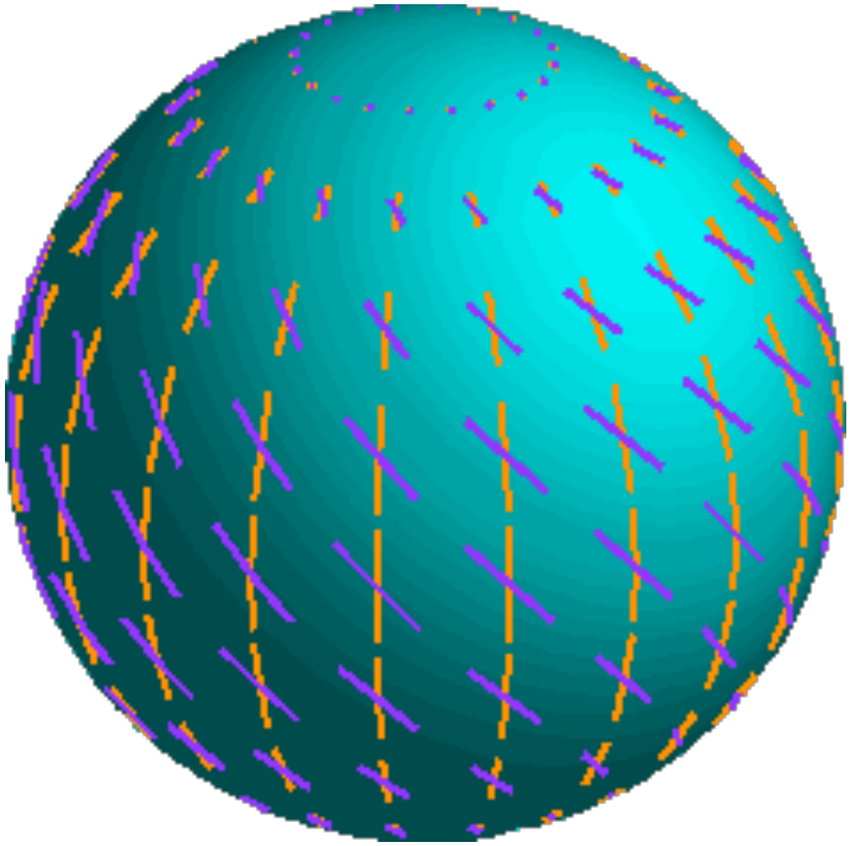

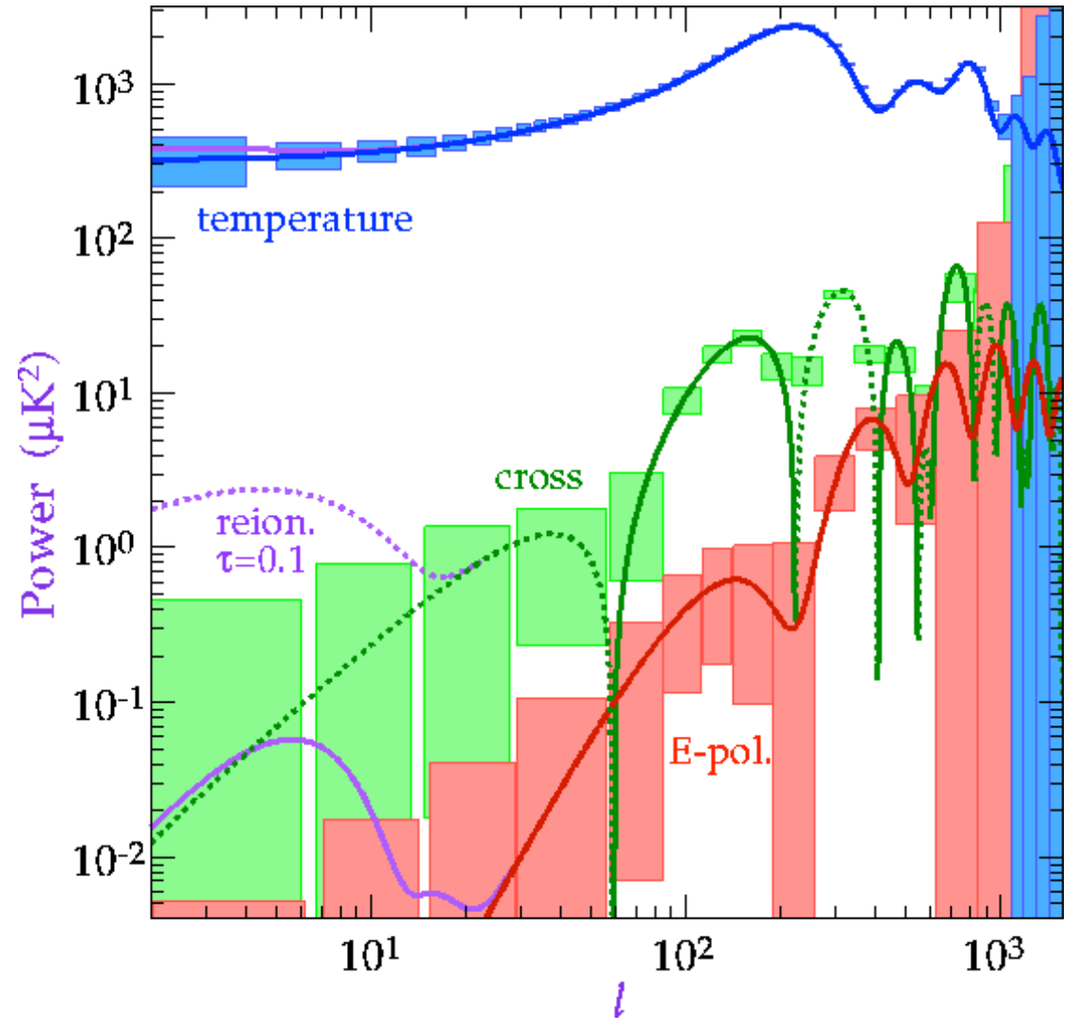

Detecting polarization is difficult!

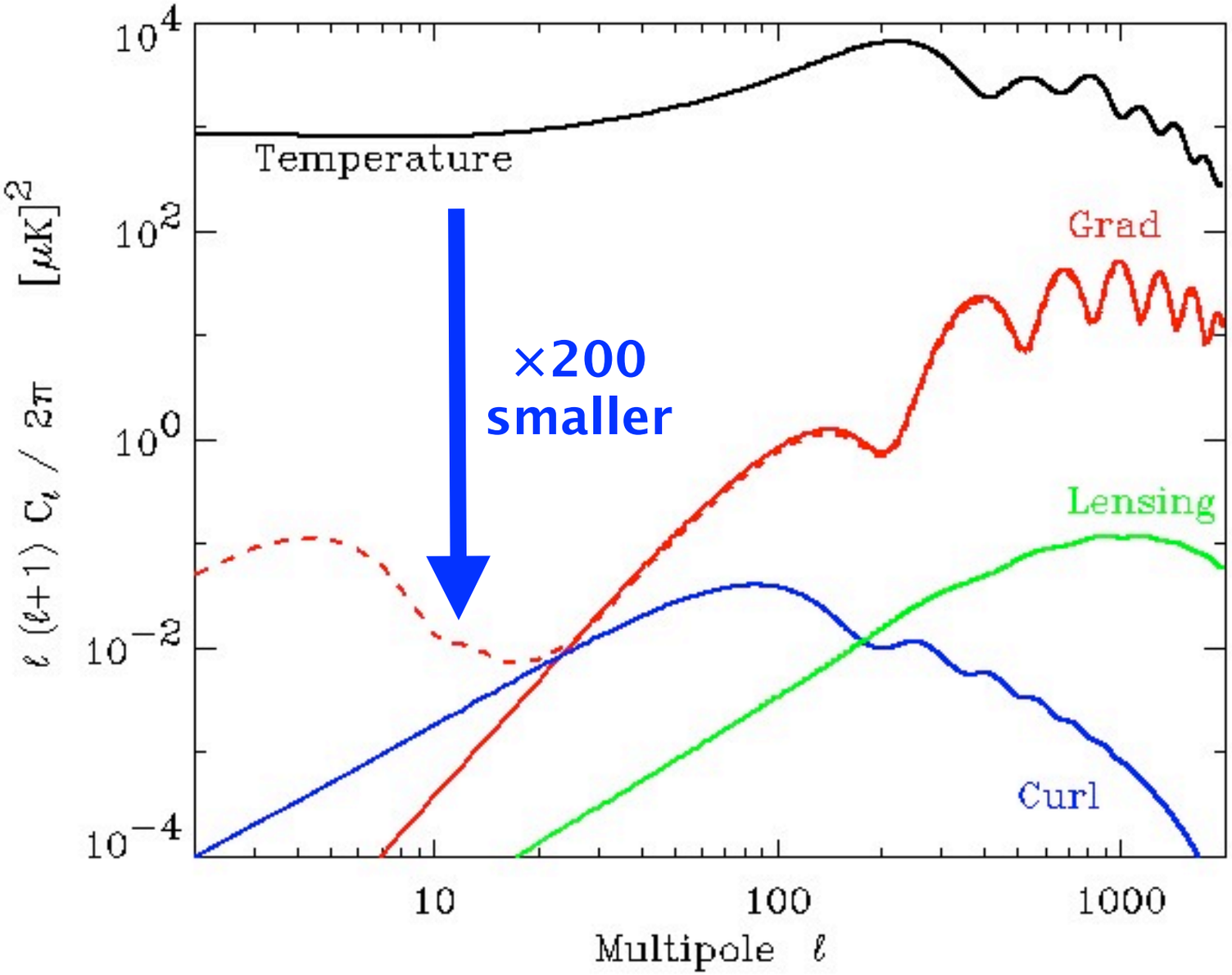

Power spectra of CMB temperature anisotropies (black), grad polarization (red), and curl polarization due to the GWB (blue) and due to the lensing of the grad mode (green), all assuming a standard CDM model with T/S = 0.28. The dashed curve indicates the effects of reionization on the grad mode for $\tau = 0.1$.

Quadrupole + Thomson scattering

Polarization is induced by Thomson scattering, either at decoupling or during a later epoch of reionization.
(No circular polarization, i.e. V=0)

$$P(\theta,\phi) \propto 1-\cos^2\theta$$

$$\frac{d\sigma}{d\Omega} = \left(\frac{e^2}{4\pi m c^2}\right)^2 |\hat{\epsilon}\cdot\hat{\epsilon}'|^2$$

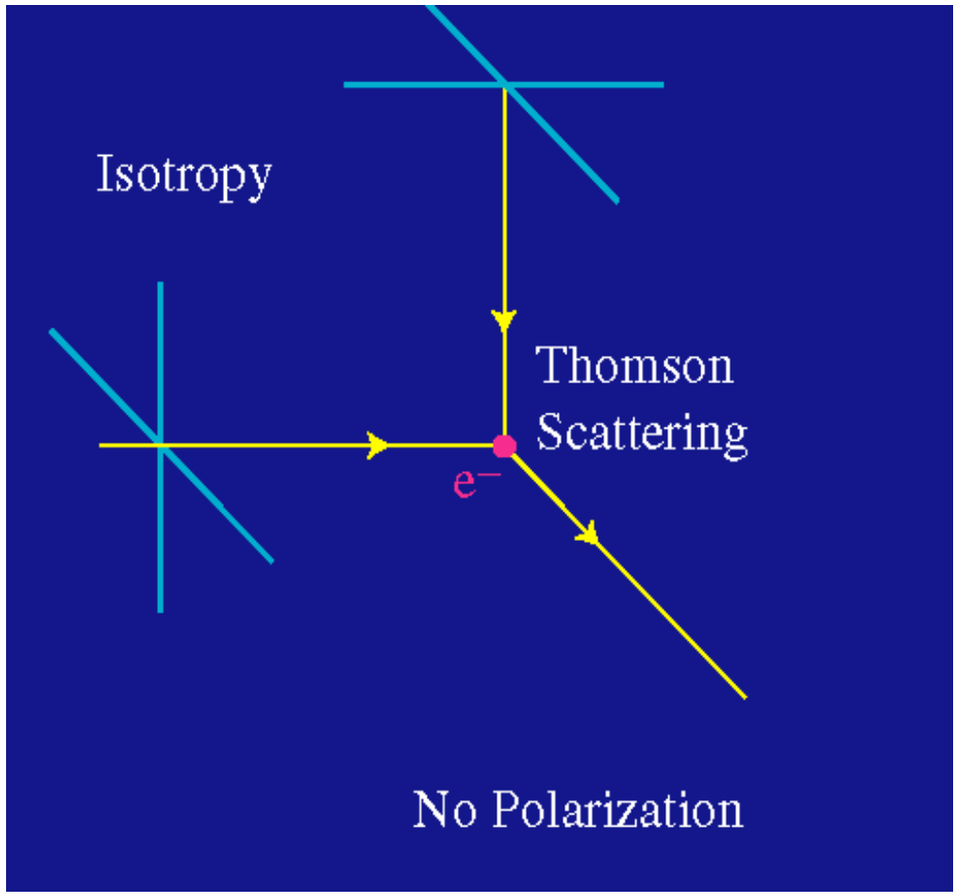

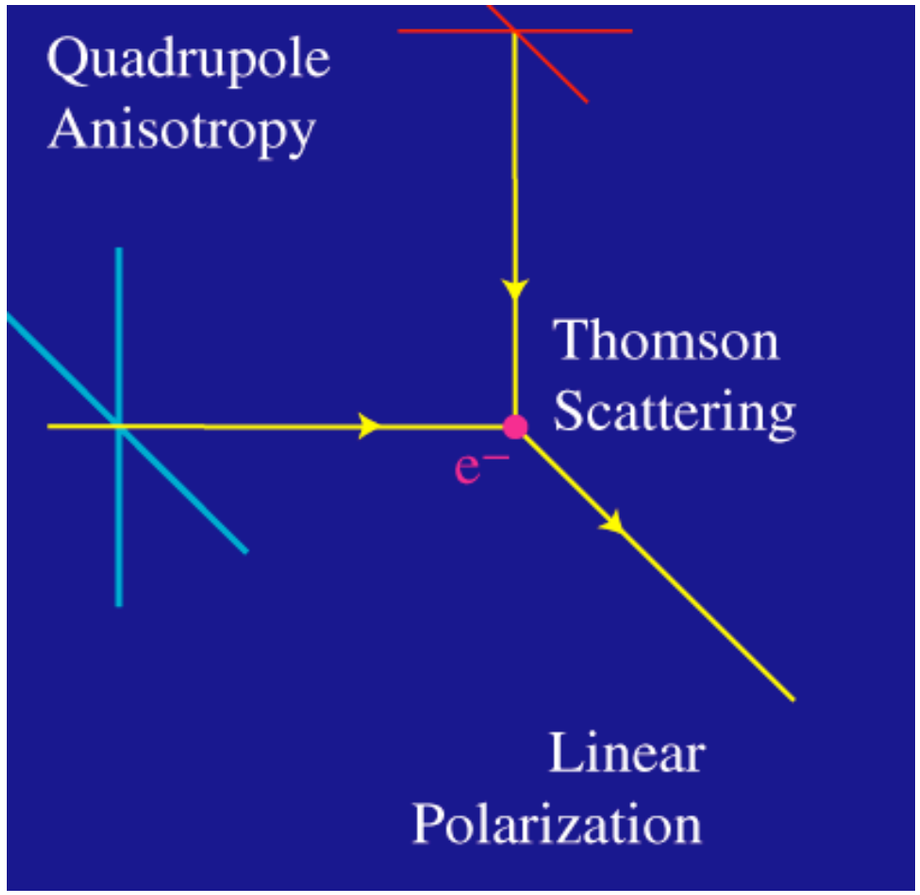

What causes the CMB quadrupole?

Two things:

"Normal" CDM: Density perturbations at z=1100 lead to velocities that create local quadrupoles seen by scattering electrons.

=> "E-mode polarization" (no curl)

Gravity waves: create local quadrupoles seen by scattering electrons.

=> "B-mode polarization" (curl)

Polarization power spectra

The polarization power also exhibits acoustic oscillations since the quadrupole anisotropies that generate it are themselves formed from the acoustic motion of the fluid.

The peaks are out of phase with TT peaks since polarization is maximum when the velocity field is maximum.

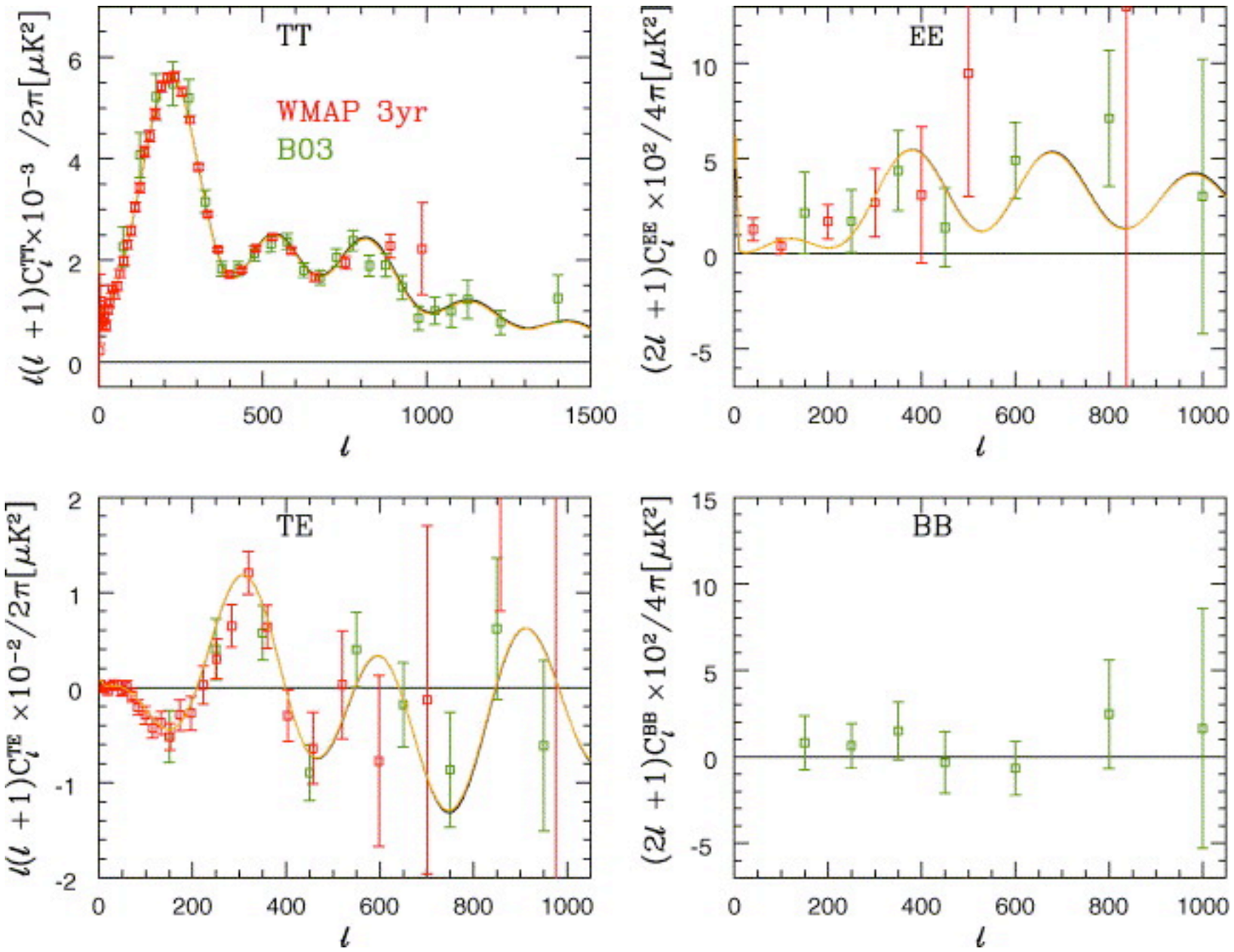

E and B modes

Two flavors of CMB polarization:

Density perturbations: curl-free, "E-mode"
Gravity waves: curl, "B-mode"

E-mode

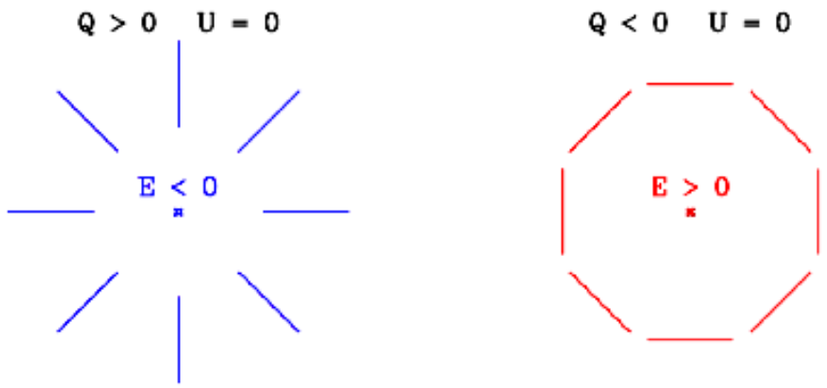

B-mode

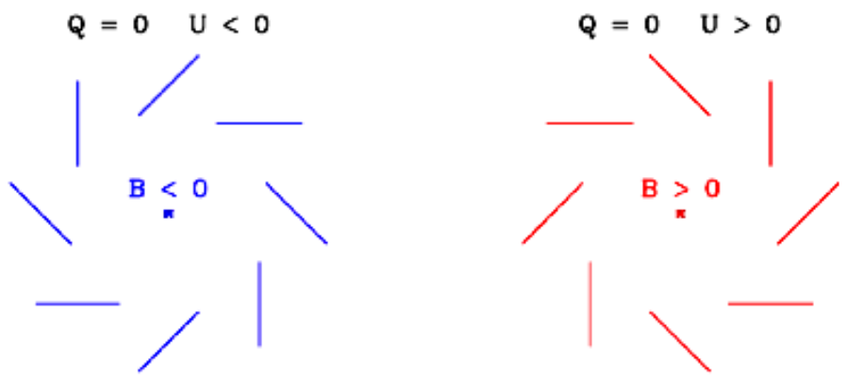

- We can break down the polarization field into two components which we call E and B modes. This is the spin-2 analog of the gradient/curl decomposition of a vector field.

- E modes are generated by density (scalar) perturbations via Thomson scattering.

- B modes are generated by gravity waves (tensor perturbations) at last scattering or by gravitational lensing (which transforms E modes into B modes along the line of sight to us) later on.

Polarization power spectra

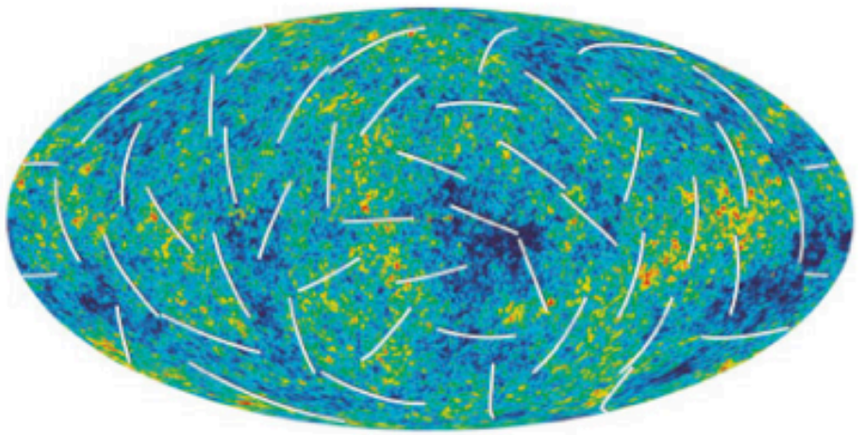

Temperature field $\Delta T(\mathbf{n})$

In Fourier space:

$$T(\mathbf{l}) = \int d^2\mathbf{n}\, T(\mathbf{n}) e^{i\mathbf{l}\cdot\mathbf{n}}$$

Polarization fields $Q(\mathbf{n})$, $U(\mathbf{n})$

E-B decomposition:

$$\begin{pmatrix} E(\mathbf{l}) \\ B(\mathbf{l}) \end{pmatrix} = \begin{pmatrix} \cos(2\varphi_l) & \sin(2\varphi_l) \\ -\sin(2\varphi_l) & \cos(2\varphi_l) \end{pmatrix} \begin{pmatrix} Q(\mathbf{l}) \\ U(\mathbf{l}) \end{pmatrix}$$

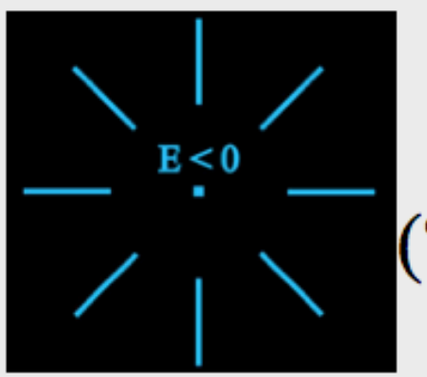

E-mode
("gradient-like")

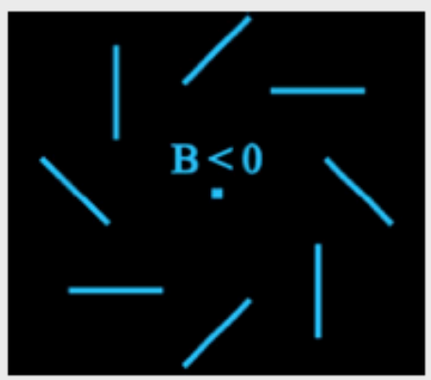

B-mode
("curl-like")

Polarization pattern

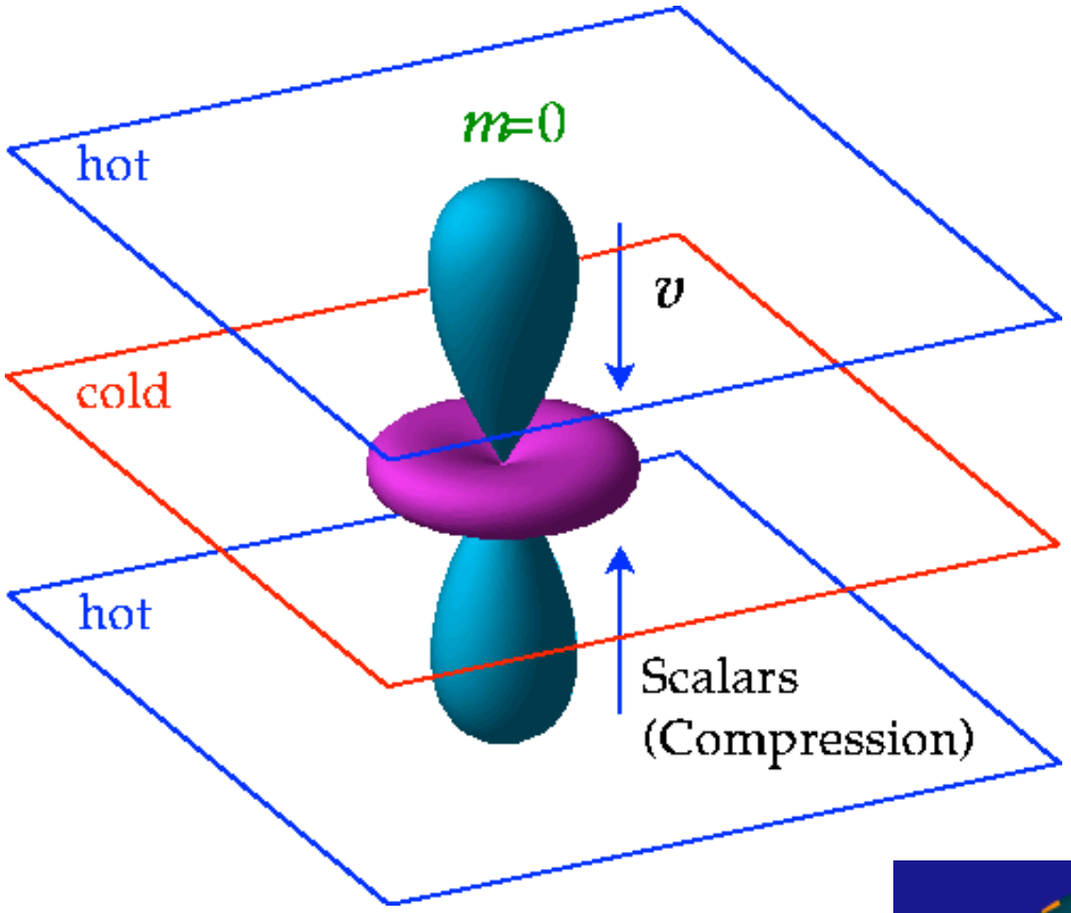

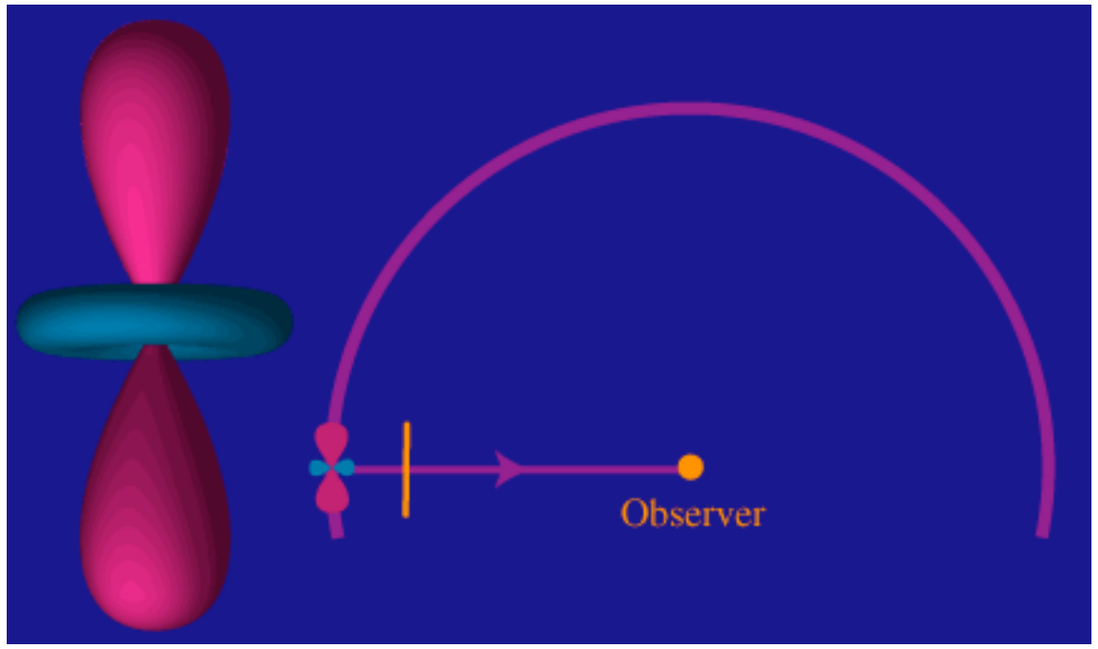

The scaler quadrupole moment, l=2, m=0. Note the azimuthal symmetry in the transformation of this quadrupole anisotropy into linear polarization.

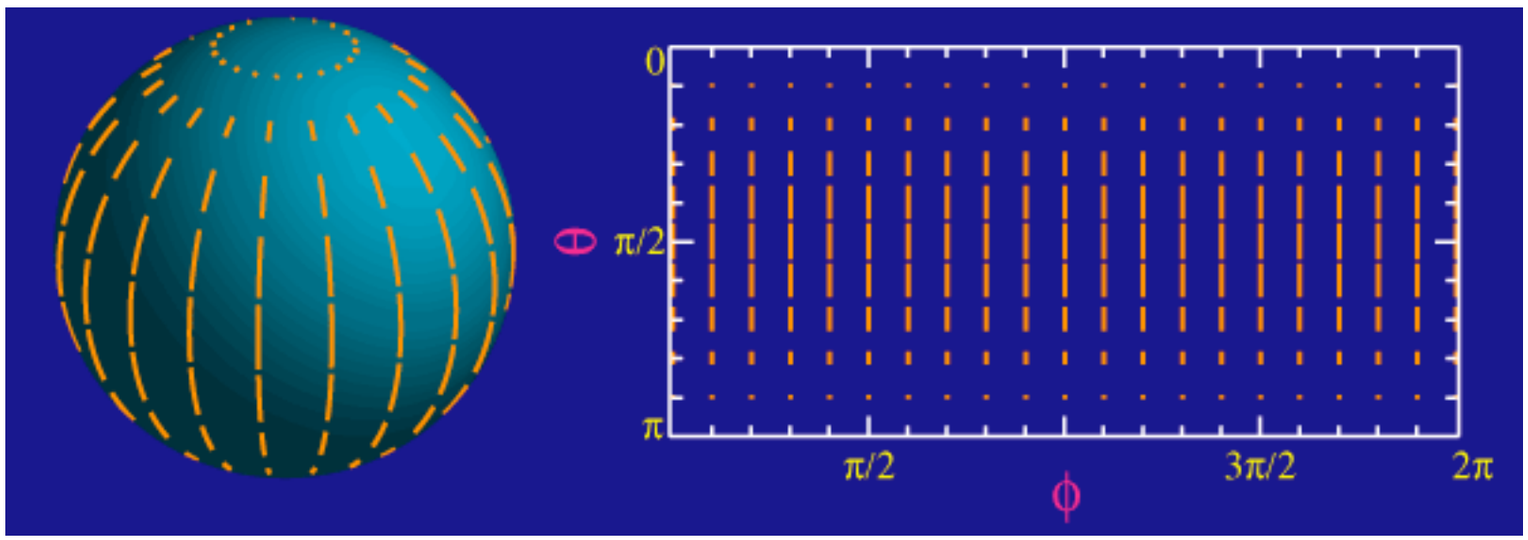

Polarization pattern

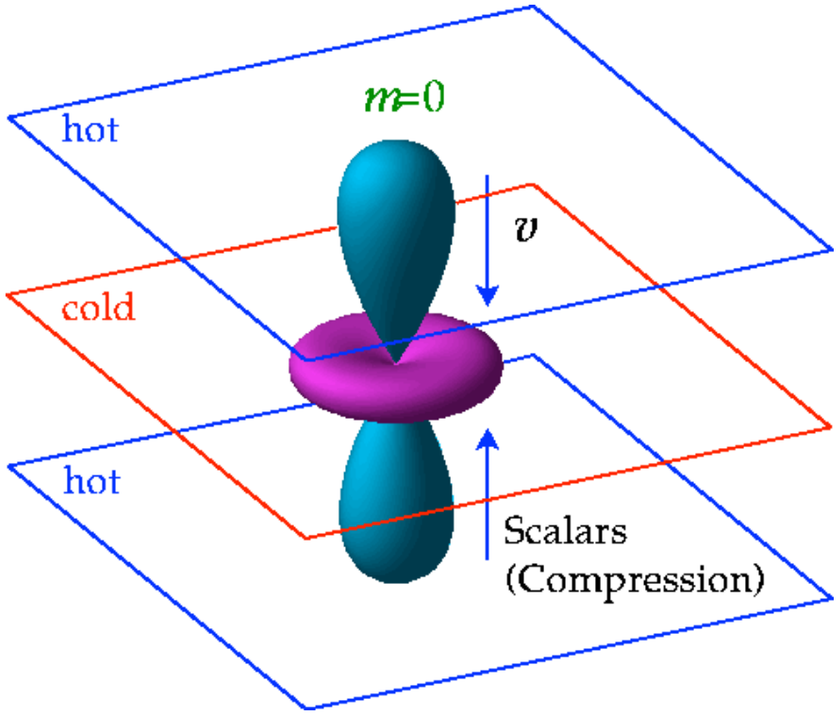

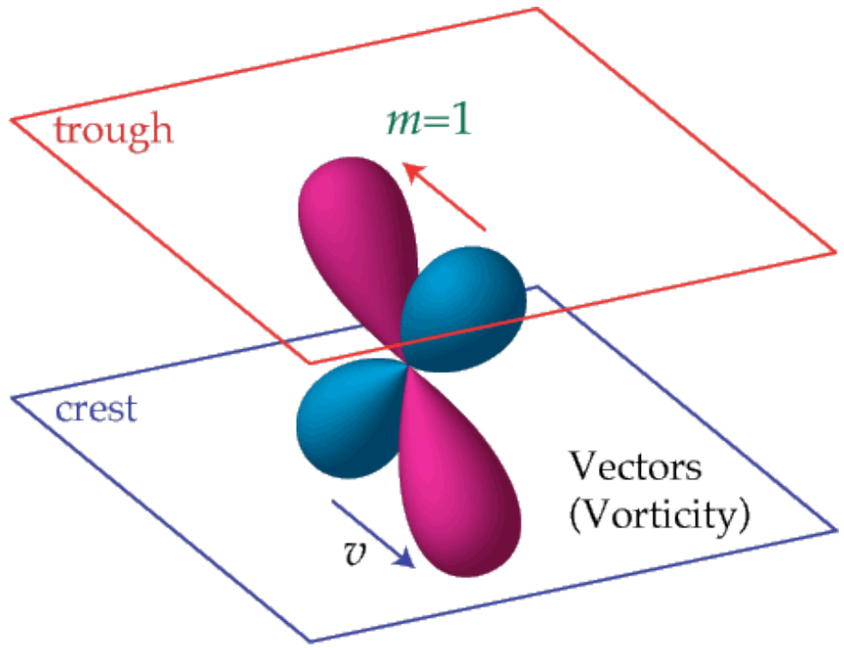

In general there are three sources to the quadrupole anisotropy at recombination:

- scalers (m=0) for density fluctuations
- vectors (m=1) for vorticity *(negligible)*
- tensors (m=2) for gravity waves

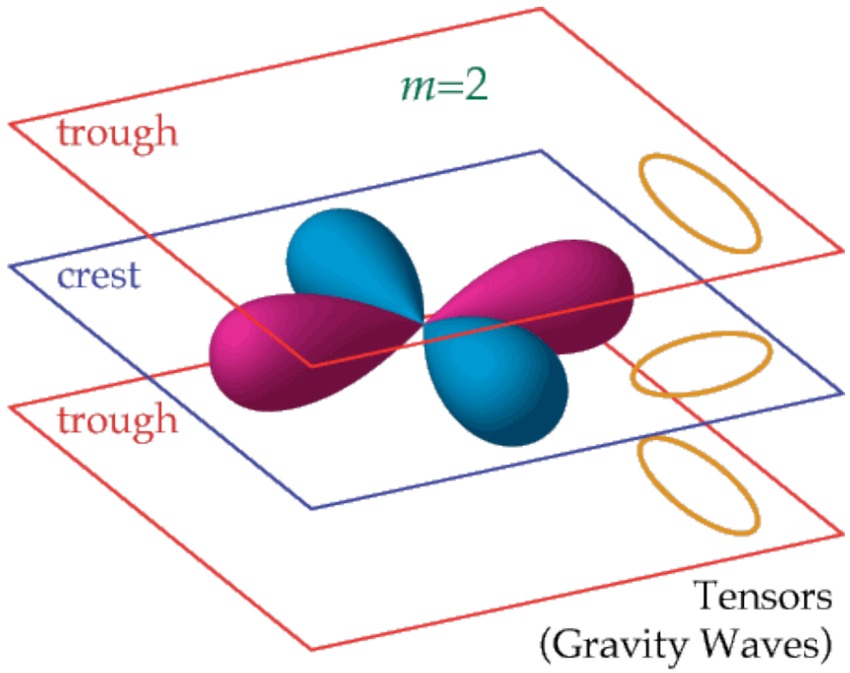

Parity of E & B modes

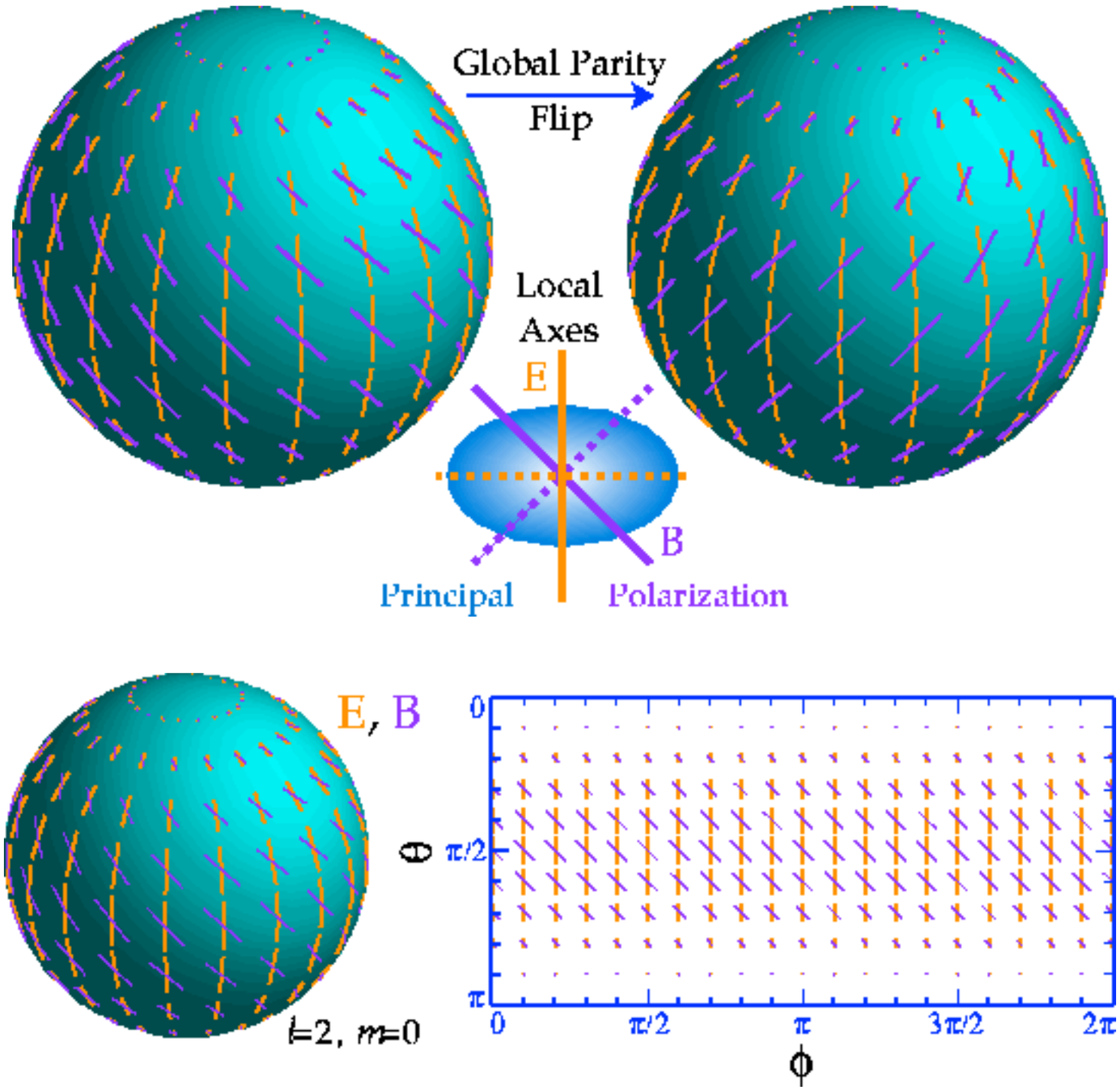

Polarization power spectra

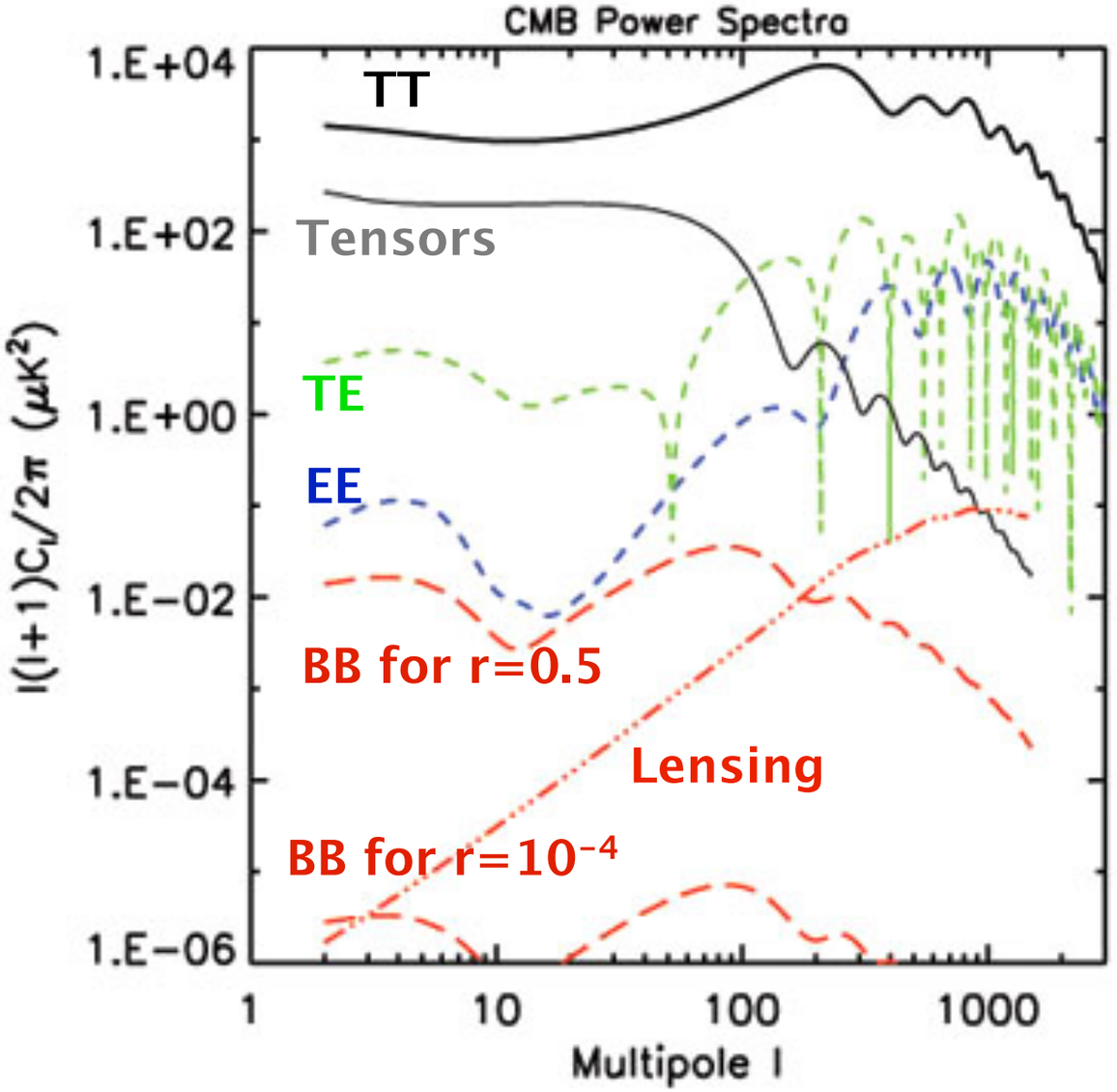

r = T/S: Tensor to scaler ratio, generated by the primordial gravity waves at last scattering

E & B modes have different reflection properties ("parities"):

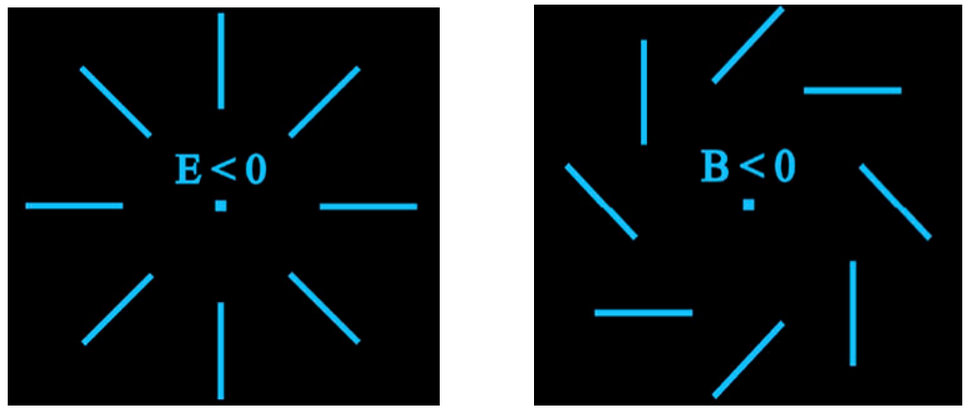

Parity: $(-1)^l$ for E and $(-1)^{l+1}$ for B

The cross-correlation between B and E or B and T vanishes (unless there are parity-violating interactions), because B has opposite parity to T or E.

We are therefore left with 4 fundamental observables.

Shape of the power spectra

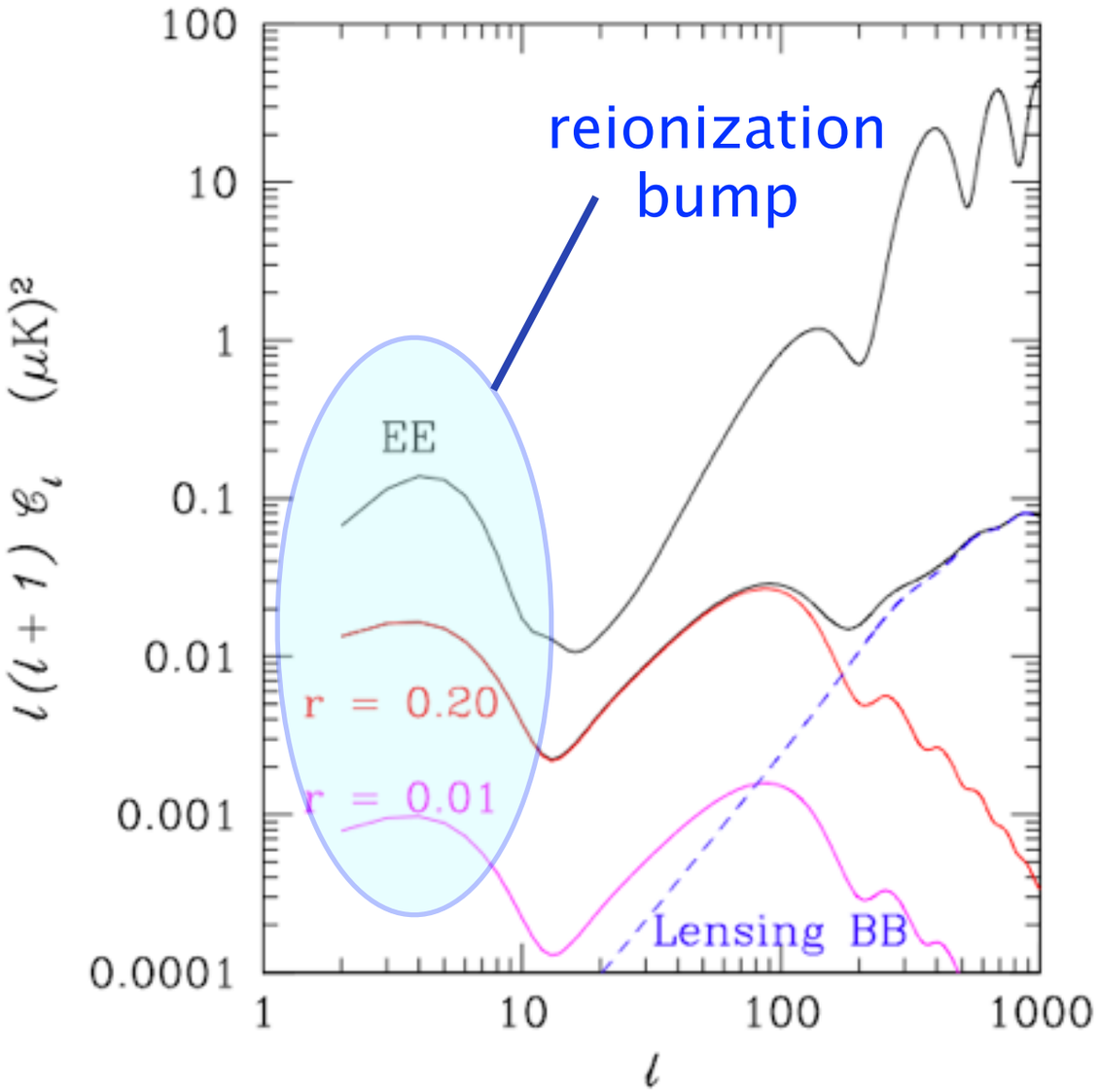

- The primordial B-mode signal (due to a stochastic background of gravitational waves) dominates only at intermediate angular scales

- On very large scales, the polarization signal is dominated by secondary fluctuations imprinted by reionization

- The lens-generated signal grows at smaller scales

Shape and amplitude of EE are predicted by ΛCDM.

Shape of BB is predicted "scale-invariant gravity waves".

Amplitude of BB is model dependent, and not really constrained from theory.
Measuring this amplitude would provide a direct handle of the energy scale of inflation!

EE power spectrum

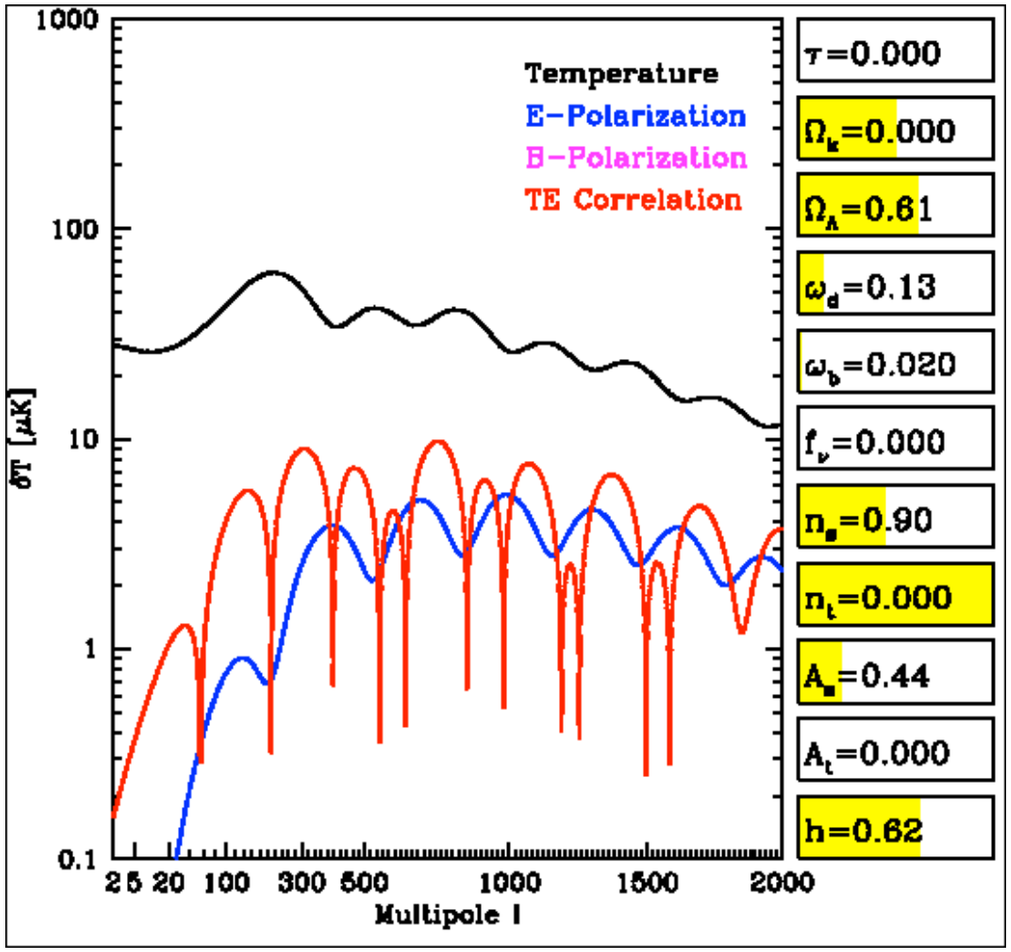

MCMC simulations from K. Vanderlinde

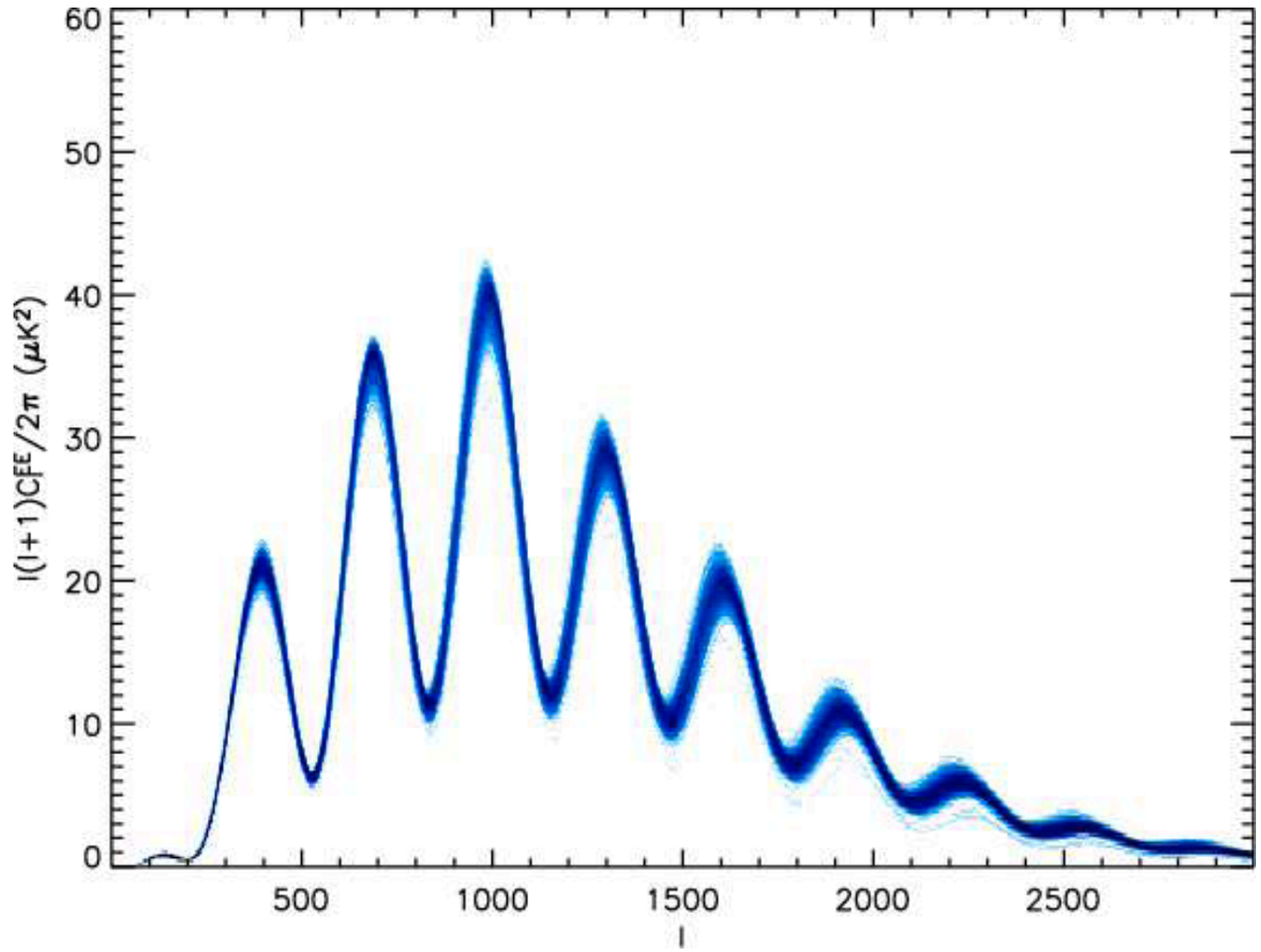

- Most parameters already well measured from TT.
- EE spectrum is a fundamental check on our understanding.
- EE is also sensitive to nonstandard model effects

(e.g. isocurvature)

BB spectrum uncertainties

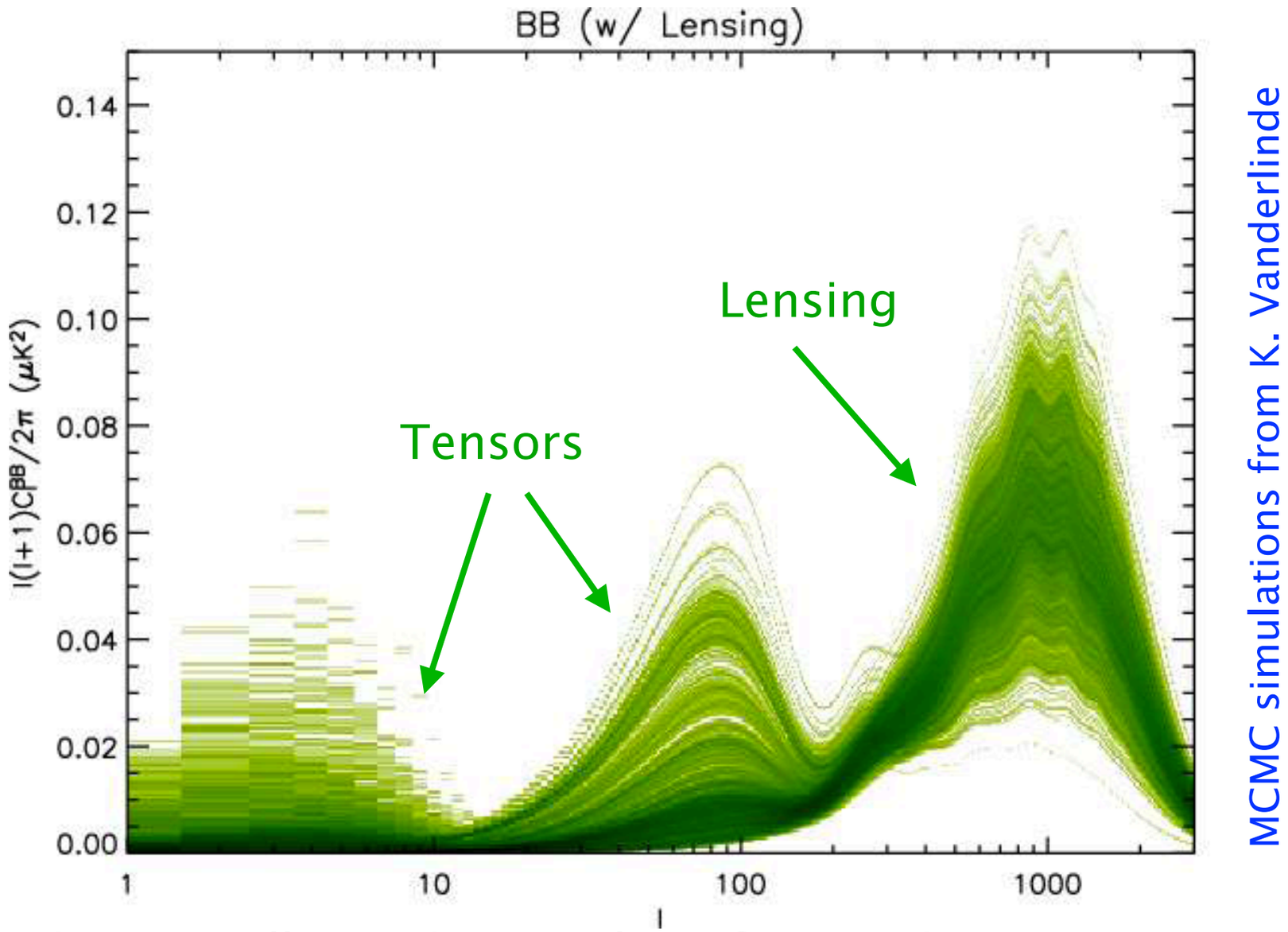

BB mode can tell us about a lot of new physics (energy scale at inflation, neutrino mass, etc.), but its prediction is still very uncertain.

Current data only puts the limit r = T/S < 0.2

Detection of polarization

- The DASI experiment at the South Pole was the first to detect E-mode CMB polarization
- It was followed by WMAP's measurement of $C^{TE}(l)$ for $l<500$
- Both the BOOMERANG and the CBI experiments have reported measurements of C^{TT}, C^{TE}, C^{EE} and a non-detection of B modes
- E-mode has also been measured by CAPMAP and Maxipol
- B-mode polarization has not been detected yet (current noise level is 50 K at the arcmin scale, future ground-based experiment will go down to 5 K)

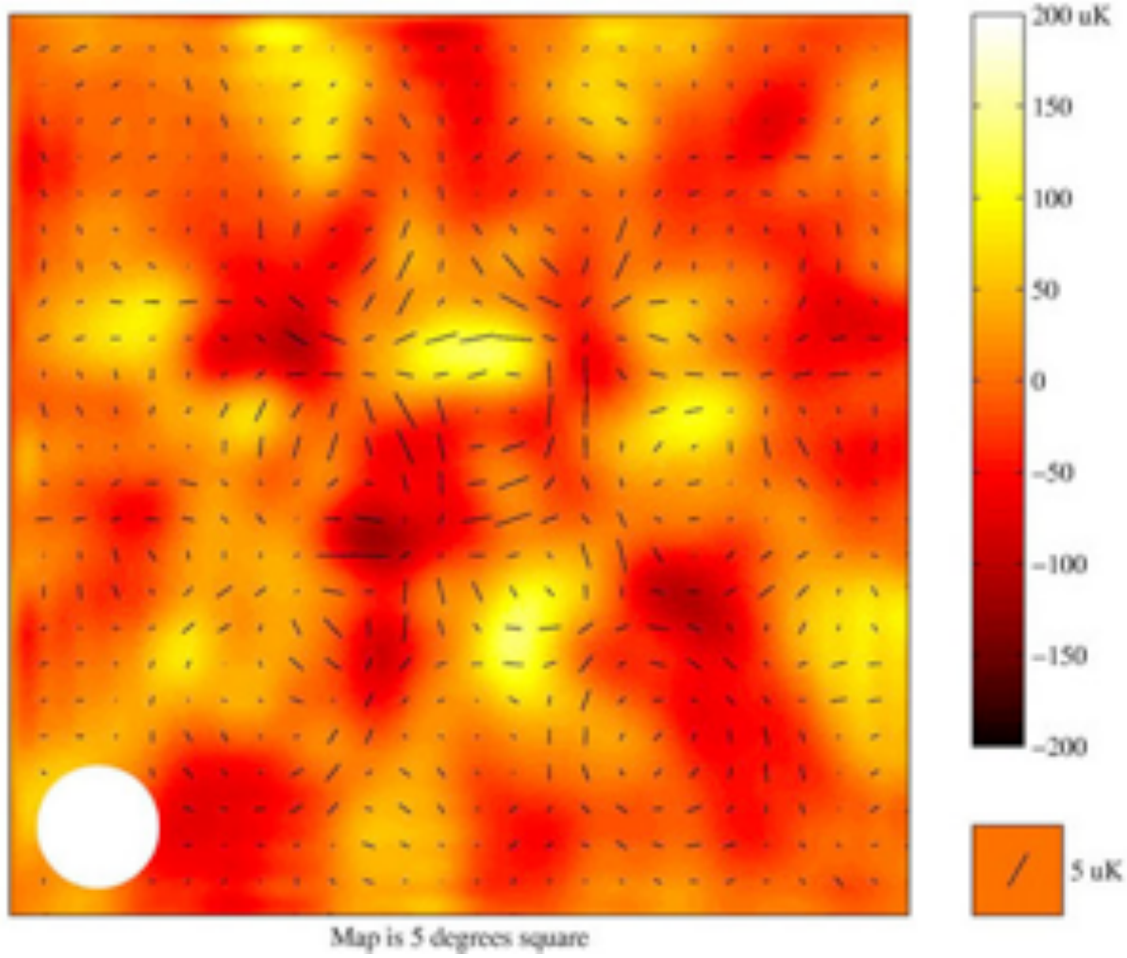

DASI collaboration, 2002

Current status

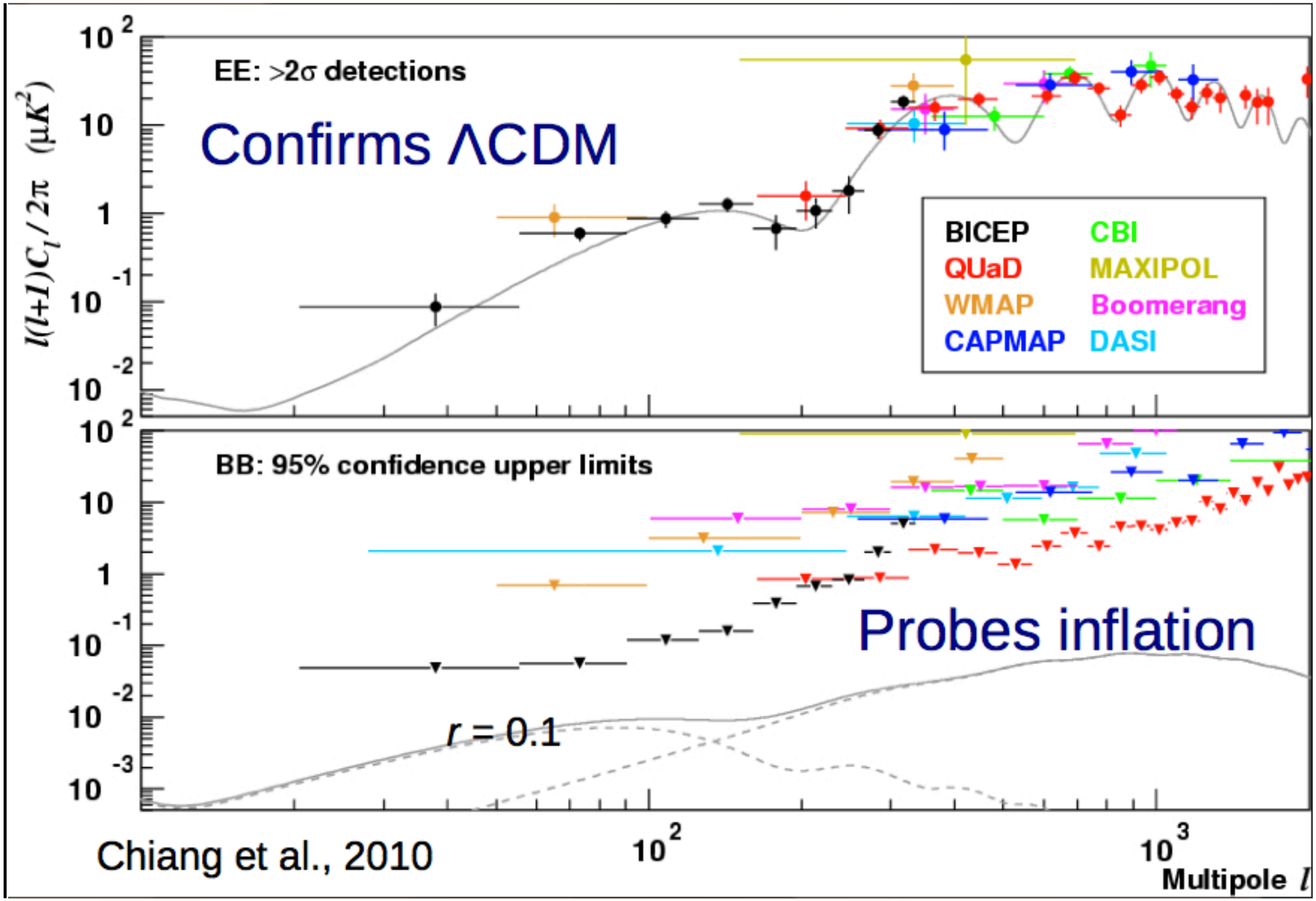

WMAP measurement

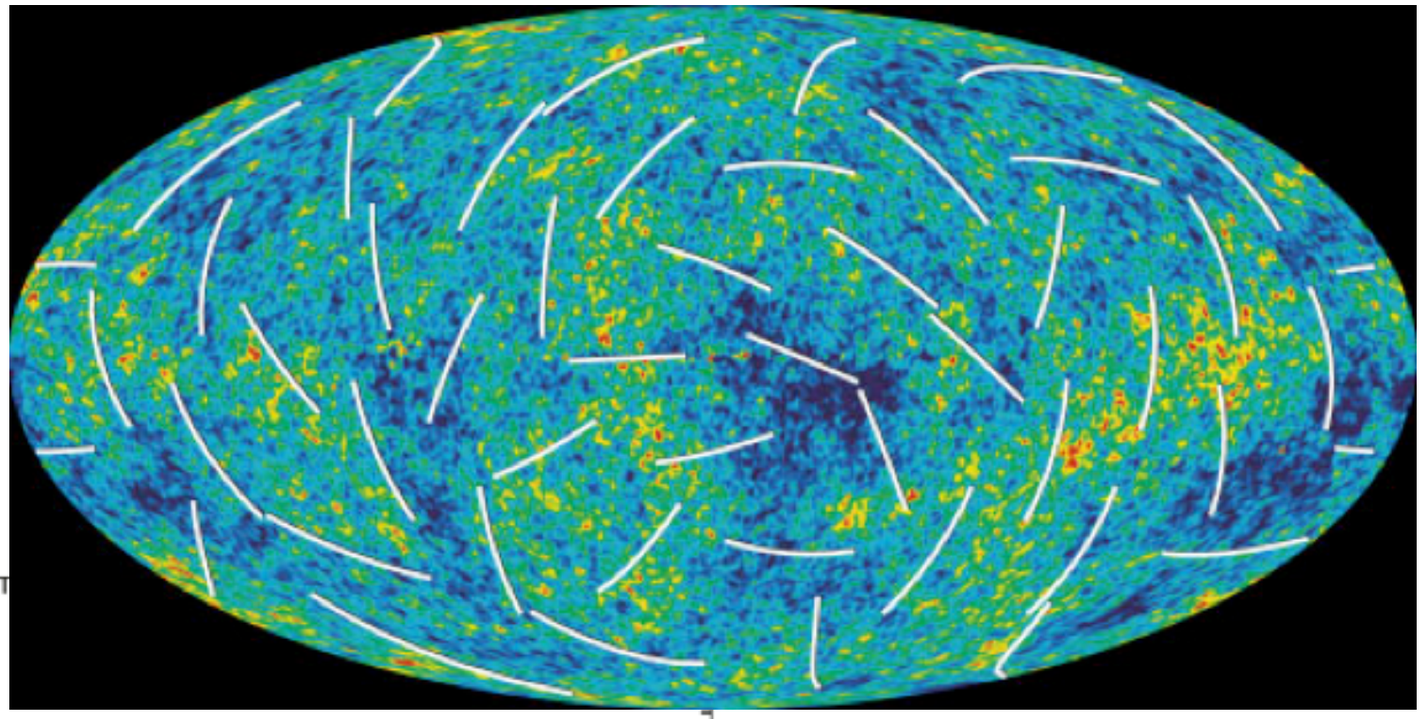

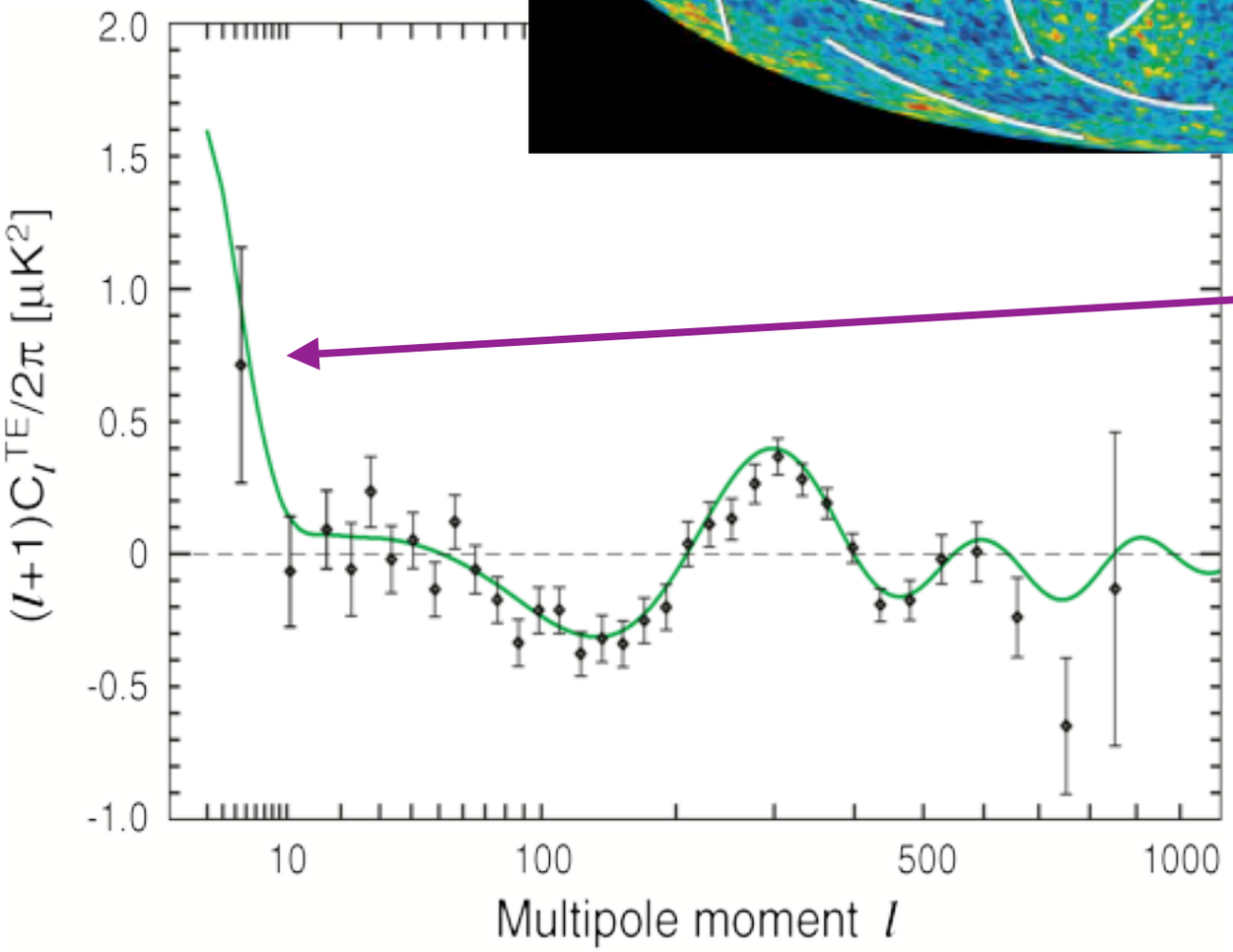

Re-scattering of the CMB photons during and after reionization added to the polarized power on large angular scales

(scale comparable to the horizon, H^{-1}, at the epoch of scattering)

List of polarization experiments

(slightly outdated)

Table 1. Current and Pending CMB Polarization Experiments

Experiment	Frequencies in GHz(# of pixels)	Beamsize	Site	Technique
CAPMAP	40 (4), 90 (10)	13', 6'	NJ	Correl. rad. array
DASI	30 (13)	20'	S. Pole	Interferometer
CBI	30 (13)	3'	Atacama	Interferometer
ATCA	8.7 (5)	2'	Australia	Interferometer
AMiBA	90 (19)	2'	M. Loa	Interferometer
Polatron	90 (1)	2'	OVRO	Bolo, halfwave plate
QUEST	100, 150 ($\approx$ 30)	6'	M. Kea	Bolo array, halfwave plate
POLARBEAR	150 (3000 dt'rs)	10'	TBD	Bolo array
Boom2K1	150(4), 240(40), 340(4)	10'	Antarctic LDB	Bolo array
MAXIPOL	150 (12), 420 (4)	10'	US-Balloon	Bolo array, cold halfwave plate
BaR-SPOrt	32, 90	30', 12'	Antarctic LDB	Correl. rad. array
MAP	22, 30, 40(2), 60(2), 90(4)	13'	L2, full-sky	Correl. rad. array
SPOrt	22, 32, 60, 90	7°	ISS, full-sky	Correl. rad. array
PLANCK-LFI	30(4), 44(6), 70(12),100(34)	33',23',13',10'	L2, full-sky	Correl. rad. array
PLANCK-HFI	143(12), 217(12), 353(6)	8', 6', 5'	L2, full-sky	Bolo array

From Timbie et al. 2002
(ASP Conference vol. 257)

Planck: polarization sensitivity

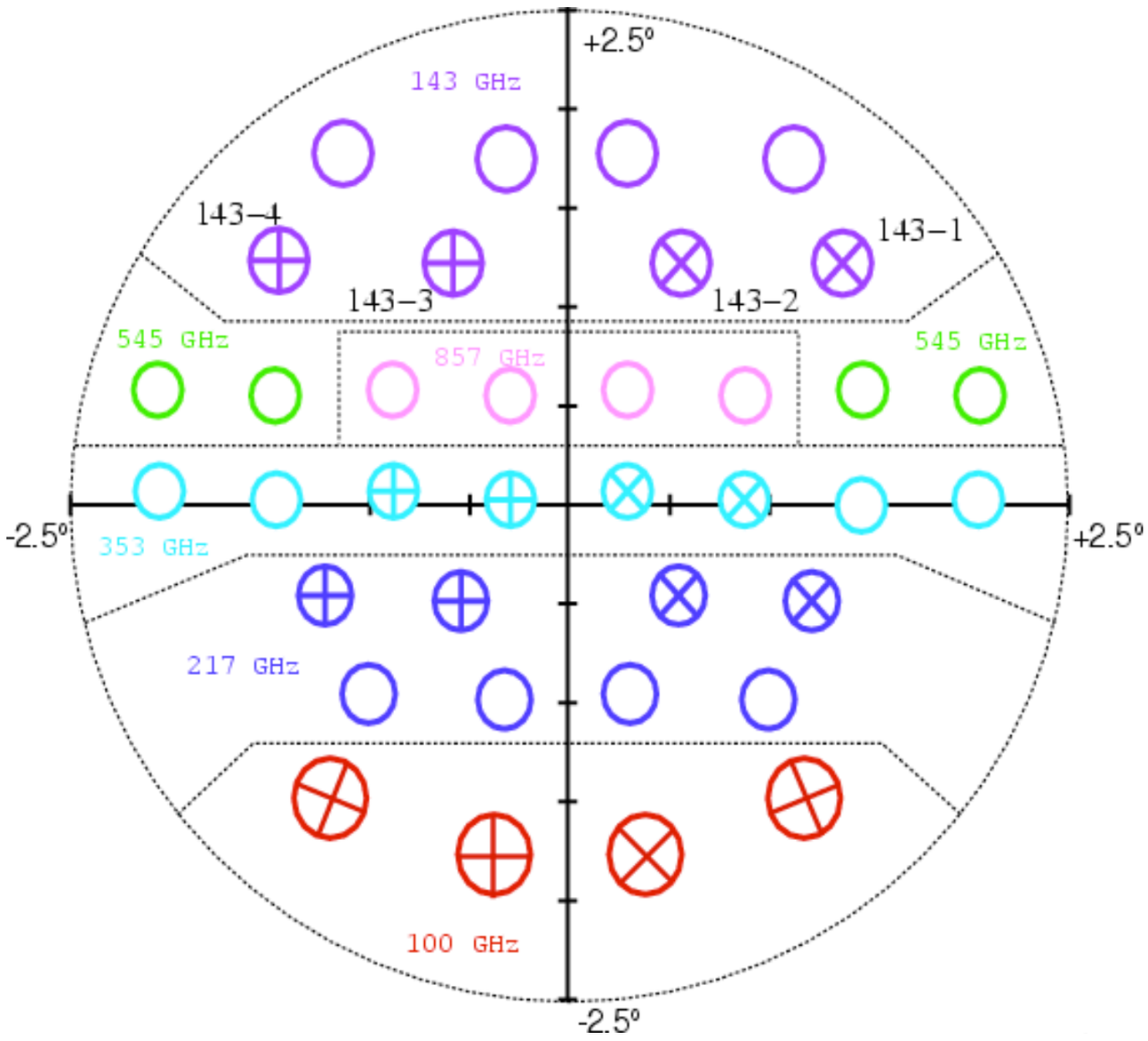

Planck Focal Plane Unit with polarization sensitive bolometers

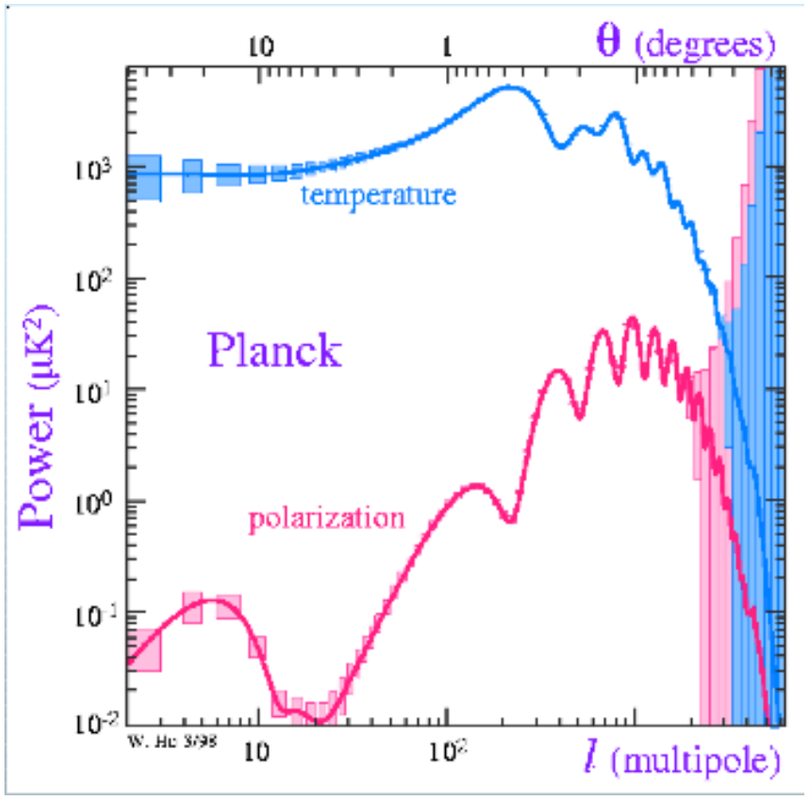

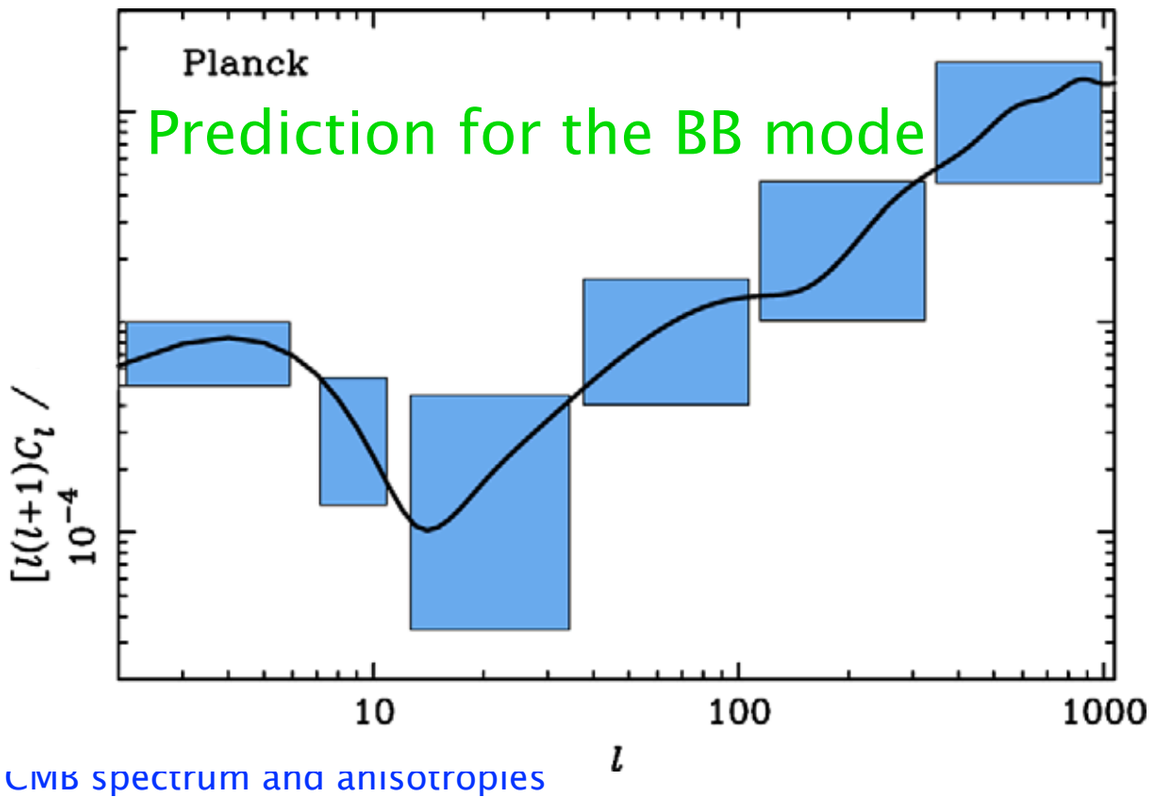

Planck instruments

Instrument Characteristic	LFI			HFI					
Detector Technology.....	HEMT arrays			Bolometer arrays					
Center Frequency [GHz].....	30	44	70	100	143	217	353	545	857
Bandwidth ($\Delta\nu/\nu$)	0.2	0.2	0.2	0.33	0.33	0.33	0.33	0.33	0.33
Angular Resolution (arcmin)	33	24	14	10	7.1	5.0	5.0	5.0	5.0
$\Delta T/T$ per pixel (Stokes I)[a].....	2.0	2.7	4.7	2.5	2.2	4.8	14.7	147	6700
$\Delta T/T$ per pixel (Stokes Q &U)[a] ...	2.8	3.9	6.7	4.0	4.2	9.8	29.8	...	...

[a] Goal (μK/K, 1σ), 14 months integration, square pixels whose sides are given in the row "Angular Resolution".

Planck Bluebook

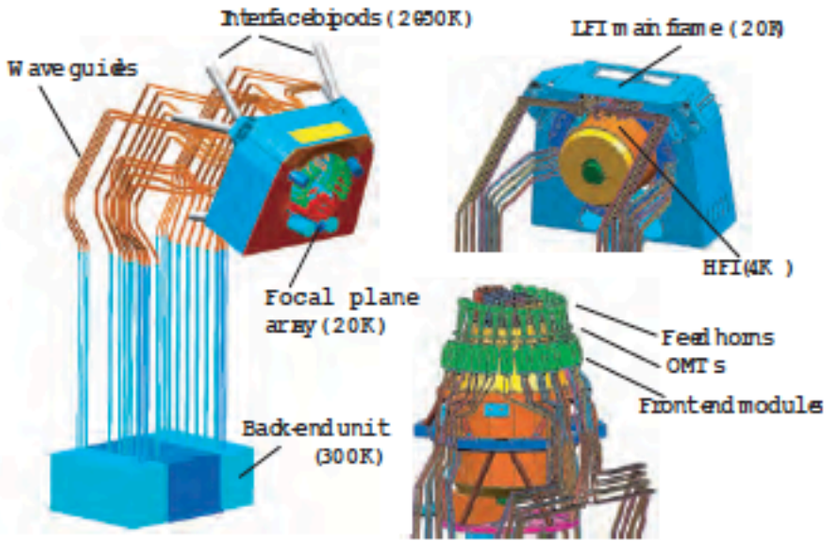

Planck Bluebook

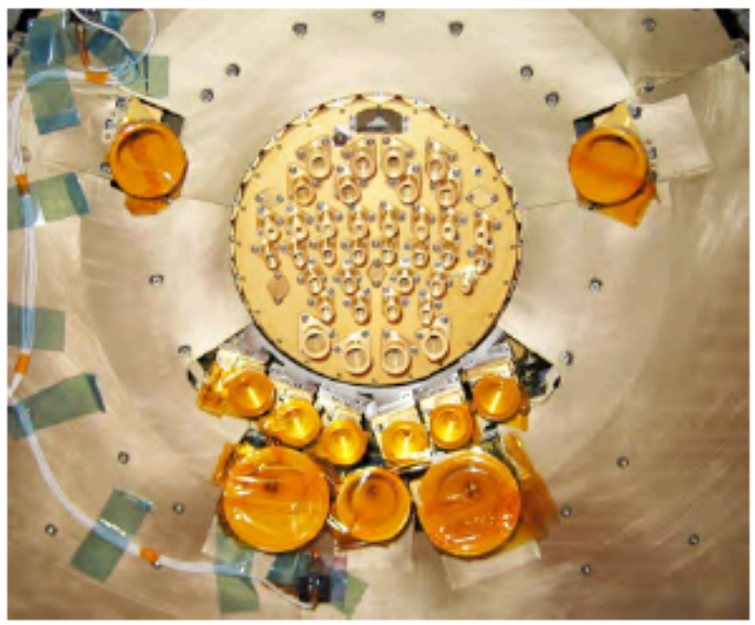

Thales/Alenia Space+ESA

Planck Bluebook

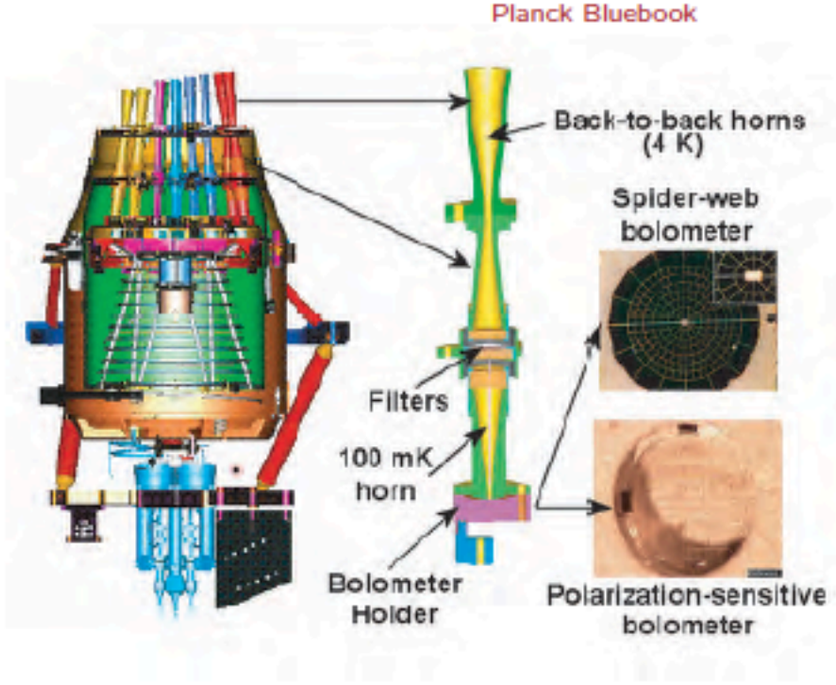

Planck Bluebook

Polarized foregrounds

(CMB Task Force Report)

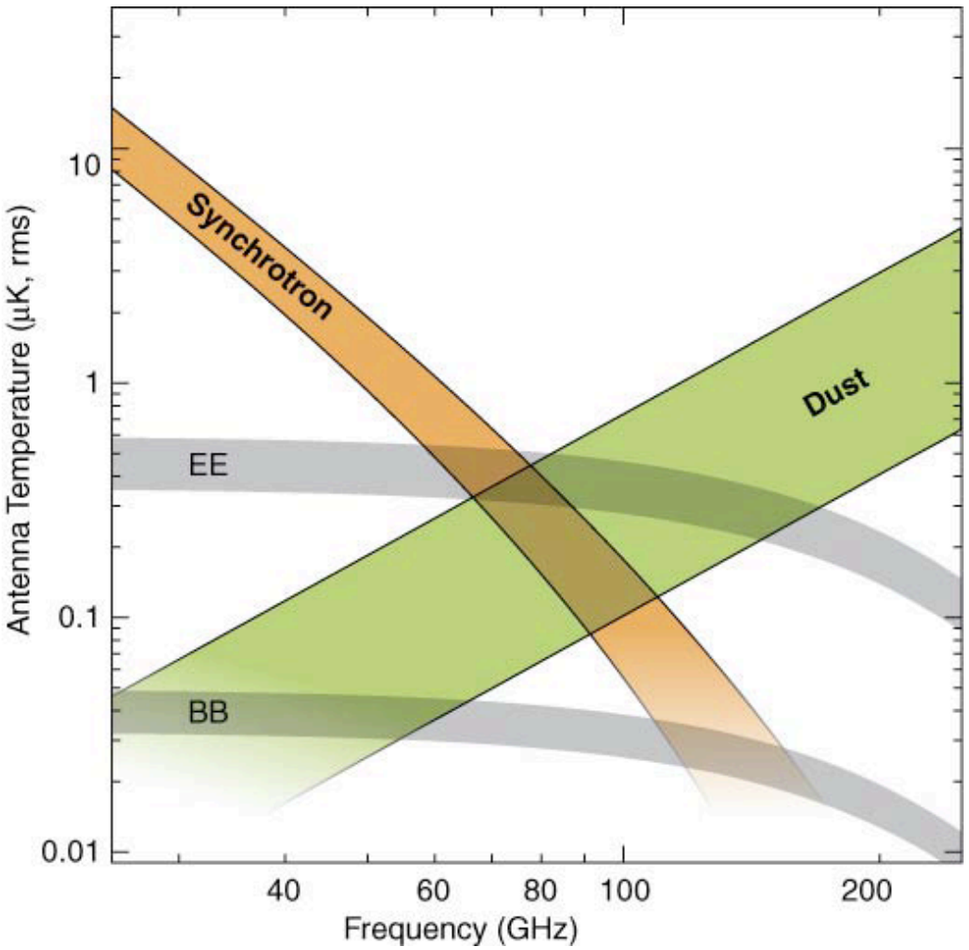

RMS fluctuations in the polarized CMB and foreground signals as function of frequency

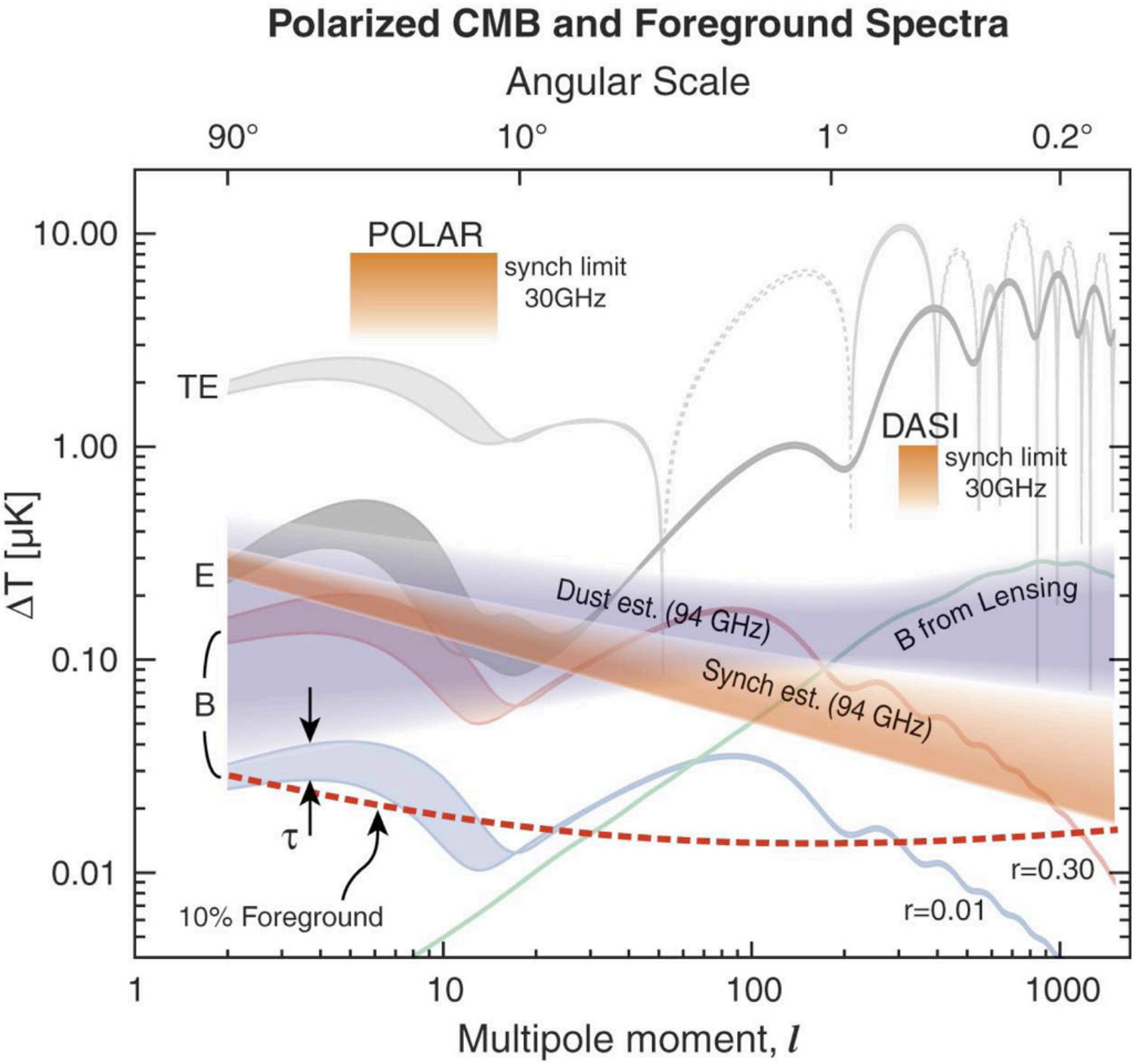

CMB Data Analysis

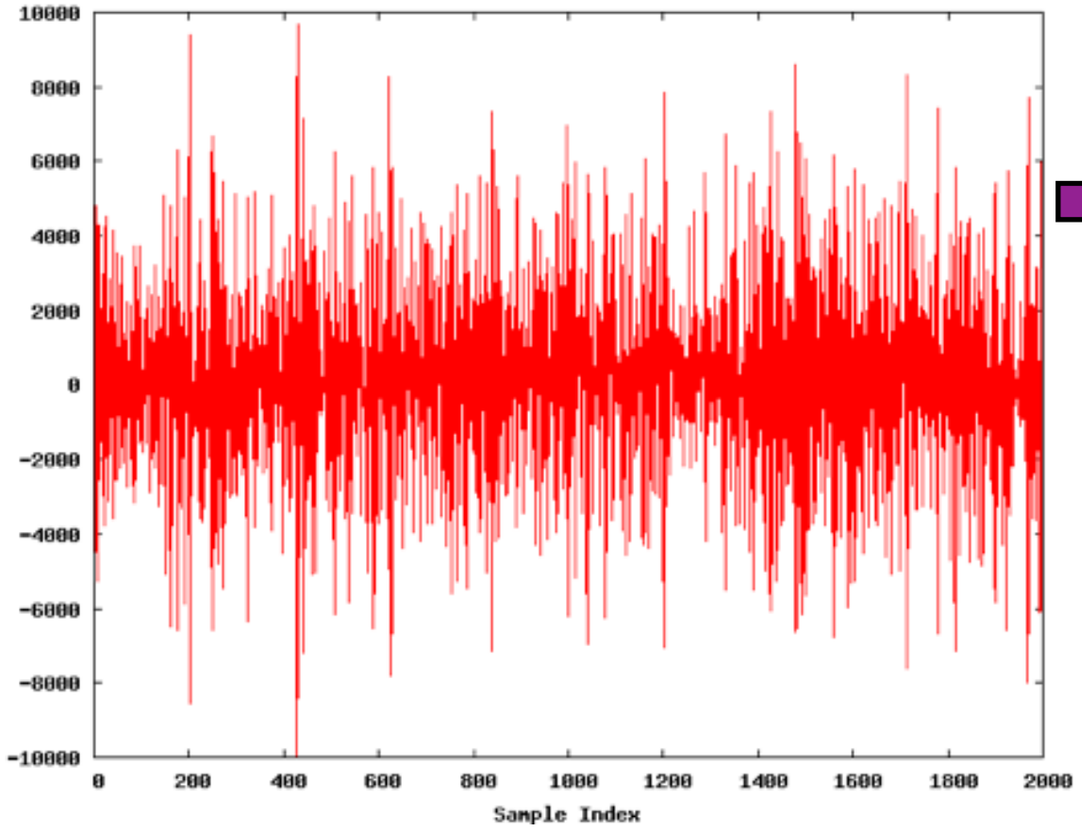

Data time-stream

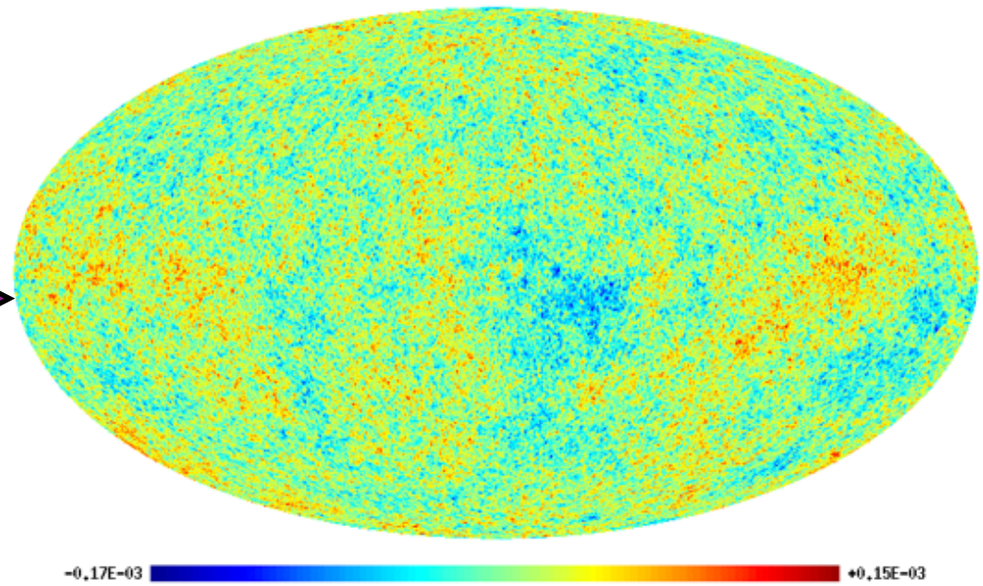

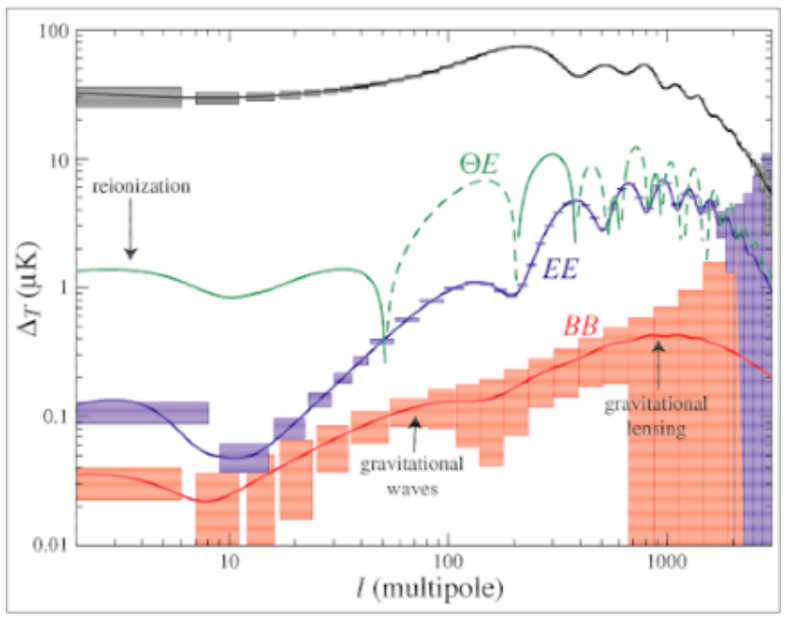

Striping

Common to get stripes in the scan direction.

Removal easy in Fourier space.

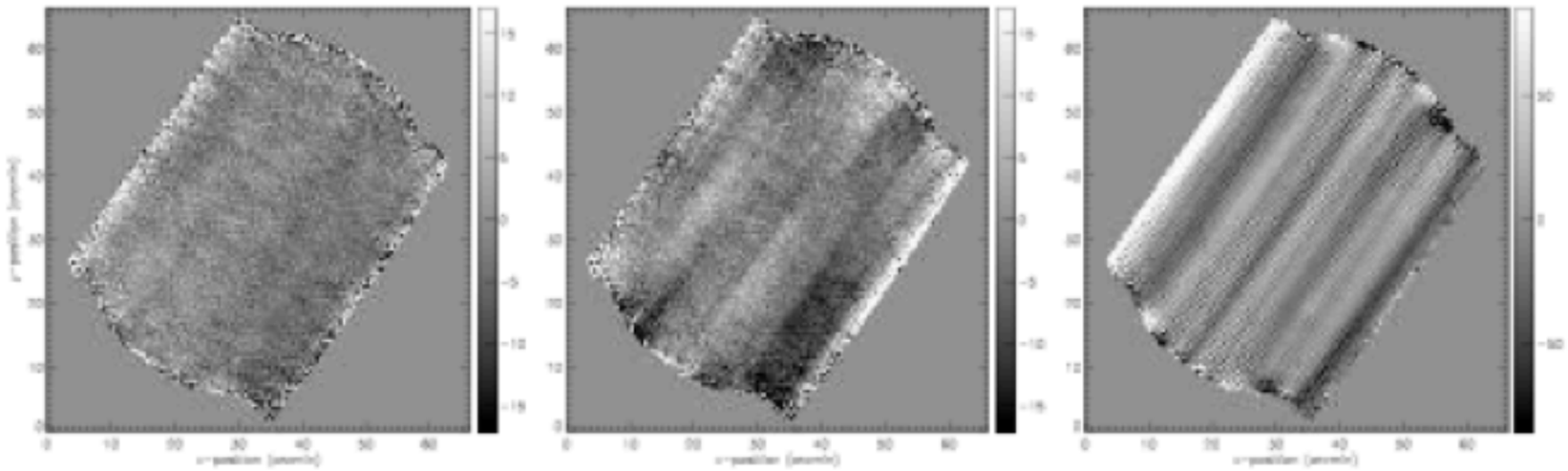

map space

Fourier transformation also helps to separate signal and noise better (different temporal signal).

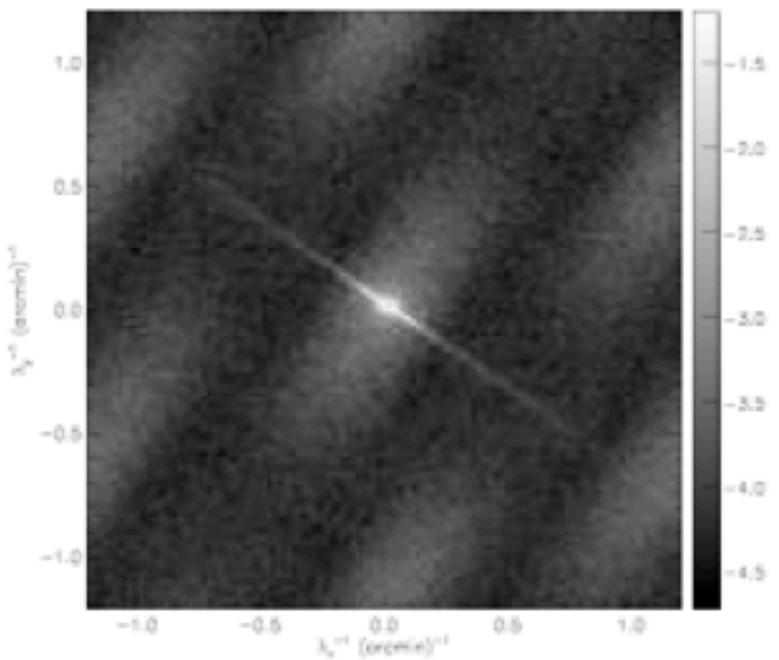

Fourier space

Patanchon et al ; BLAST data

Map making

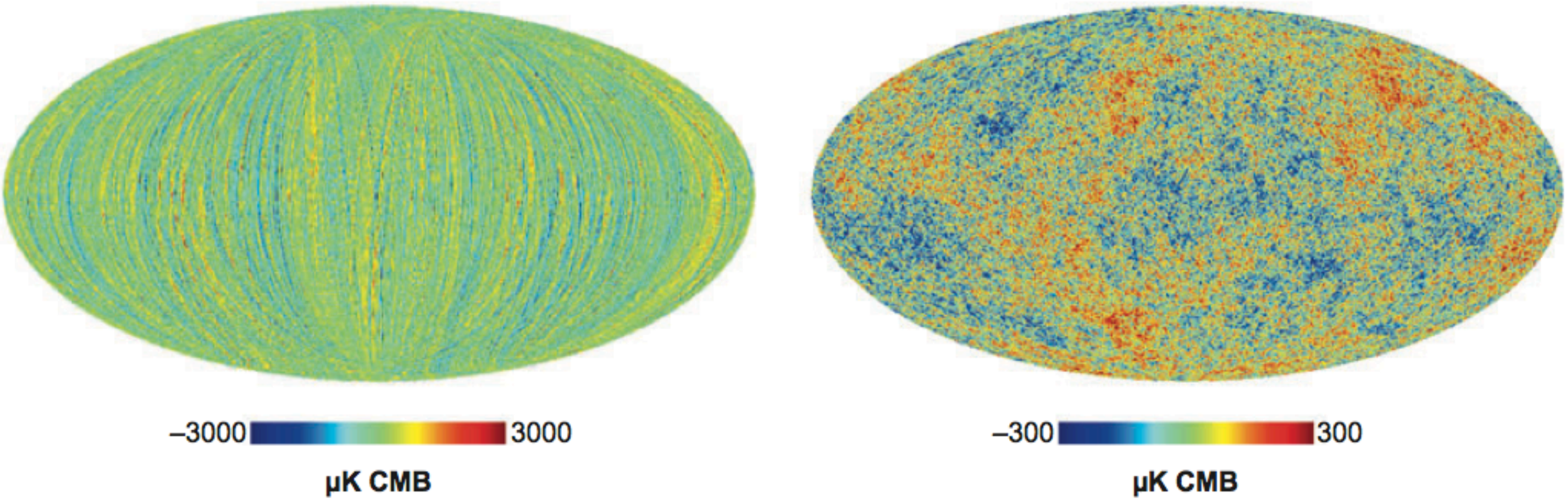

Figure 10

Effect of destriping on simulated sky maps. (*Left*) Map from a raw time stream. (*Right*) Map after applying a destriping algorithm (note the different scales). This simulation was done for the Planck High Frequency Instrument (38).

Figure taken from Samtleben et al. 2007.

Removing the Galaxy

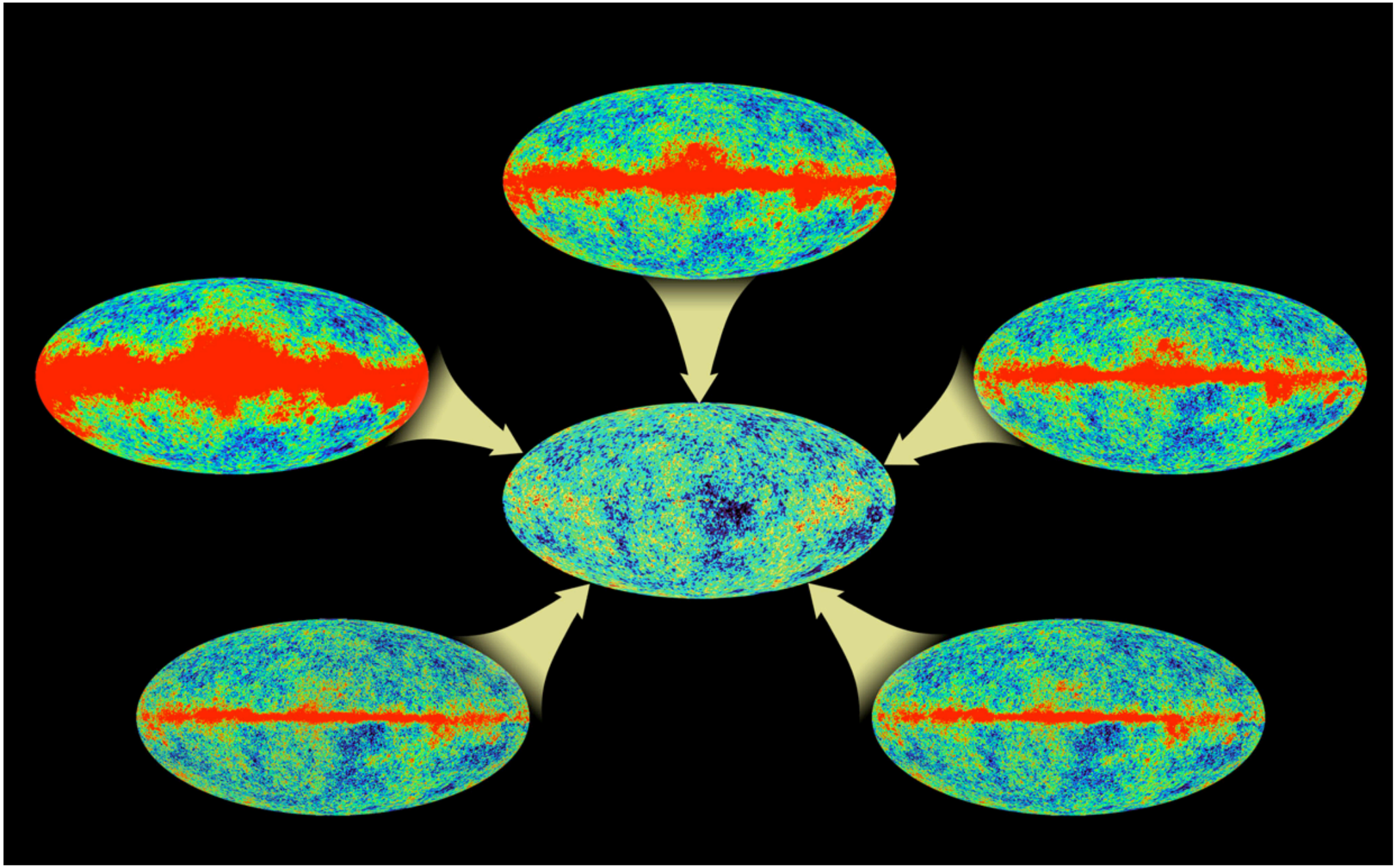

Galaxy vs. CMB

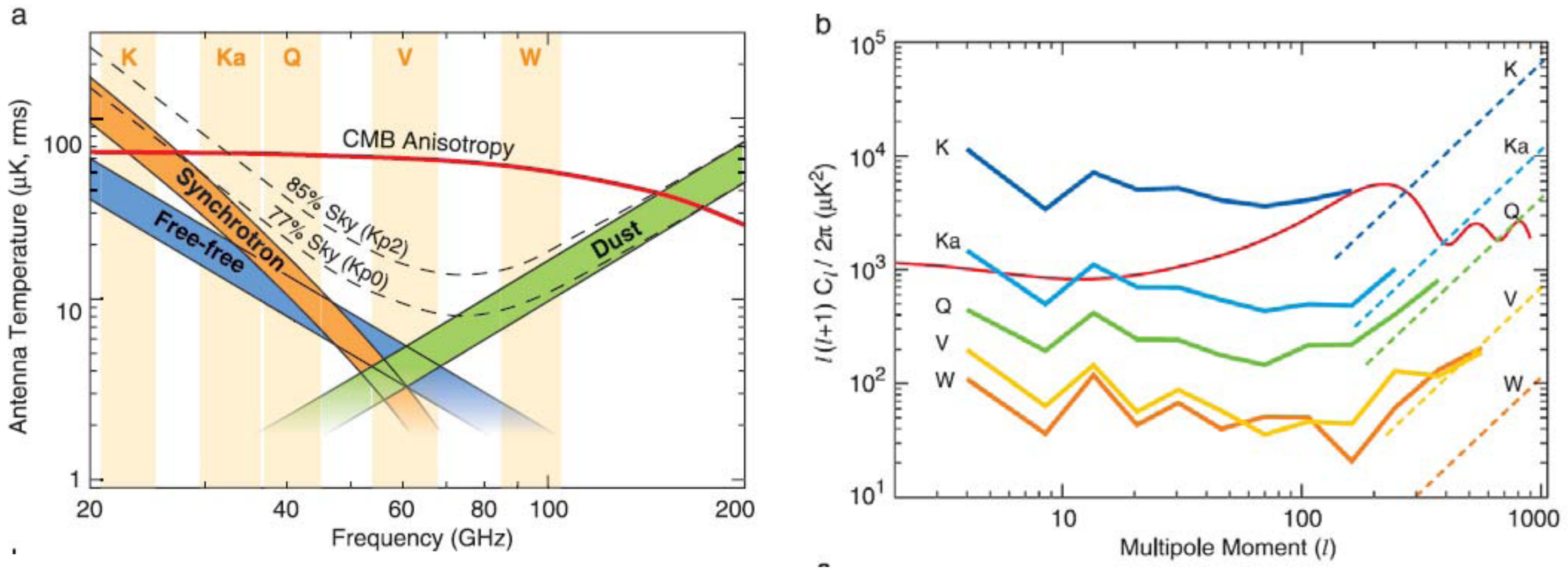

CMB vs. foreground anisotropies (Bennett et al. 2003, WMAP 1st year)

Left: Spectrum of the CMB and foreground emissions (models). WMAP frequencies were chosen such CMB mostly dominates.

Right: Foreground power spectra for each WMAP band. The dashed lines at the right are estimated point source contributions.

CMB Foregrounds

CMB

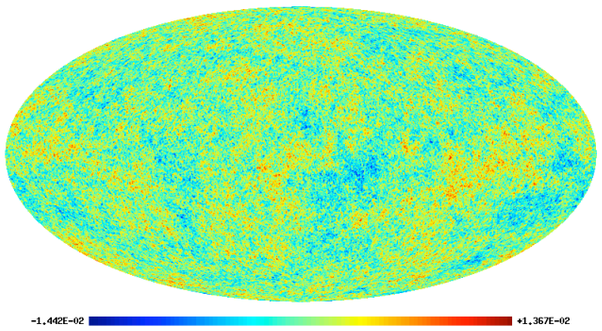

+

Foregrounds

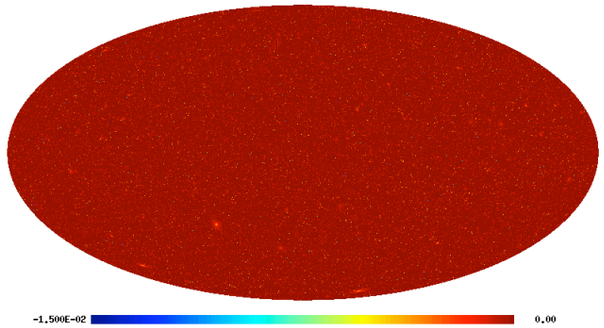

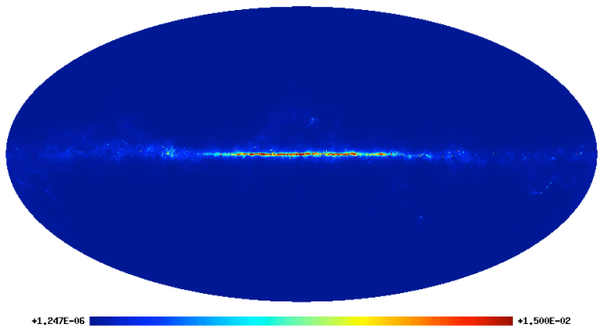

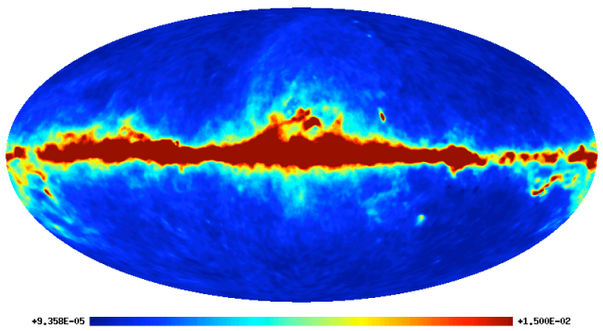

=

Observation

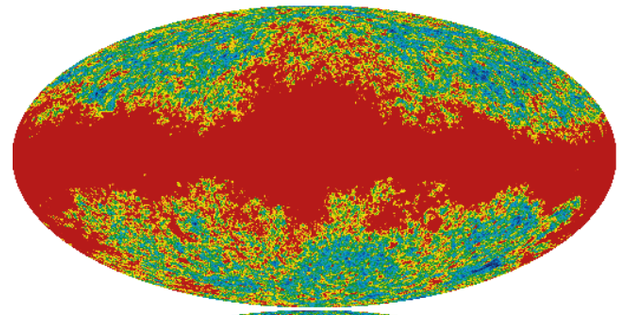

K band
23 GHz

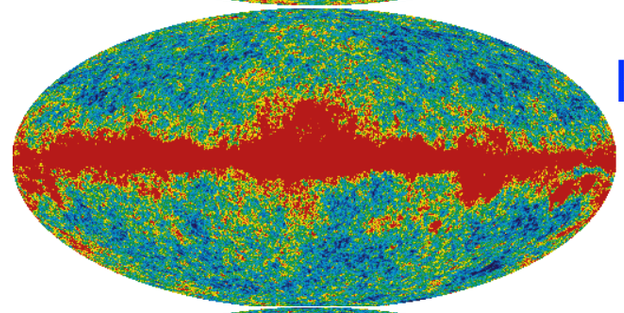

Ka band
33 GHz

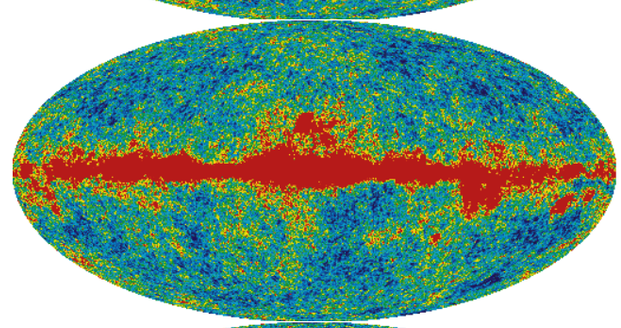

Q band
41 GHz

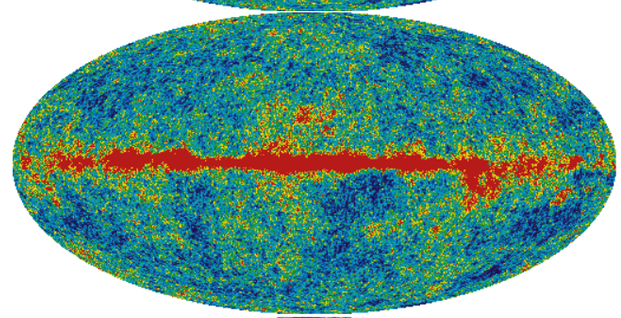

V band
61 GHz

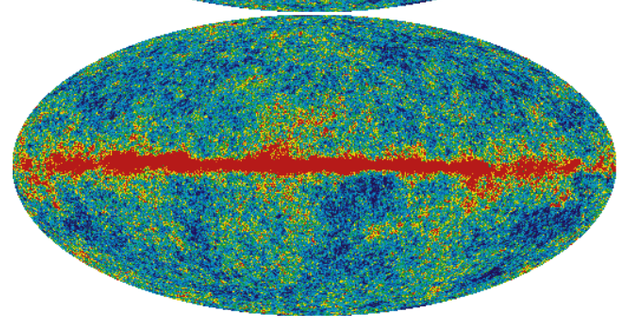

W band
94 GHz

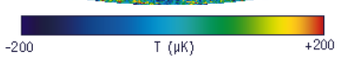

Credit: L. Colombo

Component Separation

Two observing frequencies: ν_1, ν_2

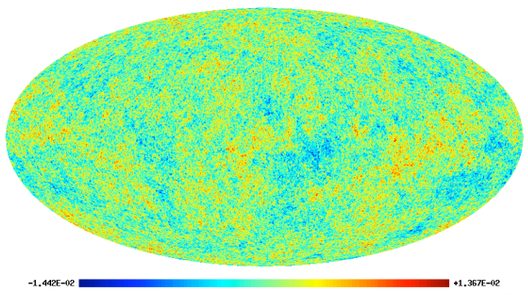

s_1

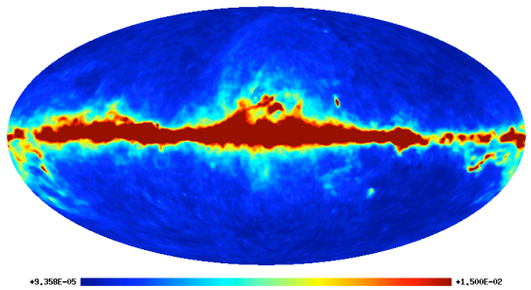

s_2

$$x_1 = a_{11}\, s_1 + a_{12}\, s_2 + n_1$$
$$x_2 = a_{21}\, s_1 + a_{22}\, s_2 + n_2$$

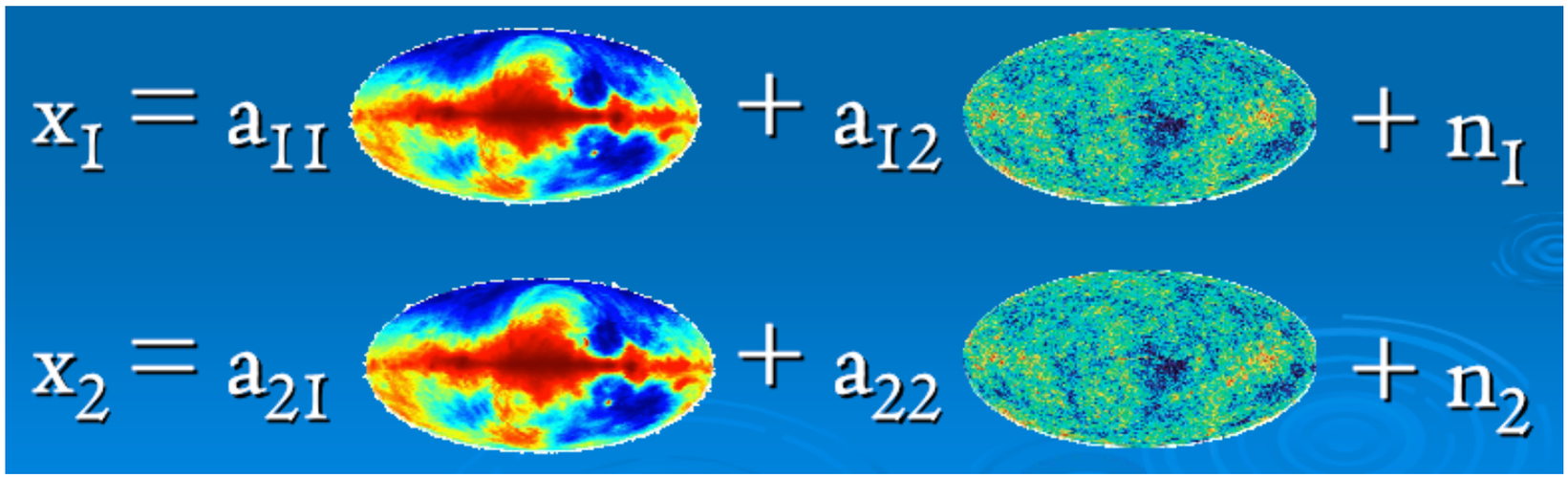

x = As + n

Invert for **s**

Ground-based measurement

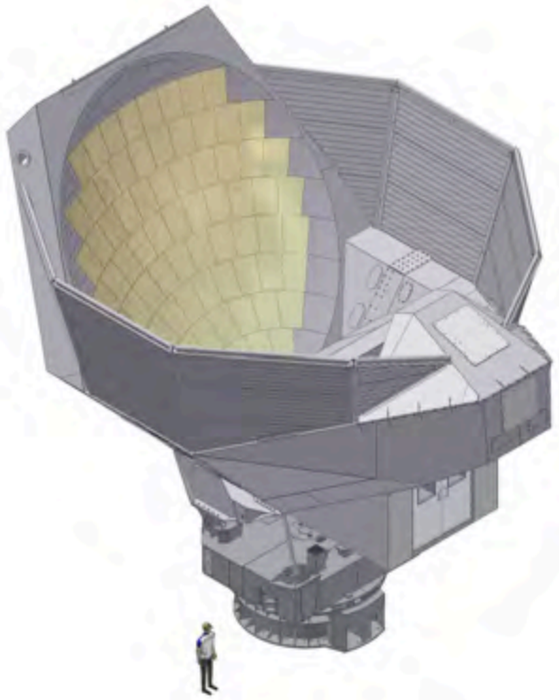

Atacama Cosmology Telescope

Since 3 K << 300 K, CMB measurements are sensitive to thermal emission from their environments

CMB telescopes are specially designed to be very directional, but 300 K in the sidelobes is always a worry

A receiver has system temperatre T_{sys}

$$T_{sys} = T_{rec} + T_{CMB} + T_{atm} + T_{ground} + \ldots$$

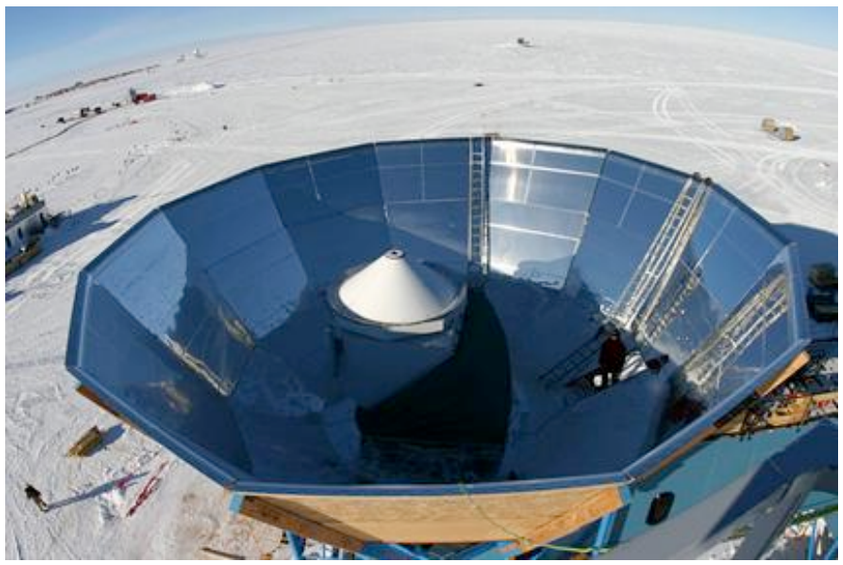

QUaD at south pole

The radiometer equation is: $$\delta T = \frac{b T_{sys}}{\sqrt{\Delta\nu\,\tau}}$$

CMB flux

Planck spectrum: $$I(\nu,T)=\frac{2h\nu^3}{c^2}\frac{1}{e^{\frac{h\nu}{kT}}-1}.$$

Example:

- Beam FWHM = 8°, beam aperture = 8 cm^2
- ν_0 = 90 GHz, $\Delta\nu$ = 10 GHz

The CMB flux (2.7K) on the horn is then: **2.5 x 10^{-13} Watts**

Temperature anisotropy: ~10^{-18} Watts

Polarization anisotropy: ~10^{-19} Watts

CMB receivers

Coherent receivers:

Phase-preserving amplification
Correlation of different polarization

- Correlation/Pseudocorrelation receiver (e.g. WMAP, CAPMAP)
- Interferometer (e.g. DASI, CBI)

Incoherent receivers (bolometers):

Direct detection of radiation,
No phase information kept
Large arrays!

- Bolometers (e.g. ACBAR, Boomerang, BICEP, Clover, Planck)

Bolometer experiments

The Bolometer

S.P. Langley invented the Bolometer,
Which is really a sort of thermometer.
It can measure the heat
Of a polar-bear's seat,
From a distance of half a kilometre.

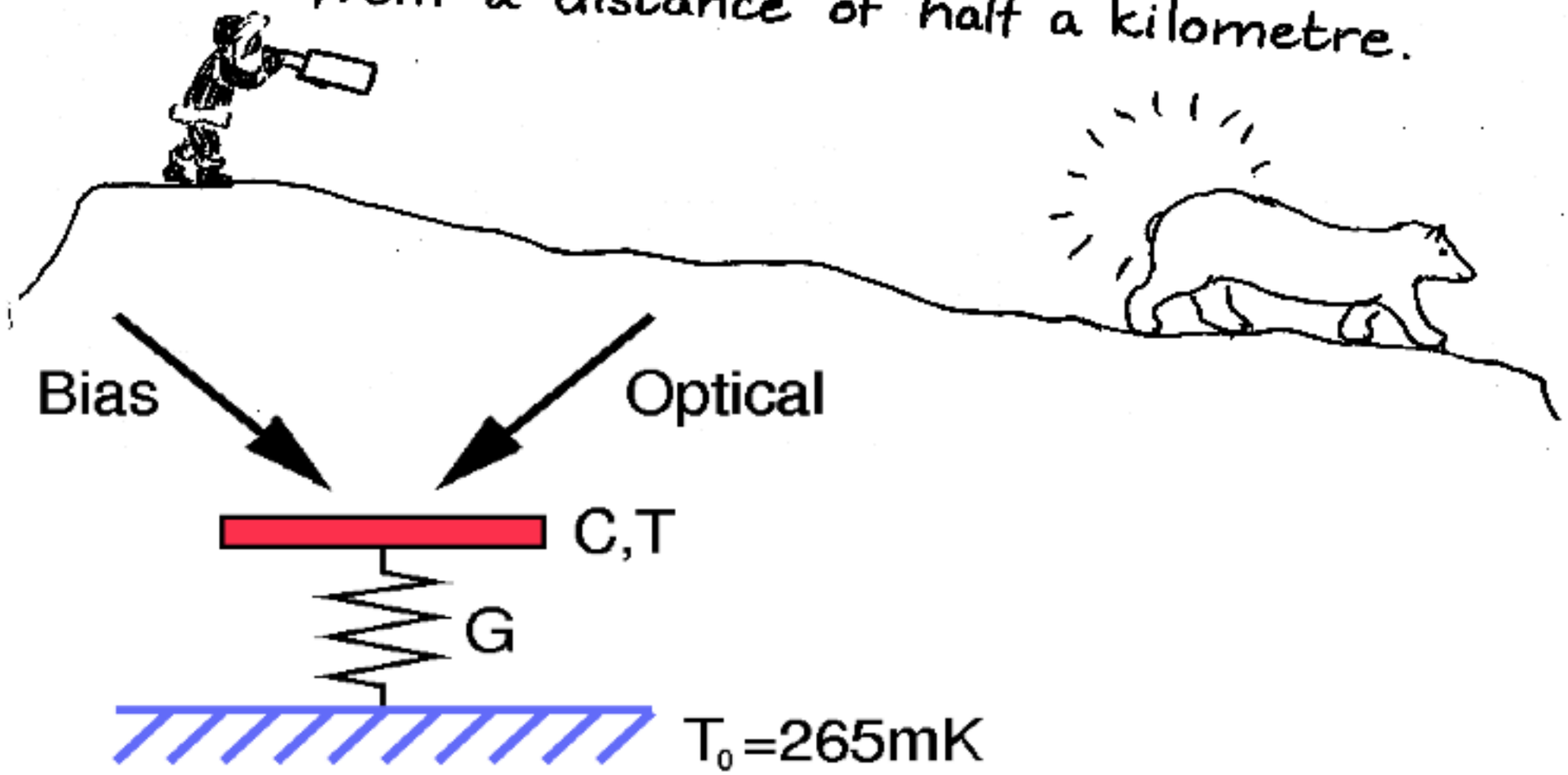

Bolometer experiments

ACBAR

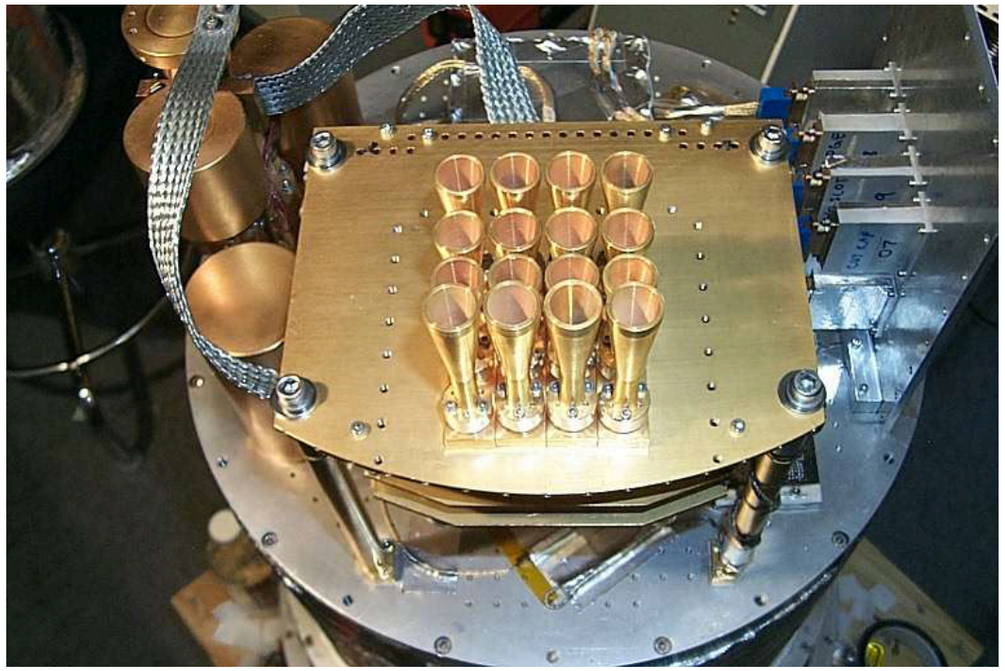

Boomerang

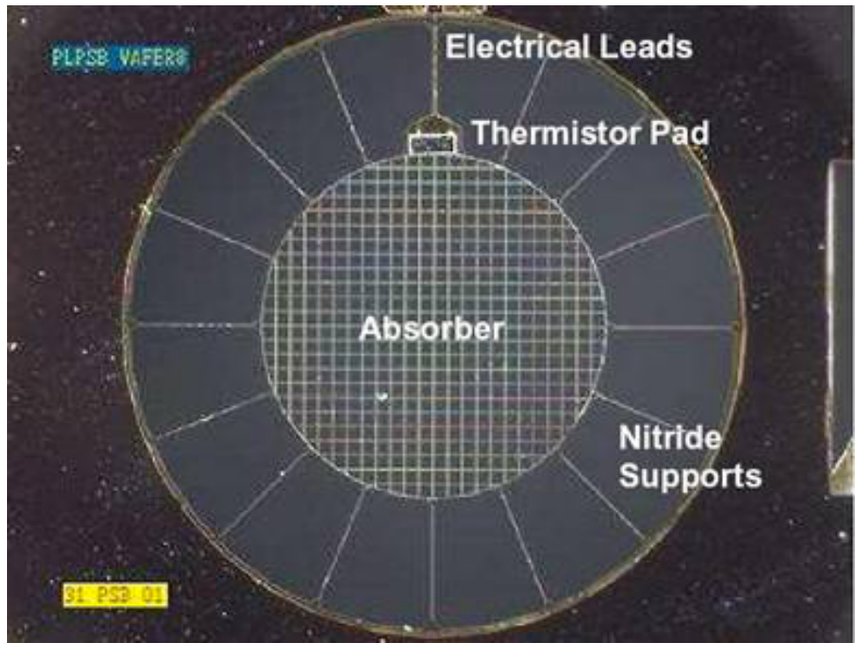

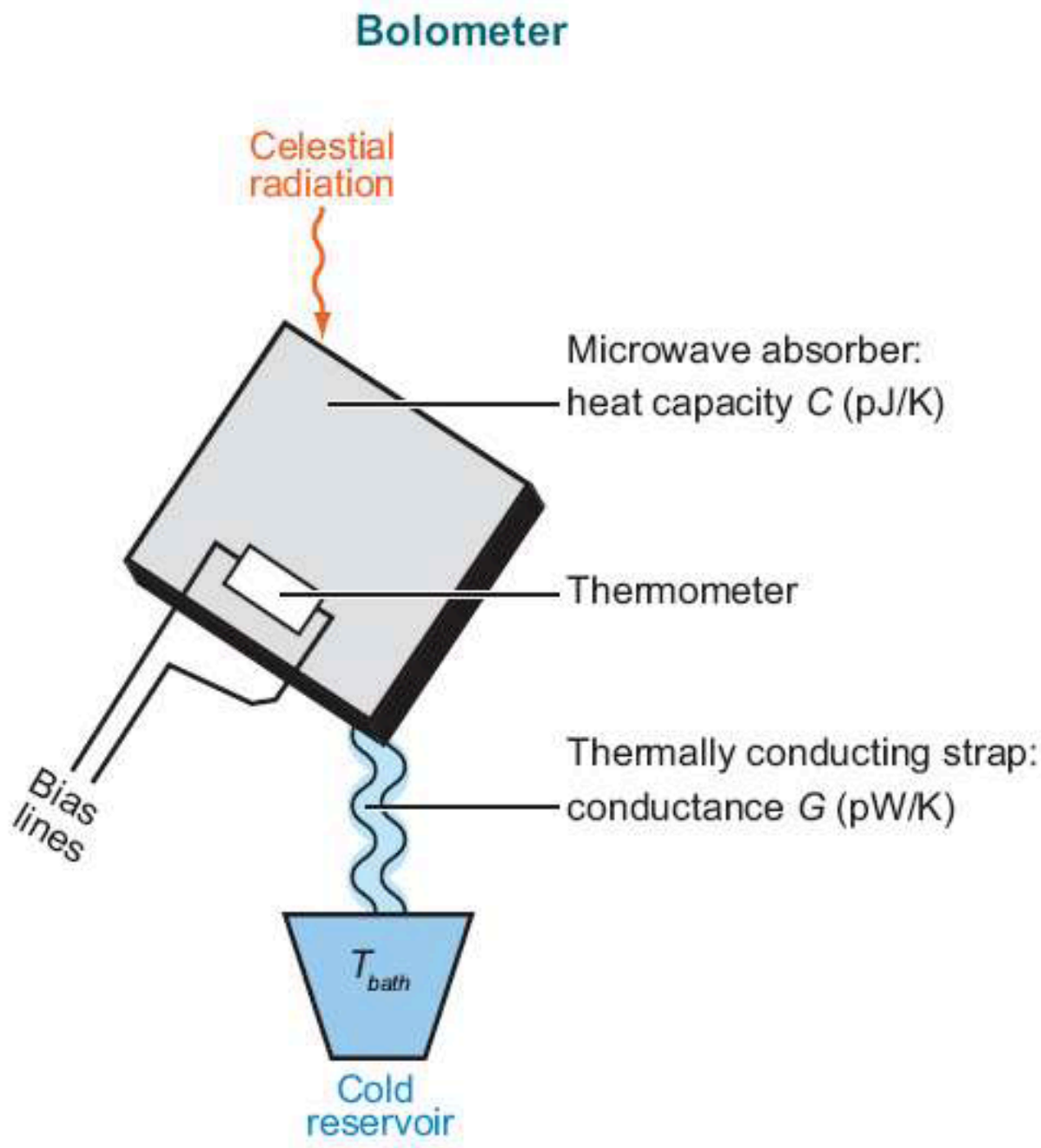

Interferometers

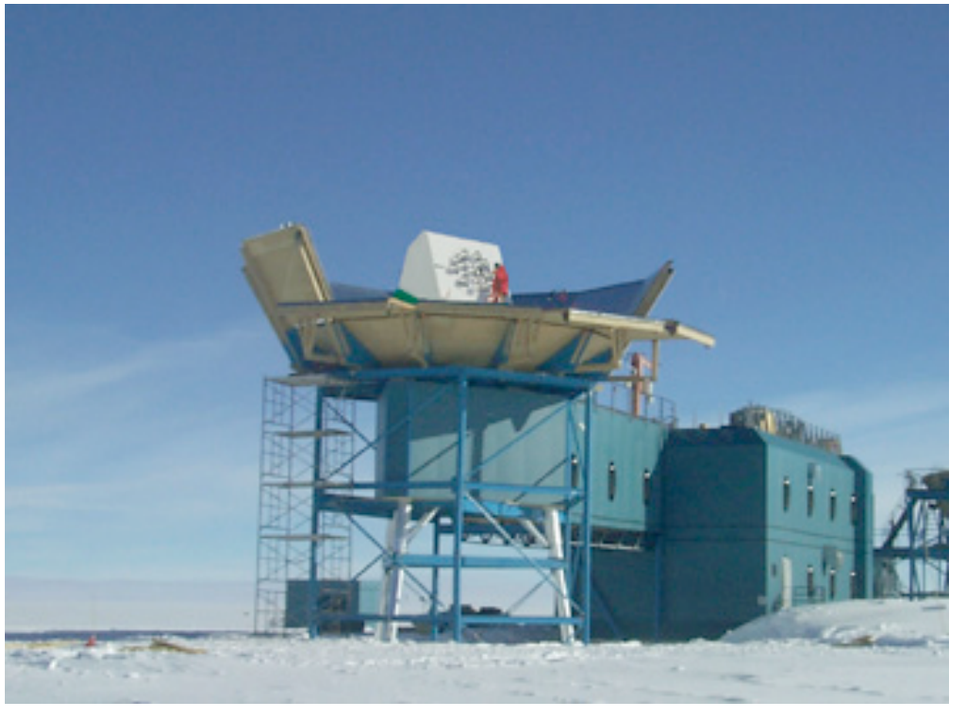

DASI in South Pole

CBI in Atacama desert

Coherent receivers: Can be configured so that the output is the correlation of two input signals.
HEMT (High Electron Mobility Transistor) allow coherent amplification with low noise and high gain.

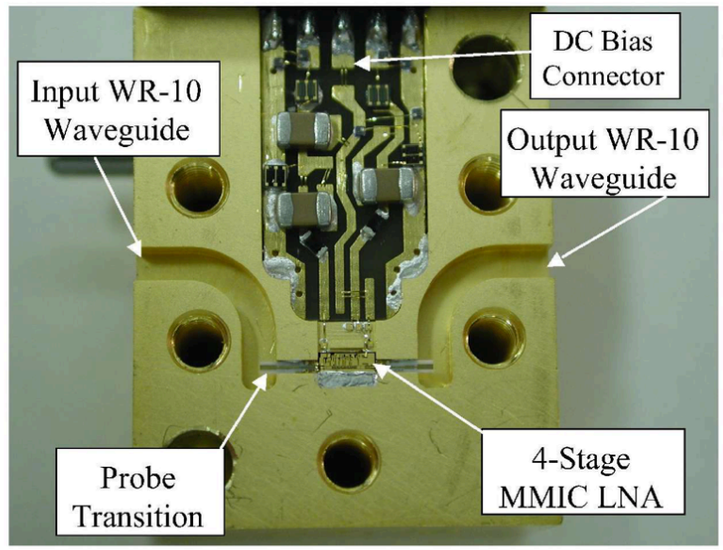

Interferometric measurements

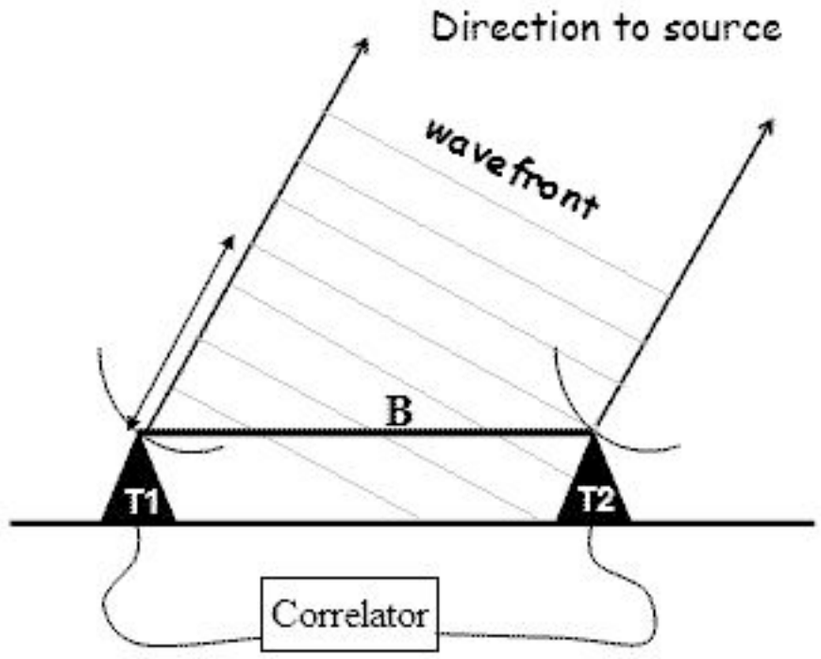

Properties of interferometers that make them ideally suited for CMB observation:

- Automatic subtraction of the mean signal
- Intrinsically stable (no skynoise)
- Beamshape is easy to obtain (and is not as important as in single dish observations)
- Direct measurement of visibilities (which are very nearly the Fourier transform of sky brightness distribution)
- Precision radiometry and polarimetry
- Repeated baselines allow variety of instrumental checks

C(θ) from interferometers

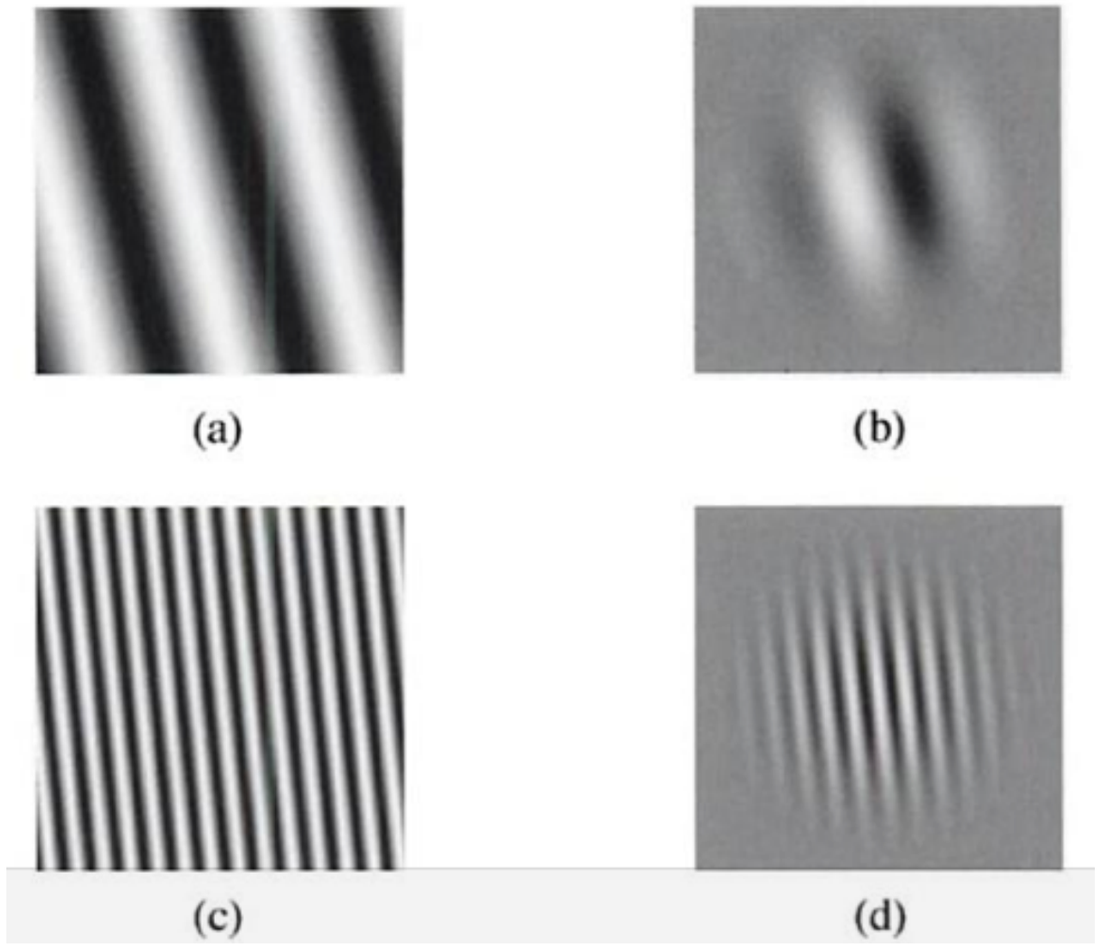

Left: Illustration of two multipole components of sky brightness over a 1.5° × 1.5° field of view. An interferometer measures directly these components multiplied by the primary beam, shown in the right. For CBI, (a) and (b) corresponds to 1-meter baselines, and (c) and (d) represents 5-meter baselines.

Bolometer and HEMT sensitivities

Fluctuations in the arrival rate of CMB photons impose a fundamental limit of ~30 μK√(sec) for detection of a single mode of radiation in a fractional bandwidth of 25% from ~30 to 220 GHz.

	2005[b]		2010[c]	
Freq.	Bolometer	HEMT /√2	Bolometer	HEMT /√2
[GHz]	[$\mu K_{cmb}\sqrt{s}$]	[$\mu K_{cmb}\sqrt{s}$]	[$\mu K_{cmb}\sqrt{s}$]	[$\mu K_{cmb}\sqrt{s}$]
30	–	93	57	48
40	–	115	51	51
60	–	175	44	60
90	67	224	40	75
120	–	–	40	93
150	48	–	43	–
220	68	–	64	–
350	224	–	220	–

(CMB Task Force Report, 2005)

Real life example: POLARBEAR

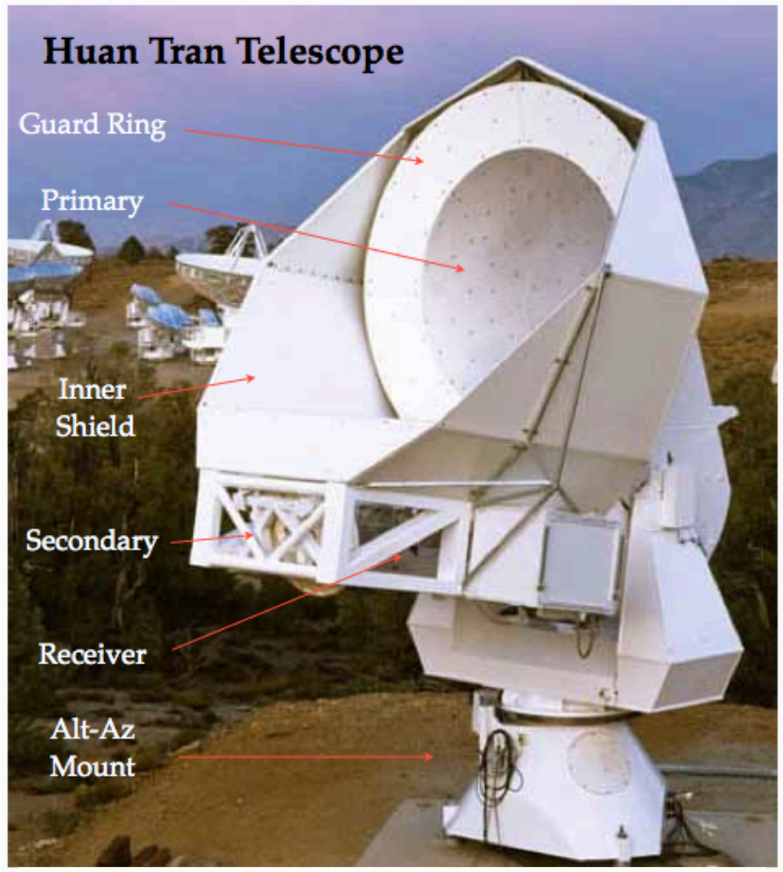

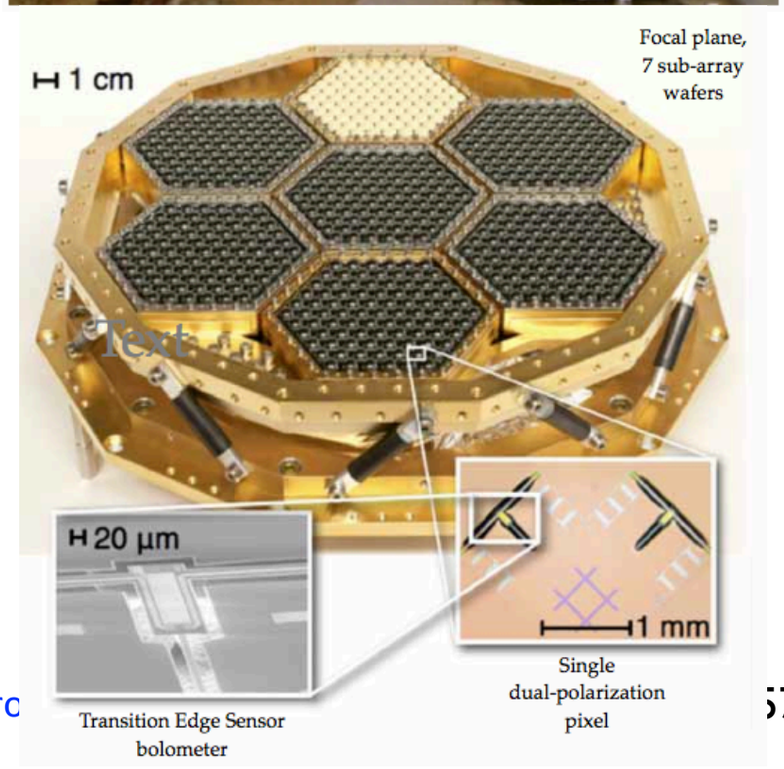

POLARBEAR currently being commissioned in Chile (not far from the ALMA and APEX sites).

Real life example: POLARBEAR

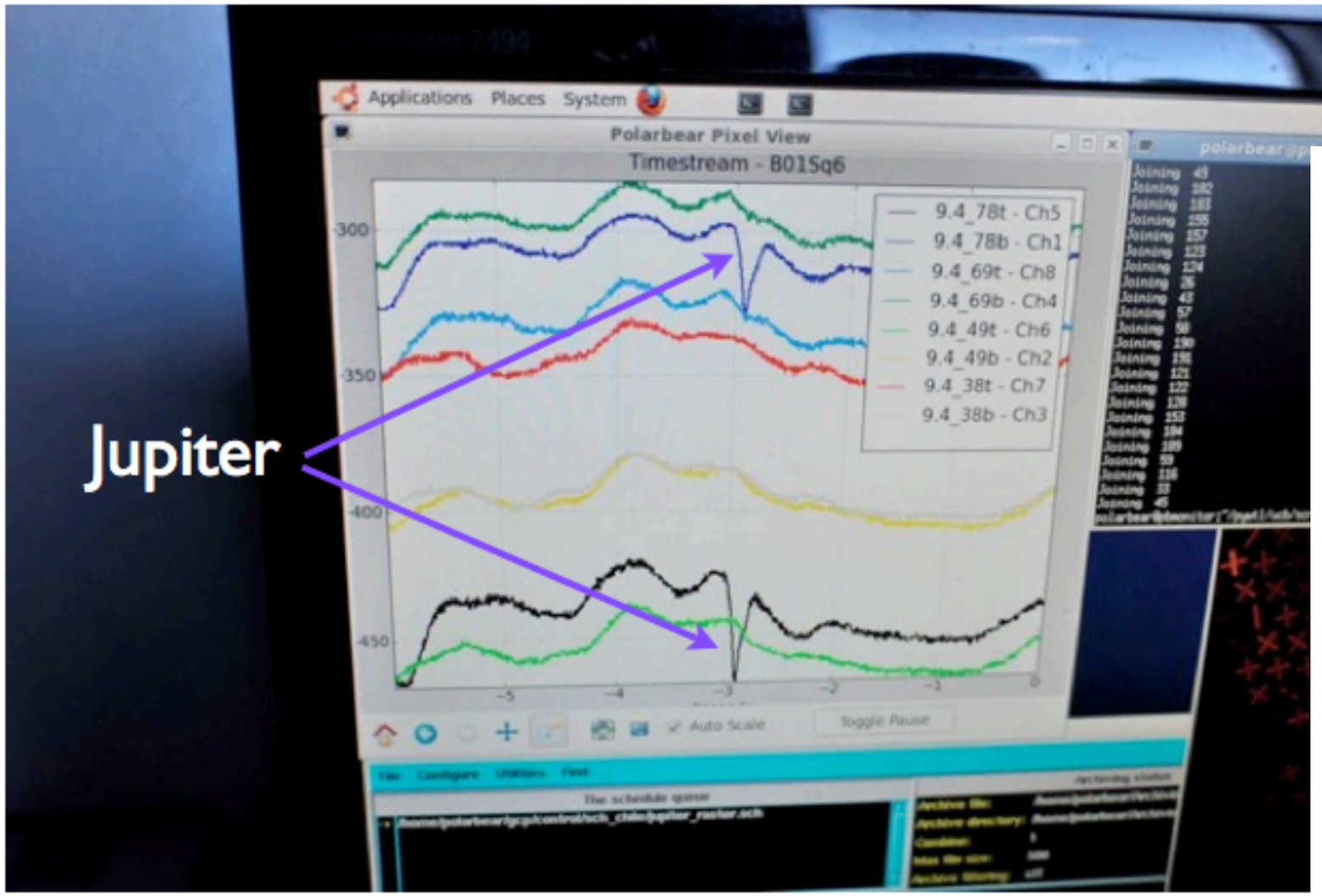

- Achieved first-light on January 10th, 2012!

Jupiter beam-map
(two polarizations!)

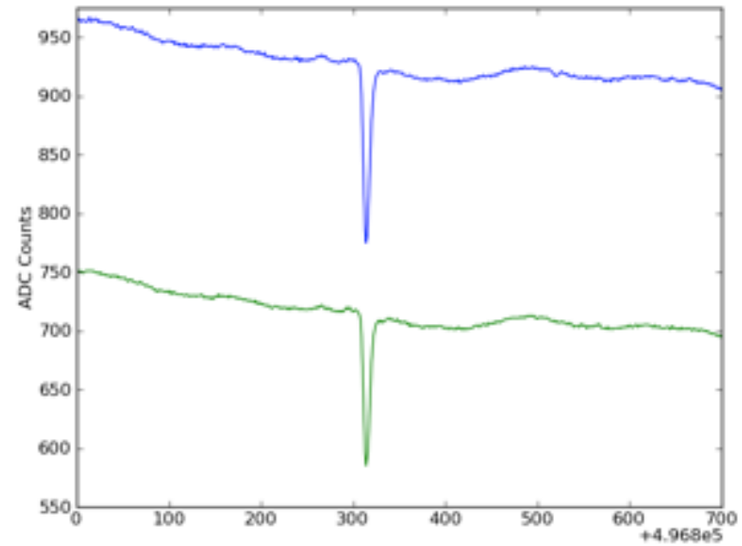

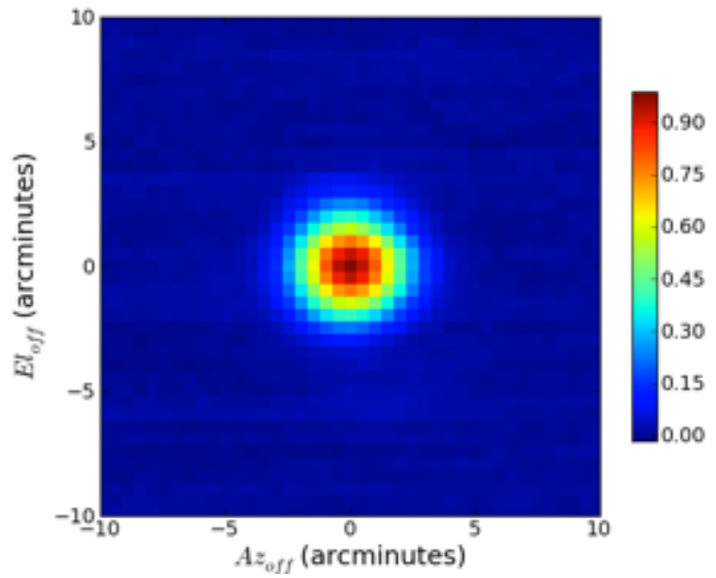

Real life example: POLARBEAR

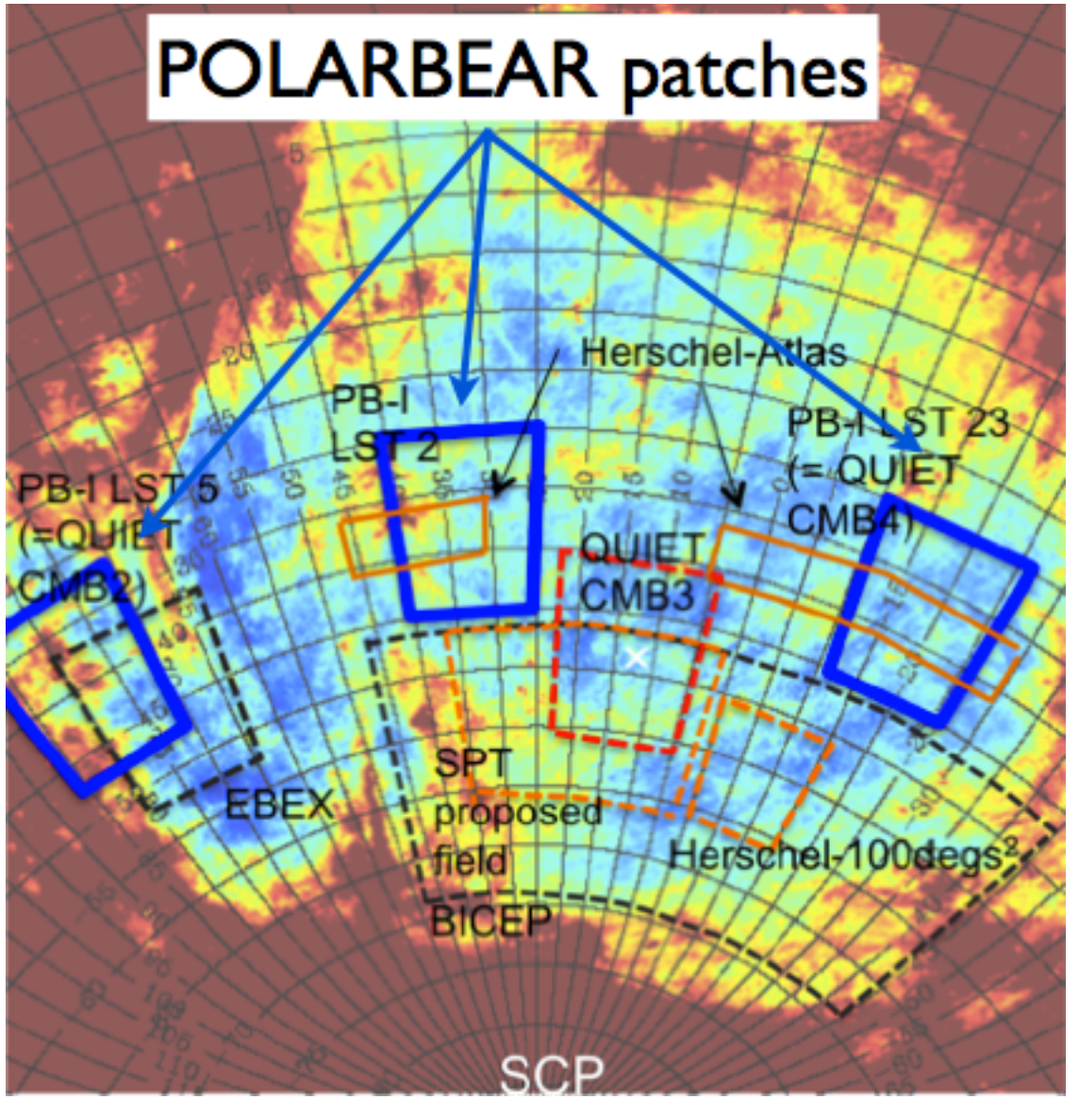

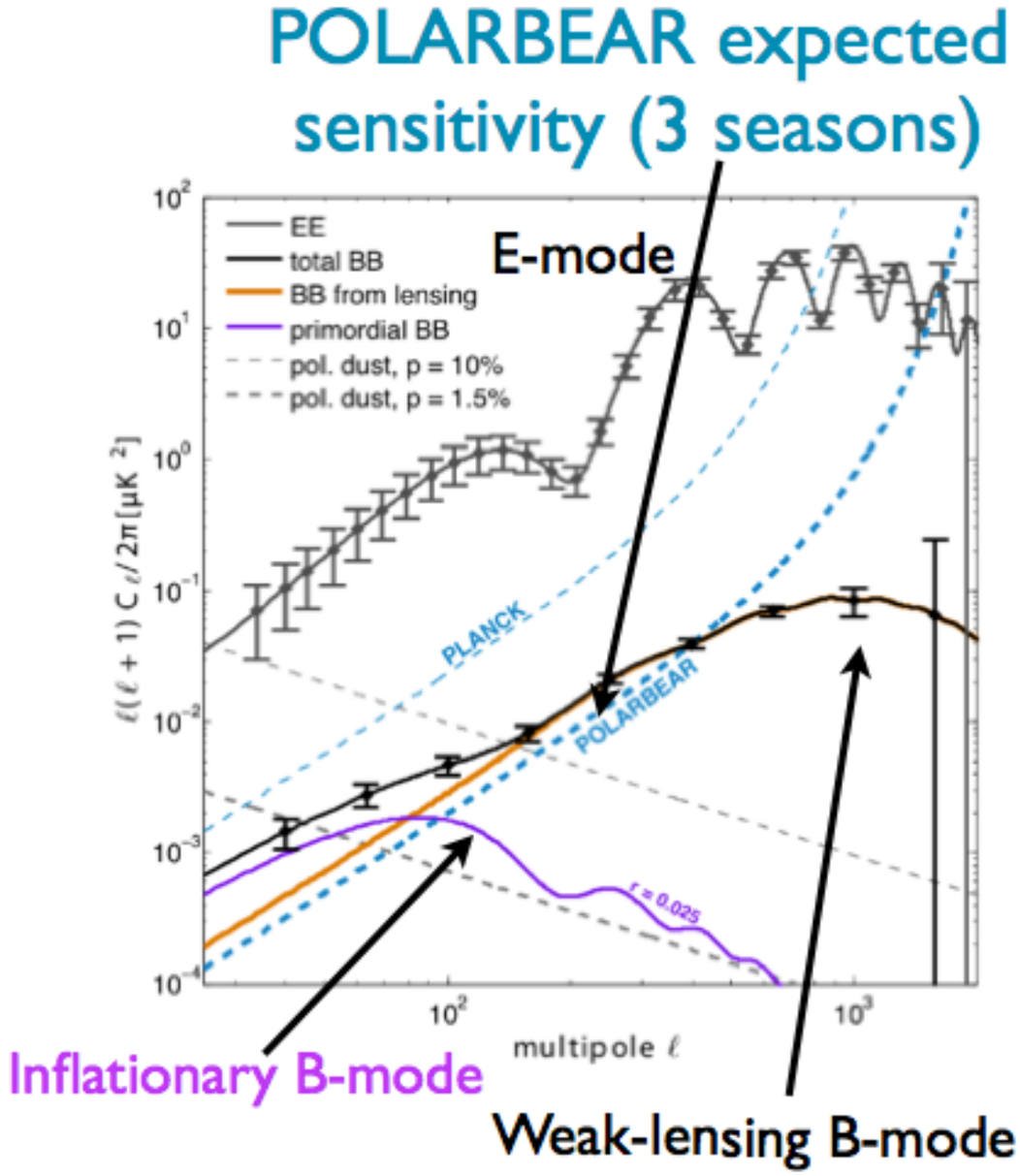

Questions?